DEPARTMENT OF PHYSICS

RESEARCH REPORT NUMBER 69-1

PENETRATION AND INTERACTION OF PROTONS WITH MATTER

PART II: EXPERIMENTAL STUDIES USING SEMICONDUCTOR DETECTORS

Edited
by

GEORGE W. CRAWFORD

Sponsored by

National Aeronautics and Space Administration
Research Grant NsG 708

Principal Investigator: George W. Crawford
Report Period: June 1, 1964 through October 31, 1969

October, 1969

SOUTHERN METHODIST UNIVERSITY
DALLAS, TEXAS 75222

SOUTHERN METHODIST UNIVERSITY

DEPARTMENT OF PHYSICS

RESEARCH REPORT NUMBER 69-1

PENETRATION AND INTERACTION OF PROTONS WITH MATTER

PART II: EXPERIMENTAL STUDIES USING SEMICONDUCTOR DETECTORS

CONTENTS

CHAPTER 1

A NEW APPROACH TO THE ANALYSIS OF MEASUREMENTS OF PROTON STOPPING POWER

by Martin Leimdorfer, Claes Johansson and George W. Crawford

INTRODUCTION

A computational procedure for extracting theoretically relevant information from measurements of the energy lost by protons in passing through a chosen material has been developed. The measured quantities include the initial energy of the proton, E_o, the energy lost, $\Delta E = E_o - E_i$ by the proton in passing through an absorber of thickness X having a density ρ . The energies E_o and E_i are recorded as multichannel pulse height distributions of charge as created in and collected from the active region of lithium-drifted silicon detectors. The detectors used were in each case long enough to totally absorb the entering proton. In order that these pulse height distributions be closely related to proton energy distributions, the detector was aligned in the proton beam so that the protons traveled parallel to the length of the detector. By keeping the parallel beam small in size as compared to the cross-section of the active region, and by centering the entrance point, the proton, whether of energy E_o (direct from the accelerator) or E_i (after passing through an absorber), entering the detector had a high probability of being totally absorbed in the active region. See Chapter 6 Part I for a discussion of lateral leakage. The Bethe-Bloch equation as modified for shell and density corrections (see Equation 2-29, Chapter 2, Part I) describes the instantaneous rate of energy loss suffered by a charged particle along the path of migration in matter through interactions with atomic electrons.

$$-\frac{dE}{\rho dx} = \frac{z^2 Z}{A} K(\beta)\left[f(\beta) - \ln I - \frac{\Sigma C_i}{Z} - \frac{\delta}{2}\right] \qquad (1\text{-}1)$$

where

$$K(\beta) = \frac{4\pi e^4 N_o}{mc^2\beta^2} \qquad \text{(in MKSA units)}$$

$$f(\beta) = \left(\ln\frac{2mc^2\beta^2}{1-\beta^2}\right) - \beta^2$$

and

ρ = density of stopping material

z = charge number of incident particle

Z = atomic number of stopping material

A = atomic weight of stopping material

β = v/c, velocity of incident particle relative to velocity of light

C_i = shell correction of the i^{th} shell ($\Sigma C_i = C(\beta)$)

δ = density correction at high energies

I = average excitation potential per electron of the stopping atom.

m = rest mass of electron

e = electron charge

N_o = Avogadro's number

ε_o = dielectric constant of vacuum

A Monte Carlo method, described in Chapter 3, Part I, was used to relate the actual path of migration to the thickness of the absorber, giving a theoretical histrogram comparable to the experimental histogram of energy distributions. Examples of such histograms are given in Figure 1-1. The basic line of reasoning followed in this method of analysis is as follows. The first step was the development of a computational procedure which duplicated the actual experiment as accurately as possible and predicted its result. By comparing the theoretical predictions with the experimental data one can optimize the values of the unknown parameters (which are used in the calculations) to produce the closest fits between experiment and theory.

Thus the basic principle of this method of extracting data from experiment is that of adjusting parameters in a computation which, under optimum conditions, would predict the outcome of an experiment. The general form of an energy distribution of protons (proton current density in the sense of transport theory), that have slowed down by multiple atomic interactions in traversing a scattering sample, is a gaussian-type curve. One obvious possibility for a criterion for goodness-of-fit between two such distributions, would be to establish the average distance between corresponding points on the two curves in a distance-squared metric (the least squares method). This would certainly be a good method if the experimental conditions were fully predictable by the computation method. This is, however, unfortunately not completely true. To see this compare the real and the theoretical conditions in figures 2 and 3, respectively. It is obvious that the ideal method of analysis would include the detector in the theoretical "reproduction" and actually predict the output of the detector. One would then be justified in optimizing the mutual fit of the two curves. At the present stage of development, this method stops one step short of such an ideal treatment. The assumption is made that the peak of the experimental distribution corresponds on a one-to-one basis to the peak of the energy distribution of protons (current density) averaged over the exit surface of the sample. The facts that the detector-to-sample distance is large and the good resolution properties of the detector back this assumption. The correctness of this assumption is established in a following section. It is readily realized that other criteria for comparing the two distributions, such as those based on the first moment of the distribution(mean energy) will be more strongly dependent upon the finite and asymmetric resolution function of the detector and hence less suitable for this purpose. Previous workers have used comparison criteria based on the mean energy.

Such procedure will, of course, be dependent on the selection of low energy cut-off of the experimental distribution.

Parametrization of Experimental Results

The experiments result in pulse height distributions. These are recorded by a multichannel analyser and are thus in a histogram form. Such a form is not the most suitable one for evaluation of the maximum of the distribution. We therefore convert this histogram into an analytical form.

The following mathematical expression is selected on the basis of the physics of the problem.

$$f(t) = \frac{1}{\sqrt{\pi}} \{e^{-t^2} [1 + \sum_{\nu=1}^{N} a_\nu H_\nu(t)]\} \quad , \tag{1-2}$$

$t = \frac{E - E_a}{\sigma}$

E_a is the average energy (= most probable energy in the gaussian approximation to the solution of the slowing-down equation)

σ = measure of dispersion of the gaussian approximation as above. σ is equal to $\sqrt{2}$ times the standard deviation of that distribution

a_ν are unknown parameters to be determined from the experimental data

$\nu = 1, 2, 3 \ldots N$

In the procedure for evaluating the parameters a_ν we first set E_a to the middle energy of the channel with the largest number of counts. We compute σ from the following approximation formula due to Rossi (1).

$$\sigma^2 = 2r^2 x\rho \tag{1-3}$$

where

x is the thickness of the scatterer (in cms)

ρ = the material density in g/cm^3 , and

$$r^2 = 2Cmc^2 E'_m \left(1 - \frac{\beta^2}{2}\right) \tag{1-4}$$

with

$$2C = 0.30058\ Z/A \quad (\text{in } cm^2/g) \tag{1-5}$$

and

$$E'_m = 2mc^2 \frac{p^2c^2}{m^2c^4 + M^2c^4 + 2mc^2 (p^2c^2 + m^2c^4)^{1/2}} \tag{1-6}$$

where

$$p^2c^2 = E^2 + Mc^2E \tag{1-7}$$

E'_m is the maximum kinetic energy loss (in MeV) suffered by a collision of a proton of energy E (MeV) with an unbound electron at rest.

$H_\nu(t)$ is the Hermite polynomial of order ν:

$$H_\nu(t) = (-1)^\nu e^{-t^2} \frac{\partial^\nu}{\partial t^\nu} (e^{-t^2}) \tag{1-8}$$

$$\int_{-\infty}^{\infty} e^{-t^2} H_\nu(t) H_\mu(t) dt = \delta_{\nu\mu} \sqrt{\pi} 2^\nu r! \ . \tag{1-9}$$

As $H_o(t) \equiv 1$, equation 1-2 will always fulfill the condition

$$\int_{-\infty}^{\infty} f(t)\,dt = 1 \tag{1-10}$$

We intend to fit an expression of the form of equation 1-2 to the experimental histogram by a least-squares criterion applied to solve the parameters a_ν , $\nu = 1, 2, 3 \ldots N$ where the appropriate value of N will be determined on the basis of practical considerations. We introduce our notation in figure 4.
We let F_i denote the number of counts between the energies E_i and E_{i+1} (corresponding to $t_i < t_{i+1}$) and set

$$\sum_{i=1}^{N} F_1 = f \tag{1-11}$$

We have silently assumed that there is a (not necessarily linear) one-to-one relation between channel boundaries and proton energy. This is, of course, the basis of the usefulness of the detector as a spectrometer. This problem will be scrutinized in a later section.
In order to change the range of definition of the function f(t) from an infinite one to a finite one (in t) we set

$$f^*(t) = \frac{K}{F} f(t) \tag{1-12}$$

K being a constant determined by the criterion

$$\int_{t_1}^{t_{n+1}} f^*(t)\,dt = 1 \tag{1-13}$$

K will have the meaning of the total number of counts predicted for the interval $-\infty < E < \infty$ by the fitting function $Ff^*(t)$.
We now set

$$\phi_i = F \int_{t_i}^{t_{i+1}} f^*(t)\,dt = K \int_{t_i}^{t_{i+1}} f(t)\,dt \tag{1-14}$$

By comparing equations 1-13 and 1-14 we see that

$$\sum_{i=1}^{N} \phi_i = F \tag{1-15}$$

Our least-squares expression reads

$$S = \sum_{i} (F_i - \phi_i)^2 \tag{1-16}$$

We want to minimize S to obtain optimum values of the parameters $a_1, a_2 \ldots a_N$. We prefer equation 1-16 to one where the terms in the sum are weighted inversely with some power of the estimated error in F_i. The reason is that we want the fit to be best at the peak of the distribution and do not so much mind deviations in the flanks.
Using equations 1-12, 1-13, and 1-16 we obtain

$$S = \sum_{i=1}^{\sim} \left[F \int_{t_i}^{t_{n+1}} f(t)\,dt - F \int_{t_i}^{t_{i+1}} f(t)\,dt\right]^2 \tag{1-17}$$

The parameters $\{a_\nu\}$ are solved by minimizing the expression S of equation 1-16 utilizing the GAP language for automatized criterion fulfillment (2).

The integrals in equation 1-16 may be written

$$\int_a^b f(t)dt = \frac{1}{\sqrt{\pi}}\left(\frac{\sqrt{\pi}}{2}[\mathrm{erf}(b)-\mathrm{erf}(a)+\sum_{\nu=1}^{N} a_\nu [e^{-a^2}H_{\nu-1}(a) - e^{-b^2}H_{\nu-1}(b)]\right) \qquad (1\text{-}18)$$

Using the properties of Hermite polynomials as given in (3) where the erf functions are also defined.
It is readily seen that the equations minimizing S represent a linear system in the variables $a_1, a_2, \ldots a_N$.
The fit will be exact in the sense that $F_i = \Phi_i$ for all values of i if N = n-1, i.e. the number of parameters is equal to the number of channels minus one. The case N = n-1 may produce computational instabilities and may give fluctuations in the function f(t). Therefore, we apply the condition

$$N \leq n-2 \qquad (1\text{-}19)$$

We have found it practical to use values of N ranging from 4 to 8. In each fitting problem all these values of N are used and the best one is selected on the basis of the criterion that the sum of the terms $(\Phi_i - F_i)^2$ over the five channels nearest to the peak should be as small as possible.
By differentiating equation 1-2, we obtain

$$\frac{df(t)}{dt} = \frac{1}{\sqrt{\pi}}\{-e^{-t^2}[2t + \sum_{\nu=1}^{N} a_\nu H_{\nu+1}(t)]\} \qquad (1\text{-}20)$$

using again the properties of the Hermite polynomials (see refs. (3) and (4)). By setting $df(t)/dt = 0$ we may solve equation 1-20 for the value of t at which the curve has its maximum. In general, the function f(t) may have more than one real extremum. We must therefore check that the root $t = \delta$ that is selected is a meaningful one, and that there is not more than one maximum in the range $t_1 < t < t_{n+1}$. This condition is applied before an optimum value of N is selected on the basis of the criterion cited above. The condition of equation 1-13 is generally sufficient to automatically make the uniqueness condition fulfilled.
In order to make the value of the root $t = \delta$ independent upon the choice of numerical value of the constant E_a we iterate the fitting procedure by exchanging for E_a (in definition of t) the peak energy

$$E_p = E_a + \delta\sigma \qquad (1\text{-}21)$$

so many times until two subsequent values of δ differ by less than 10^{-5}. This iteration technique has as a result that the functions e^{-t^2} and f(t) will have numerically coincident maxima at t = 0 in the last iteration.
As seen from equation 1-20 this implies that, for the converged set of a_ν, the following condition will hold (to within the accuracy dictated by the convergence criterion):

$$\sum_{\nu=1}^{N} a_\nu H_{\nu+1}(0) = 0 \qquad (1\text{-}22)$$

which may be rewritten

$$\sum_{\substack{\nu=1 \\ (\text{odd values of } \nu)}}^{\nu} a_\nu (-1)^{\frac{\nu+1}{2}} \frac{(r+1)!}{\left(\frac{r+1}{2}\right)!} = 0 \qquad (1\text{-}23)$$

The fitting procedure constitutes the subprogram PARA in the ORACLE

code system performing the complete analysis. A sample result is given in Table 1.
The experimental data have been manually cut off at the high and low energies shown. This truncation could also have been done according to some mathematical criterion, e.g. when the counts in two subsequent channels differ by less than the probable error in the number of counts. This problem is, however, not crucial to the accuracy of determination of the position of the peak.

Statistical Error in Experimental Value of Peak Energy

Having established the procedure for obtaining a value of the most probable energy in the measured distribution, the statistical accuracy of this quantity must be determined. It is difficult to calculate the error analytically as the peak energy is a non-linear function of the parameters a_ν. We choose instead to apply the principle of statistical sampling and assume that the number of counts F_i in channel i in the measurements is normally distributed with mean F_i and variance $F_i(1 - F_i/F)$. By applying well-known computer methods for sampling of a normally distributed stochastic variable we may produce a new set of F_i which might have been the outcome of a repeated experiment. We then find the maximum of this experimental analogue. In the parametrization we use the value of N, found to be best for the actual experiment, according to the criterion described above equation 1-20. The resampling process is repeated and the distribution of peak position values is analysed with regard to its dispersion. In our computerized implementation of this idea we resample eight times and compute the mean square deviation. The shape of the distribution of the peak position has been studied and appears to be very near to a normal distribution as indicated by a standard non-normality test. (5).

The Monte Carlo calculation gives rise to histograms of the same type as those obtained experimentally. This treatment is, of course, applicable also to the computed distributions and we proceed in exactly the same way, in fact the Monte Carlo computation is always followed by an analysis of the peak position and of its statistical error.

Test of Overall Consistency

As was pointed out in the beginning, our correlation of the peak of the experimental distribution to the most probable energy in the spectrum of proton current density, leaking across the exit surface of the absorber, is not rigorously justified. We may, however, give a proof of the correctness of this assumption in the case of aluminum where the physical data that govern the proton transport are known.
Let us call the parametrized form of the energy distribution measured by the detector with no absorber $f_0(t)$ with $t = \frac{E-E_0}{\sigma_0}$,
E_0 being known through calibration and $\sigma_0 = \sqrt{2}\,\Delta$, where Δ^2 is the mean square deviation of the experimental distribution. We may assume that the shape of $f_0(t)$ remains unchanged for values of E_0 varying slightly around its actual value. Let us now set the parametrized

version of the theoretical (Monte Carlo calculated) energy distribution, for a certain thickness of aluminum, equal to

$$g(t_1),\ t_1 = \frac{E' - E_{MC}}{\sigma} \ .$$

The folding integral

$$g^*(E) = \int_{auE'} g\left(\frac{E' - E_{MC}}{\sigma}\right) f_o\left(\frac{E-E'}{\sigma_o}\right) dE' \qquad (1\text{-}24)$$

thus represents the theoretical spectrum smeared by the response function of the detecting system. If our basic assumptions are correct, the function $g^*(E)$ should have its maximum at the same place as the function $f(E)$ representing the parametrized version of the measured spectrum for the same aluminum absorber thickness. Agreement in this case is, of course, to be considered in relation to statistical accuracies.
We now go on to look for a mathematical formulation of this consistency test.
Set

$$g(E') = g(t_1) = \frac{1}{\sqrt{\pi}} \left[e^{-t_1^2} \left(1 + \sum_{\nu=1}^{N_1} b_\nu H_\nu(t) \right) \right] \qquad (1\text{-}25)$$

with $t_1 = \dfrac{E' - E_{MC}}{\sigma}$ and

$$f_o(E-E') = f_o(t_2) = \frac{1}{\sqrt{\pi}} \left[e^{-t_2^2} \left(1 + \sum_{\mu=1}^{N_2} c_\mu H_\mu(t_2) \right) \right] \qquad (1\text{-}26)$$

with $t_2 = \dfrac{E-E'}{\sigma_o}$

Insertion of equations 1-25 and 1-26 into equation 1-24 gives

$$g^*(E) = \int \frac{1}{\sqrt{\pi}\sigma} e^{-t_1^2} \left[1 + \sum_{\nu=1}^{N_1} b_\nu H_\nu(t_1) \right] \frac{1}{\sqrt{\pi}\sigma_o} e^{-t_2^2} \left[1 + \sum_{\mu=1}^{N_2} c_\mu H_\mu(t_2) \right] dE' \qquad (1\text{-}27)$$

Let us now set

$$t_1^2 + t_2^2 = \frac{\left(E - E_{MC}\right)^2}{\sigma_o^2 + \sigma^2} + u^2 \qquad (1\text{-}28$$

giving

$$\frac{\left[E' \left(\frac{\sigma_o}{\sigma} + \frac{\sigma}{\sigma_o}\right) - \left(\frac{\sigma_o}{\sigma} E_{MC} + \frac{\sigma}{\sigma_o} E\right)\right]^2}{\sigma_o^2 + \sigma^2} = u^2 \qquad (1\text{-}29)$$

We insert the variable u into equation 1-27 and obtain

$$g^*(E) = \frac{e^{-\left(\frac{E-E_{MC}}{\sqrt{\sigma^2+\sigma_o^2}}\right)^2}}{\sqrt{\pi}\sqrt{\sigma_o^2+\sigma^2}} \int \frac{1}{\sqrt{\pi}} e^{-u^2} [1+\sum_{\nu=1}^{N_1} b_\nu H_\nu(A_1u+B)][1+\sum_{\mu=1}^{N_2} c_\mu H_\mu(A_2u+B_2)]du \quad (1\text{-}30)$$

where we have defined

$$A_1 = \frac{\sigma_\theta}{\sqrt{\sigma_o^2 + \sigma^2}} \quad (1\text{-}31)$$

$$A_2 = \frac{-\sigma}{\sqrt{\sigma_o^2 + \sigma^2}} \quad (1\text{-}32)$$

$$B_1 = \frac{\sigma(E-E_{MC})}{\sigma_o^2 + \sigma^2} \quad (1\text{-}33)$$

$$B_2 = \frac{\sigma_o(E-E_{MC})}{\sigma_\theta^2 + \sigma^2} \quad (1\text{-}34)$$

We note for future use that $A_1^2 + A_2^2 = 1$ (1-35)

It is convenient to set

$$\frac{E-E_{MC}}{\sqrt{\sigma_o^2 + \sigma^2}} = t \quad (1\text{-}36)$$

We now transcribe equation 1-30

$$\frac{g^*(t)dt}{dt} = \frac{1}{\sqrt{\pi}} e^{-t^2} + \frac{1}{\sqrt{\pi}} e^{-t^2} \int_{-\infty}^{\infty} \frac{1}{\sqrt{\pi}} e^{-u^2} [\sum_{\nu=1}^{N_1} b_\nu H_\nu(A_1u - A_1t)]du +$$

$$\frac{1}{\sqrt{\pi}} e^{-t^2} \int_{-\infty}^{\infty} \frac{1}{\sqrt{\pi}} e^{-u^2} [\sum_{\mu=1}^{N_2} c_\mu H_\mu(A_2u + A_1t)]du +$$

$$\frac{1}{\sqrt{\pi}} e^{-t^2} \int_{-\infty}^{\infty} \frac{1}{\sqrt{\pi}} e^{-u^2} [\sum_{\nu=1}^{N_1} b_\nu H_\nu(A_1u-A_2t)][\sum_{\mu=1}^{N_2} c_\mu H_\mu(A_2u + A_1t)]du \quad (1\text{-}37)$$

The integration range in equation 1-30 has been set equal to $(-\infty, \infty)$. This is justified only if the parametrized distribution functions f_o and g represent meaningful extrapolations outside the range of the histogram on which these distributions are based. In practice the areas under the extrapolated tails of the distributions are found to be

negligible.
This is indicated by the very good agreement, that is always found, between the total number of actual counts F and the extrapolated number of counts K. We now evaluate the derivative of the function $g^*(t)$ at $t = 0$. The hypothesis that we want to test is whether $(\partial g^*/\partial t)_{t=0}$ is equal to zero within the statistical accuracy of the quantities involved. We know that the corresponding experimental distribution $f(t)$ has its maximum at $t = 0$ as a result of the fitting process.
Differentiation of equation 1-37 with respect to t gives at $t = 0$

$$\left[\frac{\partial g^*(t)}{\partial t}\right]_{t=0} = \frac{-A_2}{\sqrt{\pi}} \int_{-\infty}^{\infty} \frac{1}{\sqrt{\pi}} e^{-u^2} \left[\sum_{\nu=1}^{N_1} 2\nu b_\nu H_{\nu-1}(A_1 u)\right] du +$$

$$\frac{A_1}{\sqrt{\pi}} \int_{-\infty}^{\infty} \frac{1}{\sqrt{\pi}} e^{-u^2} \left[\sum_{\mu=1}^{N_2} 2\mu c_\mu H_{\mu-1}(A_2 u)\right] du +$$

$$\frac{A_1}{\sqrt{\pi}} \int_{-\infty}^{\infty} \frac{1}{\sqrt{\pi}} e^{-u^2} \left[\sum_{\nu=1}^{N_1} b_\nu H_\nu (A_1 u)\right] \left[\sum_{\mu=1}^{N_2} 2\mu c_\mu H_{\mu-} (A_2 u)\right] du -$$

$$\frac{A_2}{\sqrt{\pi}} \int_{-\infty}^{\infty} \frac{1}{\sqrt{\pi}} e^{-u^2} \left[\sum_{\nu=1}^{N_1} 2\nu b_\nu H_{\nu-1}(A_1 u)\right] \left[\sum_{\mu=1}^{N_2} c_\mu H_\mu (A_2 u)\right] du \qquad (1\text{-}38)$$

Equation 16.5.22 of (6) may be transformed to read (for even values of m+n)

$$\int_{-\infty}^{\infty} e^{-t^2} H_m\left(\frac{\alpha t}{\sqrt{\alpha^2 + \beta^2}}\right) H_n\left(\frac{\beta t}{\sqrt{\alpha^2 + \beta^2}}\right) dt =$$

$$(-1)^{\frac{m+n}{2}} 2^{m+n} (\alpha^2 + \beta^2)^{-(m+n)} \alpha^n \beta^m \left[\left(\frac{m+n+1}{2}\right)\right] =$$

$$(-1)^m (\alpha^2 + \beta^2)^{-(m+n)} \alpha^n \beta^m \frac{(m+n)!}{\left(\frac{m+n}{2}\right)!} \sqrt{\pi} =$$

$$(-1)^m (\alpha^2 + \beta^2)^{-(m+n)} \alpha^n \beta^m \sqrt{\pi}\, H_{m+n}(0) \qquad (1\text{-}39)$$

We use equation 1-36 to evaluate the integrals in equation 1-38 bearing in mind that $A_1^2 + A_2^2 = 1$.

$$\left(\frac{\partial g^*}{\partial t}\right)_{t=0} = \frac{1}{\sqrt{\pi}} \left[\sum_{\nu=1}^{N_1} b_\nu H_{\nu+1}(0) |A_2|^\nu + \sum_{\mu=1}^{N_2} c_\mu H_{\mu+1}(0) |A_1|^\mu + \right. \tag{1-40}$$

$$\left. \sum_{\nu=1}^{N_1} \sum_{\mu=1}^{N_2} b_\nu c_\mu H_{\mu+\nu+1}(0) |A_1|^\mu \, |A_2|^\nu \right]$$

If we compare equation 1-40 with equation 1-23 we observe that the derivative in equation 1-40 will be zero whenever A_1 or A_2 is equal to either 0 or 1. This corresponds to the limiting cases.

$$\frac{\sigma_o}{\sigma} = \begin{cases} 0 \\ \infty \end{cases}$$

All the parameters b_ν and c_μ are known and equation 1-40 therefore permits direct evaluation of the derivative. Its optimum value, zero, will, of course, not be obtained exactly in the practical case. We therefore establish our consistency test in the following way: Assume that the maxima of the functions $g^*(E)$ and $f(E)$ are displaced by an amount ε and that the shape of $g^*(E)$ can be approximated by a normal distribution in the vicinity of the peak. The approximate shape of $g^*(E)$ is then

$$g^*_{appr.}(E)\, dE = \frac{e^{-\{(E - E_{MC} - \varepsilon)^2/(\sigma_o^2 - \sigma^2)\}}}{\sqrt{\pi}\,\sqrt{\sigma_o^2 + \sigma^2}}\, dE \tag{1-41}$$

or

$$g^*_{appr.}(t)\, dt = \frac{1}{\sqrt{\pi}}\, e^{-(t - \varepsilon/\sqrt{\sigma_o^2 + \sigma^2})^2} \tag{1-42}$$

This means that the sign of ε is chosen so that, for $\varepsilon > o$, $g^*_{appr.}(E)$ has its maximum for $E > E_{MC}$.

We differentiate equation 1-39 at $t = 0$

$$\left.\frac{\partial g^*_{appr.}(t)}{\partial t}\right|_{t=0} = \frac{2\varepsilon}{\sqrt{\pi}\,\sqrt{\sigma_o^2 + \sigma^2}}\, e^{-\{\varepsilon^2/(\sigma_o^2 + \sigma^2)\}} \qquad 2\varepsilon/(\sqrt{\pi}\,\sqrt{\sigma_o^2 + \sigma^2}) \tag{1-43}$$

By identifying the right hand sides of equations 1-41 and 1-43 we solve for the displacement ε.
Let us now relate the deviation ε to the sources of error. We obtain errors in the determination of the most probable energies in the experimental and theoretical (Monte Carlo) distributions, respectively. Let us set the corresponding various errors equal to D^2_{exp} and D^2_{MC}, respectively (D^2_{MC} is always made to be much less than D^2_{exp}). Our consistency criterion should read

$$\varepsilon^2 \ll D^2_{exp} + D^2_{MC} \tag{1-44}$$

In practice this condition has always been very well fulfilled

$$\frac{\varepsilon^2}{D^2_{exp} + D^2_{MC}} \approx 0.01 \tag{1-45}$$

and we therefore consider the assumption discussed at the outset of the present section proven. The calculations described are incorporated in the sub program CONSIS.

REFERENCES:

1. B. Rossi: "High Energy Particles", Prentice Hall (1952).

2. A. Householder: "Principles of Numerical Analysis", McGraw-Hill (1953) ch. 6.

3. Handbook of Mathematical Functions, NBS Appl. Math. Series No. 55 (1964).

4. I.N. Sneddon: "Special Functions of Mathematical Physics and Chemistry". University Mathematic Texts (1961).

5. Biometrika Tables for Statisticians, vol. I. Ed. by E.S. Pearson and H. O. Hartley. Cambridge Univ. Press (1954) 61.

6. Tables of Integral Transforms (Bateman Manuscript Project), vol. II, p. 291. Ed. by A. Erdelyi. McGraw-Hill.

FIGURE 1-1: Monte Carlo Histogram of
99.9 MeV Protons After Transmission
Through Aluminum
E_o: 99.9 MeV

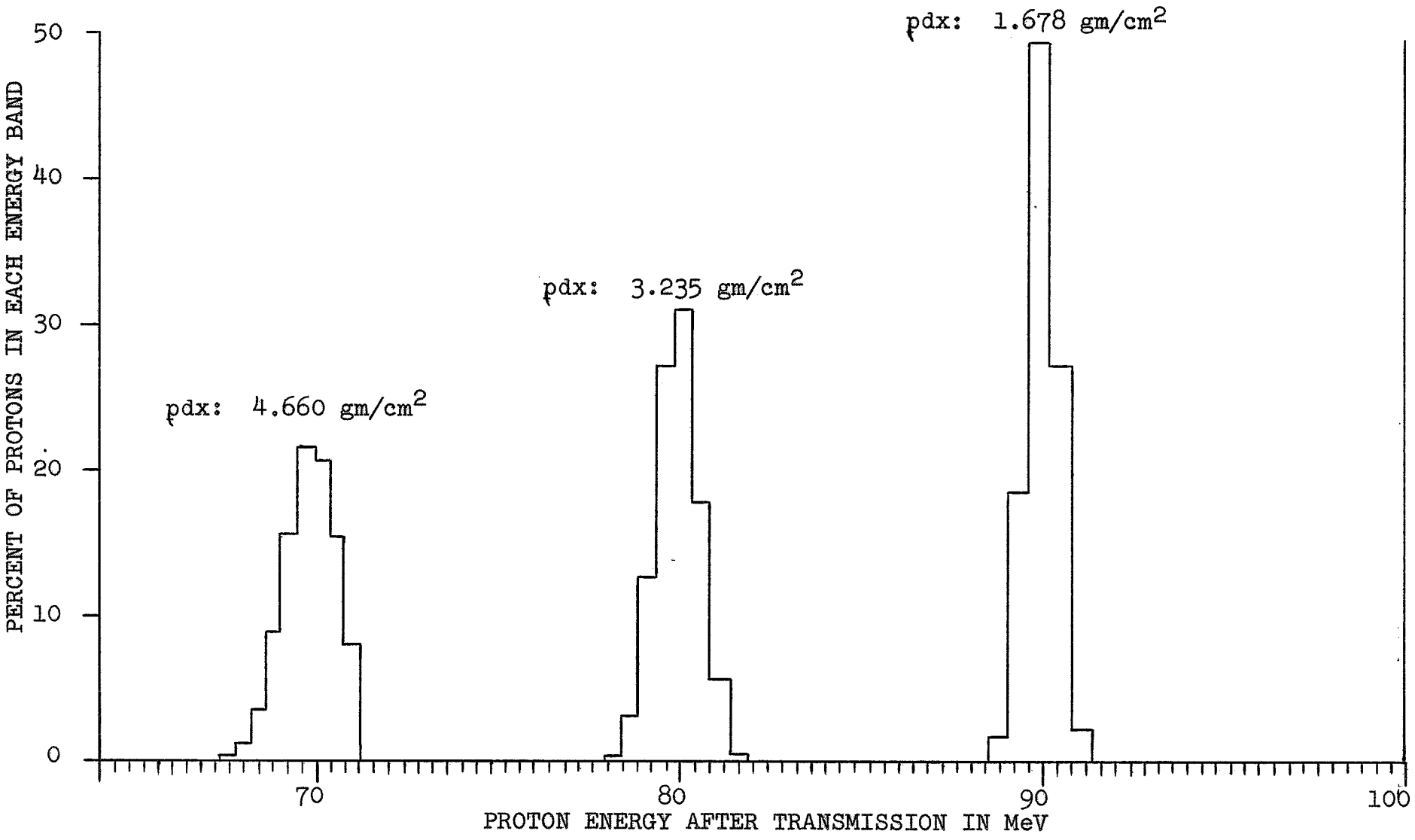

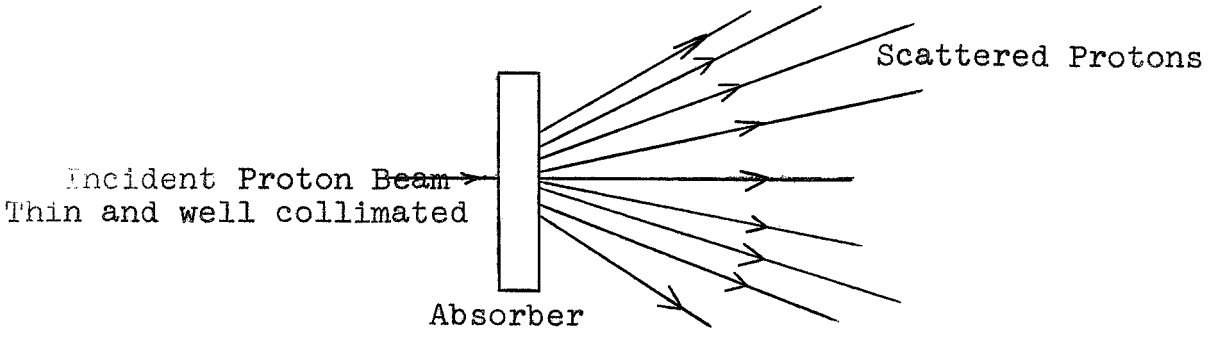

FIGURE 1-2: Calculation Geometry

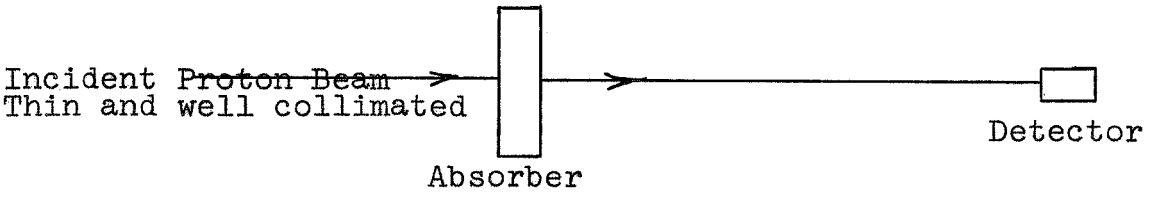

FIGURE 1-3: Experimental Geometry

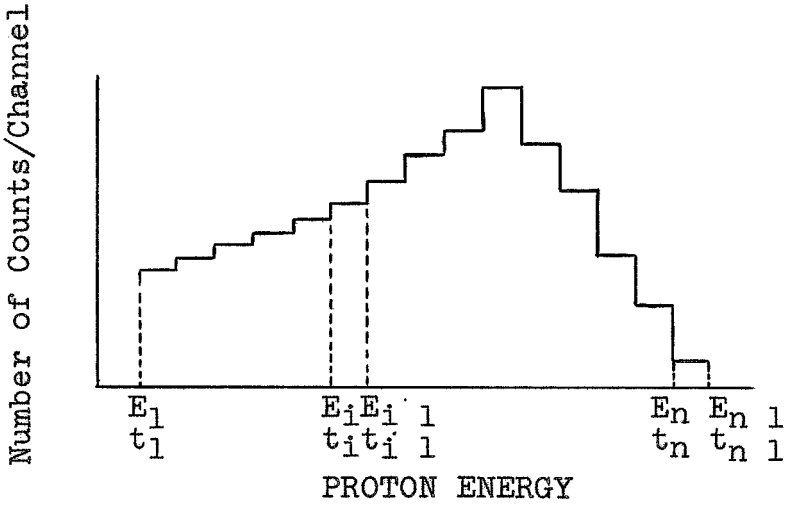

FIGURE 1-4: Representation of Experimental Histogram

AUSTIN 2*49

E=10.61 FOR CHANNEL 231.00 DE=0.00458 MEV/CH

CHANNEL NO.:	227	228	229	230	231	232	233	234	235	236
COUNTS:	2440	3180	4611	7437	11190	10453	5574	1445	138	

MEAN CHANNEL IS 230.7962 TOTAL COUNTS ARE 46468

EP	CHAN
10.653	231.93
10.651	231.89
10.651	231.90
10.652	231.92
10.651	231.89

K	A							
48461	-.27398	.11590	-.045827	.0253				
48143	-.30184	.10268	-.069153	.0234	-.0018512			
48590	-.29382	.12542	-.064615	.0297	-.0015635	.00036014		
47453	-.41639	.07809	-.145620	.0177	-.0136820	-.00029344	-.0004337	
57718	-.10384	.55408	.042399	.1863	.0120710	.01599000	.0004356	.0004144

E(I)	CHAN	EXP	4	5	6	7	8	CHAN	E(I 1)
10.43	227	2440	2192.07	2339.71	2372.33	2411.11	2440	228	10.47
10.47	228	3180	3377.26	3347.13	3314.17	3248.95	3180	229	10.52
10.52	229	4611	4582.78	4469.56	4465.39	4516.92	4611	230	10.56
10.56	230	7437	7465.88	7528.05	7554.86	7539.46	7437	231	10.61
10.61	231	11190	11097.64	11151.22	11122.98	11096.43	11190	232	10.66
10.66	232	10453	10587.89	10473.88	10474.75	10529.31	10453	233	10.70
10.70	233	5574	5543.15	5562.69	5586.70	5522.50	5574	234	10.75
10.75	234	1445	1356.15	1460.94	1423.36	1472.81	1445	235	10.79
10.79	235	138	265.17	134.82	153.45	130.51	138	236	10.84

IS BEST N AND GIVES EP=10.6 AND CHAN=231.93 ERROR IN EP IS .004917

TABLE 1-1: Determination of Experimental Peak. Multichannel Histogram Obtained by Totally Absorbing 10.61 MeV Protons in Silicon Detector.

CHAPTER 2

EVALUATION OF THE MOST PROBABLE ENERGY LOSS SUFFERED BY PROTONS PERPENDICULARLY INCIDENT ON PLANE PARALLEL ABSORBERS.

by Martin Leimdorfer and George W. Crawford

1. Introduction

In experimental determinations of charged particle stopping power, the standard procedure is to measure the average energy loss of a particle when transversing an absorber. The path length is usually designated as the thickness of the absorber, x. In that case one determines the arithmetic value of the energies of the transmitted particles after correcting for the angular deviations of the particle paths.

In many cases, however, the mean value of the measured transmission spectrum is difficult to correlate to the actual mean value of the energy distribution of transmitted particles. This difficulty occurs when the detector response distorts the real distribution and an unfolding procedure is likely to introduce large errors in the results (e.g. due to excessive escape from the detector; see Part I, Ch. 6). In most cases it may, however, be possible to use the peak value of the experimental distribution instead of the mean value since the peak is more likely to be essentially undistorted by the detector properties. A discussion of the latter phenomenon is given in Ch. 1. The purpose of the present report is to show that the value of the most probable energy loss in the experimental case is useable as the mean energy loss calculated from Monte Carlo proton transport code PROTOS III.

The average energy loss that should be the ultimate quantity to be derived from an experiment is understood to be that average energy which a charged particle loses when traveling a given path length. Since particles, penetrating through a plane parallel absorber foil have undergone coulomb interactions with the atoms of the absorber material, the actual path length is not a unique quantity in the experimental configuration for there is a distribution of path lengths, with an average value slightly larger than the foil thickness. Let us denote the desired average value of the straight-path energy loss $E_o - E_a$ where E_o is the energy of the incident particles. The mean value of the variable-path energy loss is $E_o - E_m$. Since the particles have, on the average, traveled further in the latter case than in the former, the quantity $E_a - E_m$ should be positive. In section 2 we shall derive an expression for obtaining values of the corrective quantity $E_a - E_m$. Using the results of $E_a - E_m$ we may then calculate $E_a - E_p$, where E_p is the peak energy determined by the procedure described in the preceding chapter.

The theoratical values obtained by the methods outlines in the sections 2 and 3 represent the perturbations of the average exit energy E_a due to angular deflection of the particle paths. In addition, the actual lengths of the paths have a statistical distribution, straggling, which also influence the values of E_m and E_p. It is possible, but difficult, to carry out the calculations of sections 2 and 3 with the straggling effect included. Since we have access to Monte Carlo calculated values of the quantities in question we may still study the effect of straggling, using the full theoretical treatment. (See Part I, Ch. 3).

In the derivation of the methods of calculation discussed above, we have tacitly assumed that the continuous slowing down, multiple scattering approximation of the particle transport equation is applicable. This is almost always done in related literature. The condition for validity of this approximation is that the mass of the migrating particle be large as compared to that of the electron. In our case, the mass of the proton was about 2000 times larger than that of the electron. In the degree of accuracy with which the present study is being conducted, we shall have to make appropriate corrections for departures from the picture. These efforts will be covered in section 5.

2. Analytical evaluation of $E_a - E_m$ neglecting path-length straggling.

Assume that particles of energy E_o are incident perpendicularly onto a slab of thickness z and infinite extension. The distance S traveled by a particle Before transmission is

$$S = \int_o^S dS' \qquad \text{and} \tag{2-1}$$

$$Z = \int_o^S dS' \cos\theta \tag{2-2}$$

dS' being an element of pathlength at S' where the polar angle of direction of the path is equal to θ.

E_m is equal to the mean energy of the particles that have traveled all possible wavelengths S. We may write

$$E_m - E_a = \langle (S-z)\, dE/dS \rangle \tag{2-3}$$

where dE/dS is the stopping power at the exit energy. The symbol $\langle\ \rangle$ is used to denote mean value. Since dE/dS is essentially constant over the range of possible energies, we may set

$$E_m - E_a \doteq (S-Z)dE/dS \tag{2-4}$$

$$= \langle \int_o^S (1-\cos\theta)\, dS' \rangle dE/dS \tag{2-5}$$

Since θ is generally a small angle,

$$E_m - E_a = (dE/dS) \int_o^S \langle \tfrac{1}{2}\theta^2 \rangle dS' \tag{2-6}$$

The angle θ has a Gaussian-like distribution with a width that increases with S'. If we assume that the distribution is normal, we get

$$E_m - E_a = \tfrac{1}{2}(dE/dS) \int_o^S \langle \theta^2 \rangle\, dS' \tag{2-7}$$

We have applied Moliere theory (4,5) to a calculation of $\langle \theta^2 \rangle$. Analytically evaluated values of $E_m - E_a$ are printed out by the PROTOS Monte Carlo program as an auxiliary information. The details covering the calculation of $E_a - E_m$ are given in section 6.

3. Analytical evaluation of $E_a - E_p$, neglecting straggling

We shall now address ourselves to the problem of calculating the value of the most probable energy loss of the penetrating particles in the configuration described in the preceding section. Yang (6) has developed a theory which applies to the present problem under the assumption that the energy of the particle remains unchanged (during the path). Since we shall concentrate on rather thin absorbers this assumption is acceptable. Defining the variable

$$v = 2\frac{s-z}{\langle s-z\rangle} \tag{2-8}$$

Yang obtains a distribution for v

$$Y(v) = \begin{cases} 2\sqrt{\pi}\; v^{-3/2}\left[e^{-1/v} - 3e^{-9/v}\right] & v \leq 2 \\ \frac{\pi}{4}\; e^{-\pi^2 v/16} & v > 2 \end{cases} \tag{2-9}$$

The maximum of the function Y(v) appears at $v_{max} = \frac{2}{3}$ (to within 0.02 percent)

Consequently,

$$\frac{1}{3} = \frac{v_{max}}{2} = \frac{(s-z)_{max}}{\langle s-z\rangle} = \frac{E_a - E_p}{E_a - E_m} \tag{2-10}$$

which is a universal result, rigorously applicable to thin absorbers and under the other assumptions given.

4. Effect of straggling on the quantity $E_a - E_m$

In order to be able to study the effect of including straggling in the calculation of $E_a - E_m$ we have compared an analytical evaluation of this quantity (without straggling) and a stochiastic evaluation (with straggling). For the sake of consistancy both calculations are based on the same energy grid arrangement. Fig. 1 shows the result of the comparison for a case of 99.99 Mev protons incident on aluminum absorbers, of varying thickness. We notice that the result with straggling are somewhat higher than those without straggling. Since we are using the Monte Carlo Calculated value of $E_a - E_m$ in the formula

$$\frac{E_a - E_p}{E_a - E_m} = \frac{1}{3} \tag{2-11}$$

this affect does not disturb the present study.

5. Corrections to the continium model, using the Vavilov theory

In the preceding derivations we have assumed, throughout, that the energy-loss process is a continuous one. In reality, the protons interact with only one or a few electrons at each individual collision process. The energy calculation is influenced to some degree by this approximation. In the continuous model, the particles that have traveled a certain (curved) pathlength have an energy distribution which is a Gaussian function due to the validity

of the central limit theorem to this theoretical process. In the exact theory, however, this energy distribution is not symmetrical and also has its average displaced by a small corrective energy as compared to recorresponding curve of the continuous model. Since our calculations are intended to be very accurate in their evaluations of the peak energy we shall attempt to take into account this non-continuous perturbation. We have used the Vavilov theory(7)(8) to calculate the required correction to E_p. It turns out that the corrective quantity is positive and independent of the absorber material, since it relates only to the proton-electron interaction. We have evaluated the correction $(E_{p'} - E_p)$ on the approximation that the proton energy is essentially constant. The results are in Figures 2-5 for proton energies of 50, 100, 200, and 300 Mev, respectively. The correction converges asymptotically to a fixed value at each energy as the absorber thickness increases. The asymptotic value can be shown to be well approximated by the formula

$$E_{p'} - E_p = E_o \frac{m_e}{m_e + m_p} \tag{2-12}$$

where m_e and m_p are the relativistic masses of the electron and proton, respectively. The right hand side of the equation represents the mean energy loss in the first proton-electron interaction.

In order to perform the calculations on which the Figures 2-5 are based we used the values of the Vavilov distribution, given by Seltzer and Berger (7) performed an interpolation to search for the maximum values of the difference between the maximum and the average energy loss.

6. Calculation of $E_a - E_m$ (neglecting statistical fluctuations in the stopping power)

Definitions:

E_a = mean energy of particles that have traveled a distance x (given by the the relation $x = \int_{E_o}^{E_a} \left|\frac{dE}{dx}\right|^{-1} dE$, where E_o is the source energy and $\frac{dE}{dx}$ the stopping power.) (2-13)

E_m = mean energy of particles, escaping from a slab of thickness x, after having entered at right angles to the slab surface.

$\langle\theta^2\rangle_{s'}$ = mean square of angle of the trajectory with regard to angle of incidence, measured at the pathlength s' from the point of incidence.

Following the reasoning of Fano (9), we may write

$$E_a - E_m = \tfrac{1}{2} \left|\frac{dE}{dx}\right|_{E_a} \cdot \int_o^x \langle\theta^2\rangle_{s'} \, ds' \tag{2-14}$$

in the small-angle approximation. Substituting x for s in the upper limit of the integral creates a negligible error as long as s and x are nearly equal. The numerical computation of $\langle\theta^2\rangle_{s'}$ is very complicated.

Numerical procedure: The variable SPR is defined by

$$(SPR)^2 = \frac{1}{6(s_1-s_2)} \int_{s_2}^{s_1} \langle \theta^2 \rangle_{s'} \, ds' \qquad (2\text{-}15)$$

integrated over an interval in s', s_1 obtained by adding all entries under DS from the top through the line at which the value of SPR is read off, and s_2 by adding values of DS only to the next higher position. We may then write

$$E_a - E_m = A \sum_k [(SPR)_k^2 \cdot (DS)_k] \left(\frac{dE}{dx}\right)_{E_k} \qquad (2\text{-}16)$$

The constant, A, is evaluated by comparison with values of $E_a - E_m$ obtained by Monte Carlo calculations. In these calculations, the resulting energy distributions are given in histogram form. The values of E_m are computed as the first moment of the distribution with each partial area being represented by the point in the middle between the energy limits of the interval. Representative values are given in Table 2-1. From these results, the constant A is found to be equal to 120 (A=120).

Thus the value of $E_a - E_m$ may be obtained from a Monte Carlo calculation or can be calculated from equation 2-16. The nearly symmetrical distribution of energies about the mean value for the Monte Carlo calculations produces a value for the peak energy almost that of the mean energy. Thus from the standpoint of the Monte Carlo calculations, when one has determined the value for E_m, the value for E_p has also been determined. Linear interpolation can be used to produce results for other values of ρdx.

Aluminum ρdx (gm/cm^2)	$E_o - E_a$	$E_o - E_m$	$E_a - E_m$
	(in MeV, ± 0.003)		
	E_o = 185.6 MeV		
1.6848	6.327	6.344	0.017
3.2346	12.279	12.297	0.018
4.6602	17.874	17.894	0.020
5.9259	22.961	22.984	0.023
	E_o = 159.8 MeV		
1.6848	7.010	7.024	0.014
3.2346	13.654	13.672	0.018
4.6602	19.968	19.993	0.025
5.9259	25.726	25.756	0.030
	E_o = 99.9 MeV		
1.6848	9.974	9.982	0.008
3.2346	19.935	19.949	0.014
4.6602	30.002	30.025	0.023
5.9259	39.962	39.994	0.032
	E_o = 36.2 MeV		
0.1350	1.704	1.710	0.006
0.2700	3.477	3.486	0.009
0.4055	5.329	5.342	0.013
0.5400	7.273	7.288	0.015

Table 2-1: Comparison of Linear Energy Loss, $E_o - E_a$, with Variable-Path Energy Loss, $E_o - E_m$.

References:

1. M. Leimdorfer; in M. Leimdorfer and G. Crawford (ed.) Penetration and Interaction of Protons with Matter, Part I. Theoretical Studies Using Monte Carlo Techniques Chapter 6 (1968).
2. M. Leimdorfer: et al, in G. Crawford (ed.) Penetration and Interaction of Protons with Matter, Part II. Experimental Studies, Chapter 1 (1968).
3. C. Johansson and M. Leimdorfer: in M. Leimdorfer and G. Crawford (ed.) Penetration and Interaction of Protons with Matter, Part I. Theoretical Studies Using Monte Carlo Techniques Chapter 3 (1968).
4. G. Moliere: Z. Naturforsch. 3a (1948) 78.
5. H. A. Bethe: Handbuch der Physik. 24.1 (1933) 518.
6. C. N. Yang: Phys. Rev. 84 599 (1951).
7. S. Seltzer and M. Berger: in U. Fano (ed.) Studies In Penetration of Charged Particles in Matter, Nuclear Science Report No. 39, Chapter 9, (1964) 187.
8. P. V. Vavilov: Zh. Exper. Teor. Fiz. 32, 320 (1957). Transl. JEPT. 5, 749 (1957).
9. U. Fano: in U. Fano (ed.) Studies in Penetration of Charged Particles in Matter, Nuclear Science Report No. 39, Appendix A (1964) 46.

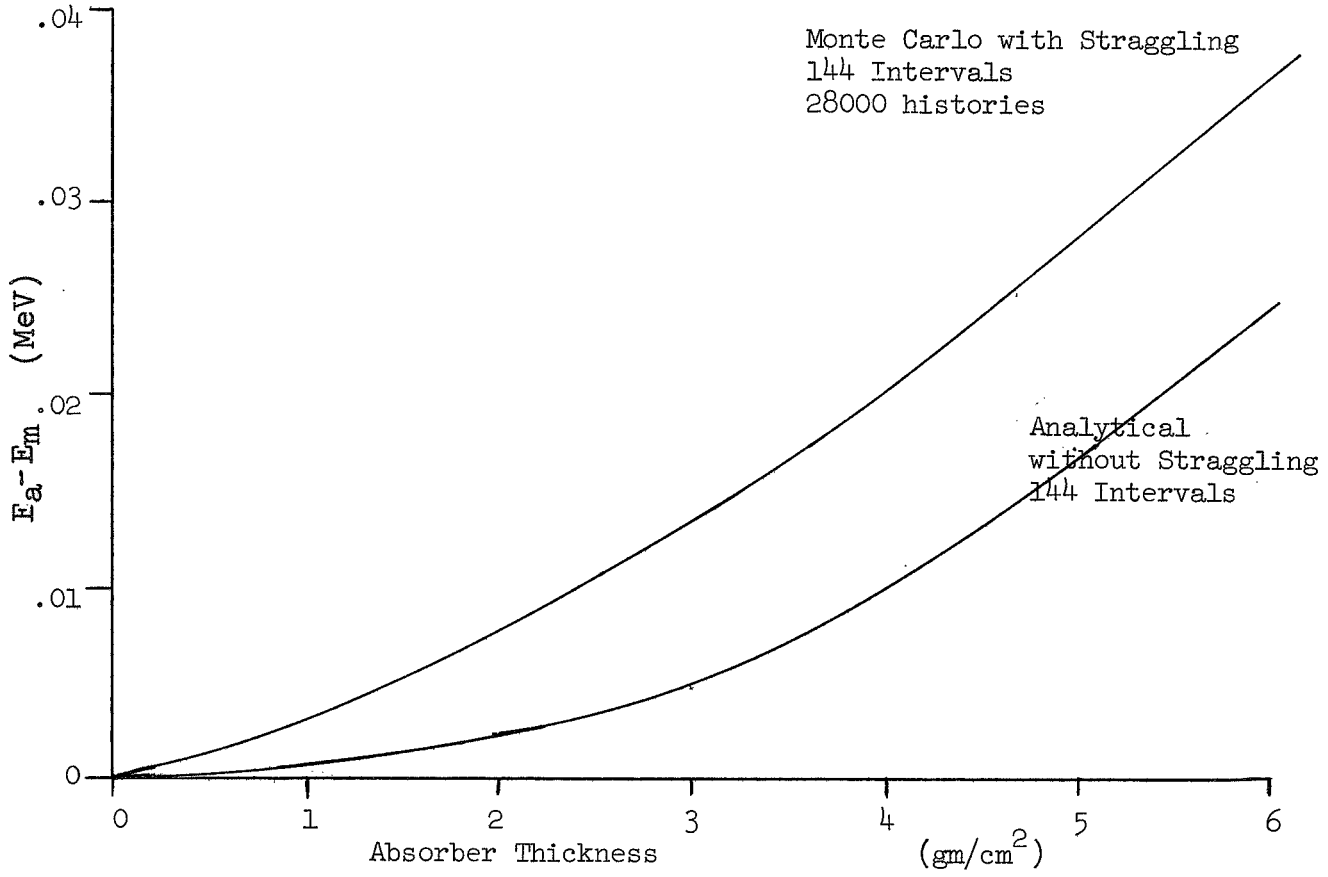

Figure 2-1: $E_a - E_m$ vs. Absorber Thickness of Aluminum. E_o = 99.9 MeV.

Figure 2-2: Energy Correction Based on Vavilov Distribution for $E_o = 50$ MeV

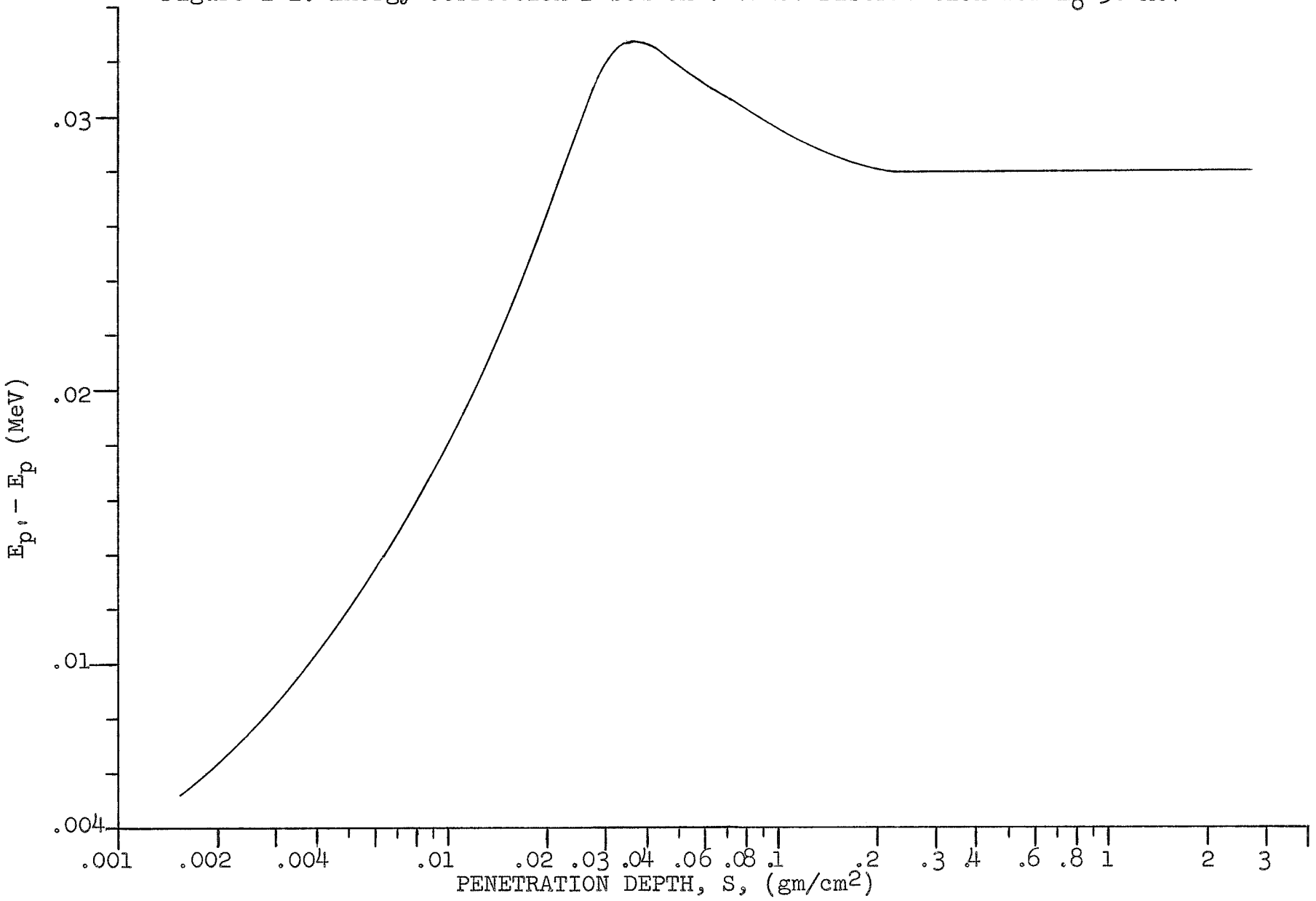

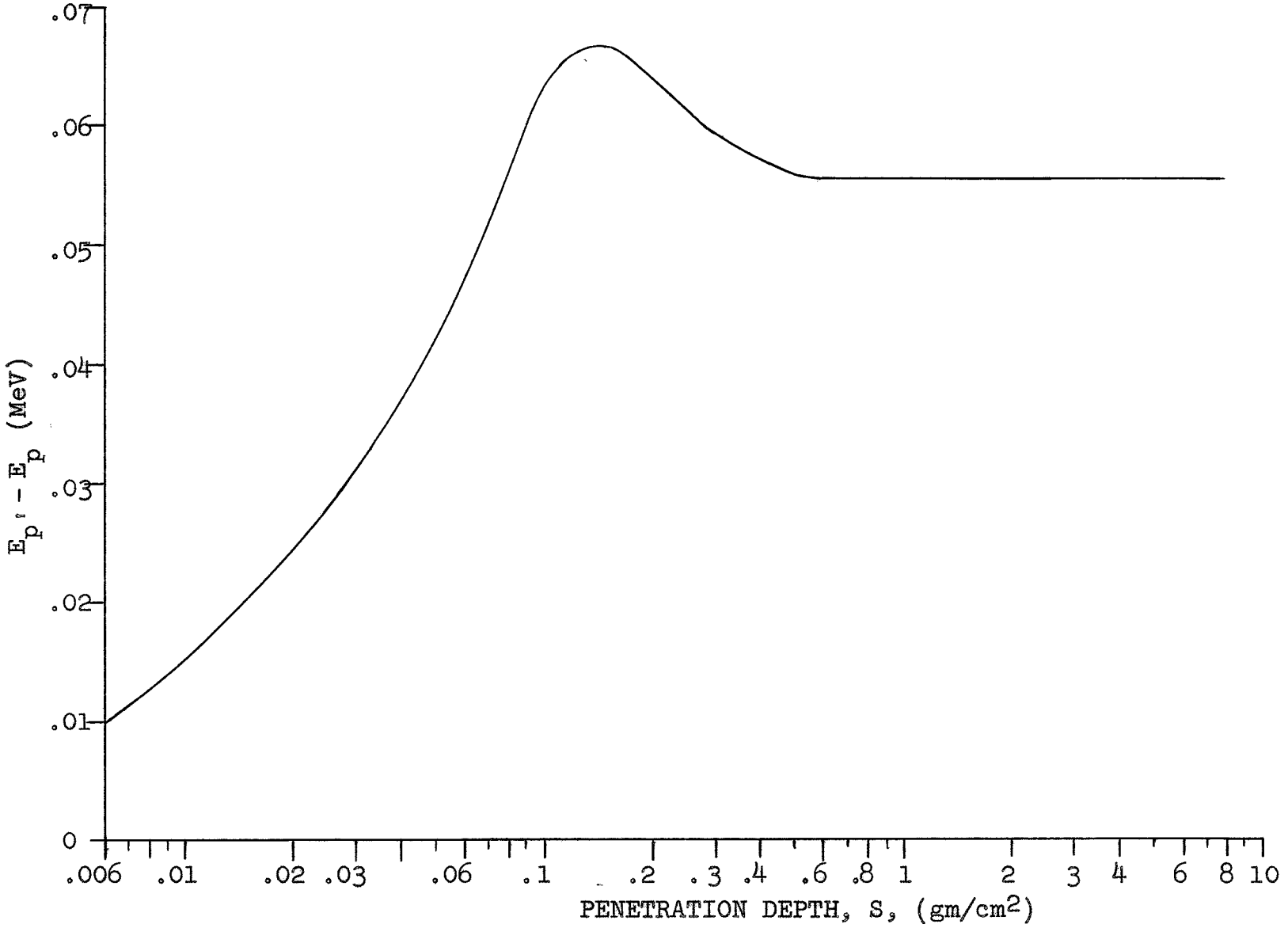

Figure 2-3: Energy Correction Based on Vavilov Distribution for E_o = 100 MeV

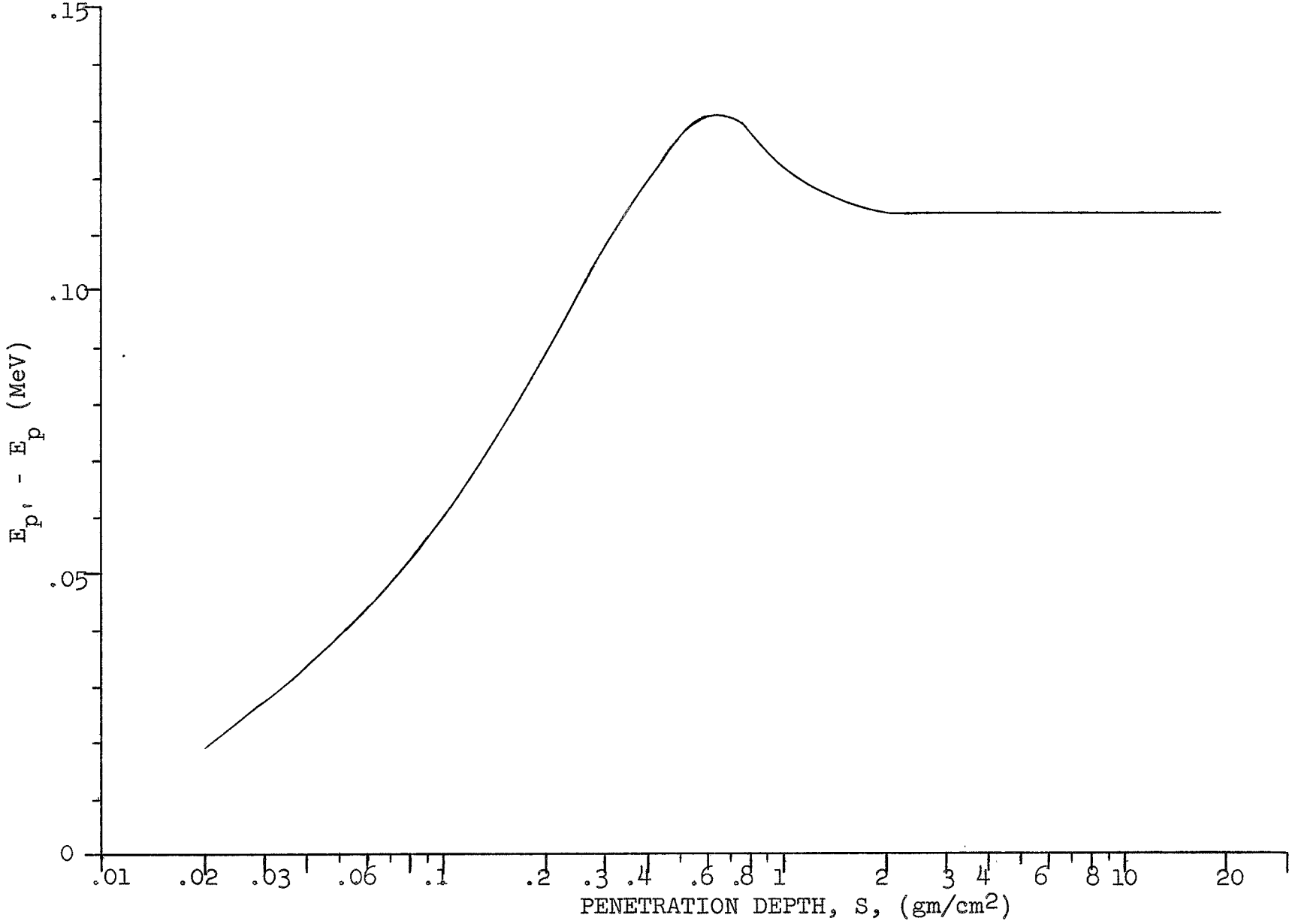

Figure 2-4: Energy Correction Based on Vavilov Distribution for E_o = 200 MeV

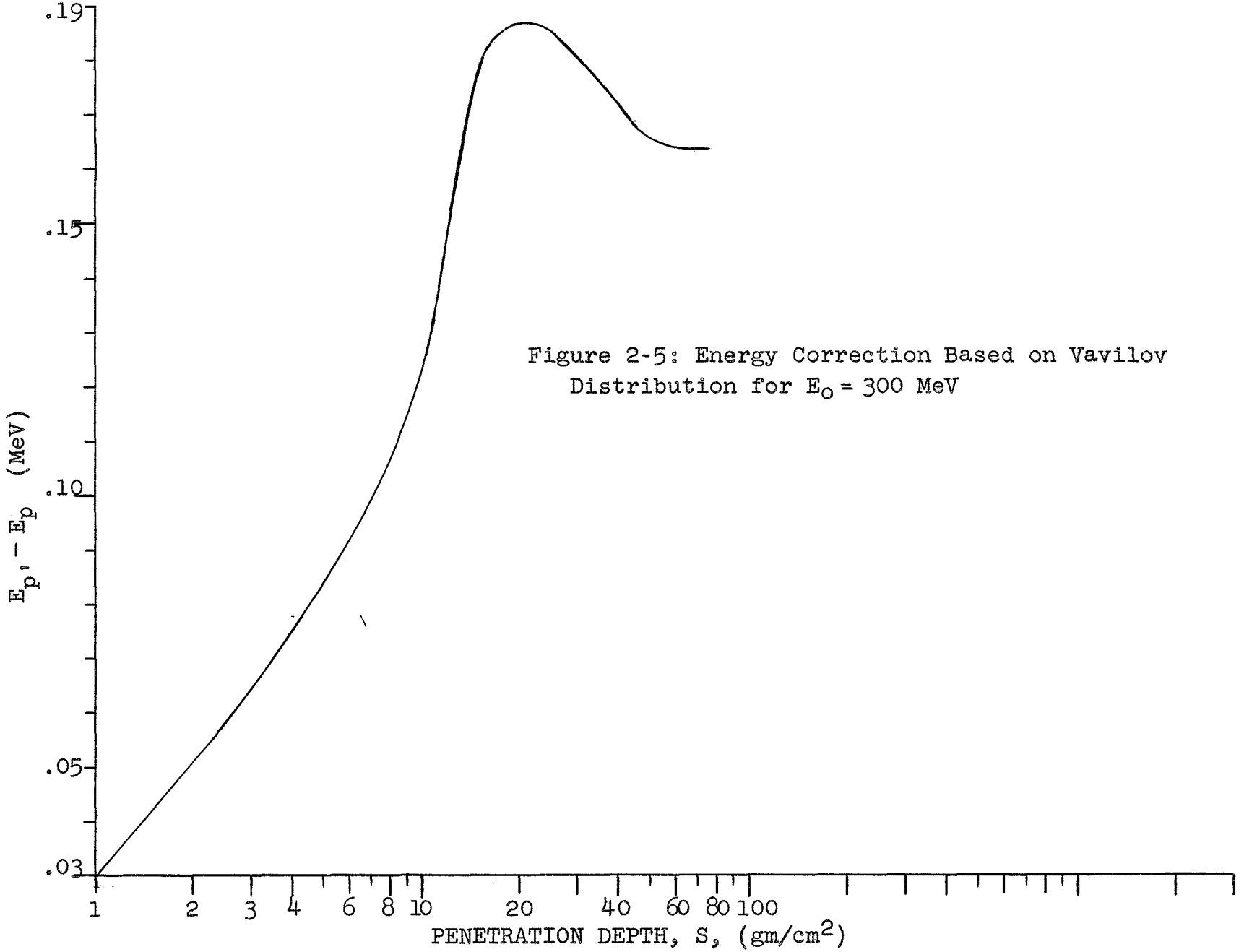

Figure 2-5: Energy Correction Based on Vavilov Distribution for $E_o = 300$ MeV

CHAPTER 3

CALIBRATION OF PULSEHEIGHT DISTRIBUTION IN TERMS OF PROTON ENERGY

by Arne Bergstrom, Martin Leimdorfer,
Elton K. Helwig and George W. Crawford

The problems to be discussed in the present section are those of establishing the conversion formula from pulseheight (voltage) to proton energy and of assessing the accelerator beam energy and its effective dispersion. In the present version of our procedure we assume the stopping power as a function of energy for aluminum to be known. This means that the calibration will be performed relative to an aluminum standard. The basic data is a set of pulseheight distributions from measurements with different aluminum absorbers of varying thickness and the pulseheight distribution taken with no absorber in the beam. The first step is to calculate the peak position of each histogram, following the procedure in Chapter I. The energies E_i will be exchanged for pulseheights in terms of channel number. The dispersion (previously calculated on the basis of physical data) is now replaced by the measure of the width of the distribution in terms of pulseheight. $\sigma^2 = 2\Delta^2$, where Δ^2 is the mean square deviation of the experimental distribution from the middle of the peak channel. All pulseheights in a single channel are assumed to lie in the middle of the channel. By way of definition we only include in Δ^2 the largest part of the distribution which is symmetrical in terms of distance from the peak but contains counts in all channels. The factor of 2 is based on the Chapter I definition of σ.

As a result we can associate to each aluminum absorber j, of thickness x_j, a peak pulseheight V_j with statistical error Δ_j. We define $j = 0$ to be the case with no absorber and x_1, $x_2 \ldots x_2$ to be thicknesses of increasing magnitude. Let us set the unknown source energy equal to E_o and the likewise unknown peak energies for the n absorbers equal to E_{p1}, $E_{p2} \ldots\ldots E_{pn}$. These energies should cover the entire range over which the calibration is desired. From the assumed knowledge of the proton stopping power of aluminum, a set of functions S are defined in the following way.

$$
\begin{aligned}
E_o - E_{p1} &= S(E_o, x_1) \\
E_o - E_{p2} &= S(E_o, x_2) \\
&\quad \vdots \\
E_o - E_{pn} &= S(E_o, x_n)
\end{aligned}
\qquad \text{n equations} \qquad (3\text{-}1)
$$

where the S functions represent the most probable energy losses suffered by protons of initial energy E_o while traversing aluminum absorbers of thicknesses x_j.

Mathematical expressions for the S functions are obtained in the following manner. A series of Monte Carlo calculations are made involving different source energies covering the range of interest. The PROTOS program gives transmission spectra for many different thicknesses in one run so all thicknesses x_j can be calculated on the same run. An analytical function (polynomial) is then fitted to the values of $E_{pj} - E_o$ versus E_o obtained for each x_j via the peak analysis program PARA. This is done by a least-squares procedure using weights equal to the inverse of the statistical error ΔE_{pj} also produced by the PARA program. The statistical errors of the Monte Carlo results are made sufficiently small (by analysing a sufficient number of histories) to be unnoticeable as compared to other errors in the calibration procedure.

Next a functional form of the calibration function is defined $E = B_o + B_1V + B_2V^2 + \ldots\ldots + B_mV^m$, which relates pulseheight, in terms of channel widths, to proton energy via the parameters $B_o \ldots B_1$ obtained in the calibration procedure. In the case of ideal linearity B_1 will be the proton energy decrement (MeV) per channel as, in that case $B_2 = B_3 = \ldots\ldots B_1 = 0$. (3-2)

We insert the connected quantities E_{pj}, V_j into equation 3-2 and obtain the n equations (corresponding to n absorbers)

$$\begin{aligned}
E_{p1} &= B_o+B_1V_1+B_2V_1^2+\ldots\ldots+B_mV_1^m \\
E_{p2} &= B_o+B_1V_2+B_2V_2^2+\ldots\ldots+B_mV_2^m \\
&\quad\vdots \\
E_{pn} &= B_o+B_1V_n+B_2V_n^2+\ldots\ldots+B_mV_n^m
\end{aligned} \qquad \text{n equations} \qquad (3\text{-}3)$$

In analogy, the equation for the source energy becomes

$$E_o=B_o+B_1V_o+B_2V_o^2+\ldots\ldots+B_mV_o^m \qquad (3\text{-}4)$$

By subtracting each of the n equations 3-3 in turn from the equation 3-4 a new set of equations is obtained.

$$\begin{aligned}
E_o-E_{p1} &= B_1(V_o-V_1)+B_2(V_o^2-V_1^2)+\ldots\ldots+B_m(V_o^m-V_1^m) \\
E_o-E_{p2} &= B_1(V_o-V_2)+B_2(V_o^2-V_2^2)+\ldots\ldots+B_m(V_o^m-V_2^m) \\
&\quad\vdots \\
E_o-E_{pn} &= B_1(V_o-V_n)+B_2(V_o^2-V_n^2)+\ldots\ldots+B_m(V_o^m-V_n^m) \\
E_o &= B_o+B_1V_o+B_2V_o^2+\ldots\ldots+B_mV_o^m
\end{aligned} \qquad (3\text{-}5)$$

The left hand sides of the first n of the equations 3-5 are identical to those of equations 3-1 which are equal to the polynomial expansions $S(E_o,x_1) \ldots S(E_o,x_n)$. By inserting these we get a system of n+1 equations for sloving the variables E_o, B_o, B_1, $B_2 \ldots B_m$.

$$S(E_o,\ x_1)=B_1(V_o-V_1)+B_2(V_o^2-V_1^2)+.....+B_m(V_o^m-V_1^m)$$
$$S(E_o,\ x_2)=B_1(V_o-V_2)+B_2(V_o^2-V_2^2)+....+B_m(V_o^m-V_2^m)$$
$$\vdots$$
$$S(E_o,\ x_n)=B_1(V_o-V_n)+{}_2(V_o^2-V_n^2)+.....+B_m(V_o^m-V_n^m) \qquad (3\text{-}6)$$
$$E_o=B_o+B_1V_o+B_2V_o^2+.....+B_nV_o^m$$

This system of equations may be written in matrix form as

$$S(E_o) = V\ B \qquad (3\text{-}7)$$

For the determination of the m+1 coefficients $B = (B_o,\ B_1....B_m)$ from these n+1 equations we want to give all equations equal weight, i.e. we divide them with the experimental standard deviations for the right membrum. (We assume that the polynomial expansions give the S functions in the left membrum with negligible truncation errors.) Since the source measurement V_o is much more accurate than the absorber measurements and $V_o - V_i \ll V_o$ the error in the right membrum will be

$$\Delta(\Sigma_j B_j(V_o^j - V_i^j)) \simeq \Delta V_i \Sigma_j B_j V_i^{j-1} \simeq \text{const. } \Delta V_i \qquad (3\text{-}8)$$

The normalized equations will then read

$$S'(E_o) = V'\ B \qquad (3\text{-}9)$$

where the primes designate that all elements are divided by ΔV_i.

We now have n+1 equations of equal weight from which we want to determine the m+2 unknown parameters B_o, $B_1.....B_m$ and E_o, where $B_o, B_1, ...B_m$ occur linearily and E_o non-linearily as a power series $a_o+a_1E_o+a_2E_o^2+....$ For this problem we shall now give an algorithm which is a generalization of the least-squares method for the determination of linearily occuring parameters to an algorithm where we may determine also a non-linearily occuring parameter from a power series expansion of arbitrary order in the parameter.

To visualize the working of the algorithm we shall, using the model of ref. (1), represent a function f(x) by a point in an (n+1)-dimensional function space where a coordinate i may be defined as the value $f(x_i)$ of the function at x_i, i=0, 1, ...n, and with a metric defined by the distance measure between two functions f(x) and g(x)

$$d = \{\Sigma(f(x_i) - g(x_i))^2\}^{\frac{1}{2}} \qquad (3\text{-}10)$$

In this picture the functions $f(x) = S(E_o,\ x)$ will be represented

as a curve $L(E_o)$ and the function

$$g(x) = \begin{cases} \sum_{j=0}^{m} B_j (V^j(x) - V_o^j)/\Delta V(x) & x \neq 0 \\ \sum_{j=0}^{m} B_j V_o^j/\Delta V_o & x = 0 \end{cases} \qquad (3\text{-}11)$$

as a hyperplane H $(B_o, B_1, \ldots . B_m)$ of order m+1. The problem now consists of finding the points on $H(E_o)$ and $H(B)$ between which the length of the normal in the sense of the above metric is minimized. One approach to solving this problem would be a linearization, as described in (3), of the non-linear parameter dependence in $S(E_o, x)$ by a Taylor expansion in $(E_o - E_{oo})$ around a guessed value E_{oo} and neglecting terms of second order or more. As is pointed out in ref. (2) this is a rather hazardous method if the function is not very simple since there may be several minima. A scanning, as described in (2), in the non-linear parameter and simultaneous solution for the linear parameters using the normal equations may then be the only safe, although very tedious, way to solve the problem. In our present problem, however, we can find a more general and much faster algorithm by using one of the assumptions made in formulating the problem, namely, that the term of order m+1 in eq. 1-21 may be neglected. By including that term in our system of equations we instead get a hyperplane H^* $(B_o, B_1, \ldots . B_{m+2})$ of order m+2 corresponding to the function

$$g(x) = \begin{cases} \sum_{j=0}^{m+1} B_j (V^j(x) - V_o^j)/\Delta V(x) & x \neq 0 \\ \sum_{j=0}^{m+1} B_j V_o^j/\Delta V_o & x = 0 \end{cases} \qquad (3\text{-}12)$$

The new dimension in the hyperplane can be regarded as orthogonal to the normal that we are looking for, since we have assumed that the additional term in the calibration expansion was neglible and thus would not reduce the length of the normal. We may now solve the normal equations

$$V^* S = V^* V^* B^* \qquad (3\text{-}13)$$

where the asterisk indicates that the term V^{m+1} is included making the V^*-matrix of order (n+1) (m+2) and B^* of order m+2. The solution gives the B:s as functions of E_o, corresponding to a curve on the hyperplane $H^*(B_o, B_1, \ldots . B_{m+1})$ which the normal from the line $L(E_o)$ describes as E_o varies. We now solve E_o from the condition $B_o=0$, selecting the solution which gives the least value of the length of the normal. This method determines the source energy E_o and the calibration function, equation 3-2. Should the uncertainty in E_o, when determined by this method, exceed that which can be obtained for the accelerator facility using any other method, an option exists which used a fixed E_o in the S-functions and only determines the B_o:s. We must, however, also evaluate the accuracies involved. We repeat the procedure used once before and resample new sets of values of the pulseheights $V_o, V_1, \ldots . V_n$ from normal distributions with means V_j and variances $(\Delta V_j)^2$. The new values are then used for repeated solutions of the calibration equations.

By doing this a number of times (in practice ten times) we obtain a distribution of E_o and may compute distributions of E at a set of given points, e.g. E_{pj}. In the same way as before we calculate the root-mean-square deviations of these quantities and interpret them as our statistical errors.

The uncertainty in the determination of the absorber thickness should also be examined with regard to its influence on the calibration error. To sufficiently good approximation we may set this physical error equal to (thickness uncertainty) $|\partial E/\partial s|_{E_p}$.

By adding the squares of the statistical error and the physical error we obtain an estimate of the square of the total calibration error at the points $E = E_{pj}$. The condition for a linear response is that for all values of V,

$$L = \frac{B_2 V^2 + B_3 V^3 + \ldots + B_{n-1} V^{n-1}}{B_0 + B_1 V} \ll 1 \qquad (3\text{-}14)$$

The reason it is possible to evaluate the source energy by the method described is that the S functions are not all proportional to the source energy itself. If that were so, the system of equations for E_o and B_j:s would not be solvable for E. This implies that the method of calibration works best where the stopping power has a large and momotonic variation with energy. If the source is known, forinstance from a magnetic deflection experiment, the calibration function can be established with this method for any form of the stopping power variation with energy. In that case E_o is no longer a variable and the system of equations will determine one more parameter in the calibration function (l = n).

The calibration method described above constitutes a part of the ORACLE code system of experimental analysis. The subprogram is called CALIB.

An example of a calibration calculation is given in Table 3-1. The histograms of 6 different thicknesses of aluminum absorber and the histogram of the "No Absorber" condition were analyzed to obtain peak channel, the error in the peak determination and the full width at half maximum, FWHM, of the peak. On Figure 3-6 are drawn 4 of the 7 histograms used in the example. The experimental histograms may be compared to the calculated Monte Carlo histograms for the same aluminum absorber thicknesses assuming a perfectly monoenergetic proton beam (see Figure 3-5). Based on the fit for the 7 data points, the calculated value for E_o was 99.74 MeV. The best experimental value for E_o was 99.9 MeV. The calculated values for the mean energy of the protons leaving the absorbers, with error evaluation are listed at the end of the table, the large deviation resulted from using $E_o - E_a$ instead of using $E_o - E_m$ values in the fitting calculations.

In Table 3-2 are given the results obtained using the same data points of Table 3-1 where the option of using $E_o - E_m$ values was employed.. The values obtained are very close to the values calculated by the program (again using $E_o - E_m$ option) using a different set of data points. The final values used as the calibration E_m's were the result of many calculations using many combinations of data points. This proedure was repeated for each set of experimental conditions. Having established a viable calibration of channel number vs. mean energy, it was possible to determine mean energy from histograms of absorbers of materials other than aluminum.

TABLE 3-1: Aluminum Calibration, Montreal Data, 2-Degree Fit to $E_o - E_a$.

Z=13 A=26.98 I=163.0 RHO=2.700 2-Degree S-Funtion E-est = 99.9 MeV

V(0)=200.60 dV=0.1000
V(1)=190.90 dV=0.0262 RHOdx=0.8406
V(2)=180.54 dV=0.0350 RHOdx=1.6846
V(3)=169.85 dV=0.0422 RHOdx=2.5063
V(4)=161.10 dV=0.0626 RHOdx=3.2346
V(5)=140.76 dV=0.2263 RHOdx=4.6602
V(6)=118.96 dV=0.3545 RHOdx=5.9292

$S(1)= -12.508644 + .11534117\ E_o - .00039022154\ E_o^2$
$S(2)= -26.431078 + .24986833\ E_o - .00084835445\ E_o^2$
$S(3)= -42.863384 + .42540854\ E_o - .00148104430\ E_o^2$
$S(4)= -60.165183 + .62547166\ E_o - .00222987345\ E_o^2$
$S(5)= -105.65214 + 1.20746408\ E_o - .00450636082\ E_o^2$
$S(6)= -172.52337 + 2.18116906\ E_o - .00855142414\ E_o^2$

E_o = 99.743 MeV
B_o = -.38936218 BETA = .498996 MeV/Channel
CHAN=190.90 CALC ENERGY=94.858 dx error=.0060 STAT error=.0160
CHAN=180.54 CALC ENERGY=89.796 dx error=.0063 STAT error=.0168
CHAN=169.85 CALC ENERGY=84.578 dx error=.0066 STAT error=.0177
CHAN=161.10 CALC ENERGY=79.781 dx error=.0069 STAT error=.0184
CHAN=140.76 CALC ENERGY=69.696 dx error=.0077 STAT error=.0200
CHAN=118.96 CALC ENERGY=59.702 dx error=.0088 STAT error=.0217

RESOLUTION IS .05089

TABLE 3-2: Repeat of Montreal Data Calibration, 2-Degree Fit to $E_o - E_m$

Input data identical to that of Table 3-1.

$S(1)= -10.589439 + .076518712\ E_o - .00019480964\ E_o^2$
$S(2)= -26.555747 + .24985534 1\ E_o - .00083708827\ E_o^2$
$S(3)= -41.980734 + .404946573\ E_o - .00136617160\ E_o^2$
$S(4)= -59.871731 + .616872022\ E_o - .00217550653\ E_o^2$
$S(5)= -102.32139 + 1.138214891\ E_o - .00414993637\ E_o^2$
$S(6)= -166.63244 + 2.059635892\ E_o - .00792904942\ E_o^2$

E_o = 99.912 MeV
B_o = -2.0927188 BETA = .50325 MeV/Channel
CHAN=190.90 CALC E=95.042 dx er=.0059 STAT er=.0127 TOT error=.0140
CHAN=180.54 CALC E=89.913 dx er=.0061 STAT er=.0126 TOT error=.0140
CHAN=169.85 CALC E=84.599 dx er=.0064 STAT er=.0144 TOT error=.0158
CHAN=161.10 CALC E=80.235 dx er=.0067 STAT er=.0169 TOT error=.0182
CHAN=140.76 CALC E=70.358 dx er=.0074 STAT er=.0621 TOT error=.0625
CHAN=118.96 CALC E=59.019 dx er=.0085 STAT er=.1654 TOT error=.1656

RESOLUTION IS .05003

TABLE 3-3: Aluminum Calibration, Montreal Data, 2-Degree Fit to $E_o - E_m$
Different Set of Data Points from Tables 1 and 2.

E_o = 99.903MeV
B_o = .5295190 BETA = .49384 MeV.Channel
CHAN=191.36 CALC E=95.035 dx er=.0059 STAT er=.0082 TOT error=.0101
CHAN=181.00 CALC E=89.925 dx er=.0062 STAT er=.0088 TOT error=.0108
CHAN=170.31 CALC E=84.652 dx er=.0064 STAT er=.0145 TOT error=.0159
CHAN=161.10 CALC E=80.109 dx er=.0067 STAT er=.0206 TOT error=.0216
CHAN=140.76 CALC E=70.077 dx er=.0074 STAT er=.0350 TOT error=.0358
CHAN=118.96 CALC E=59.324 dx er=.0084 STAT er=.0508 TOT error=.0514
RESOLUTION IS .04933

FIGURE 3-1: Monte Carlo Histogram of
185.6 MeV Protons After Transmission
Through Aluminum.
Channel Width: 0.250 MeV
pdx in gm/cm^2

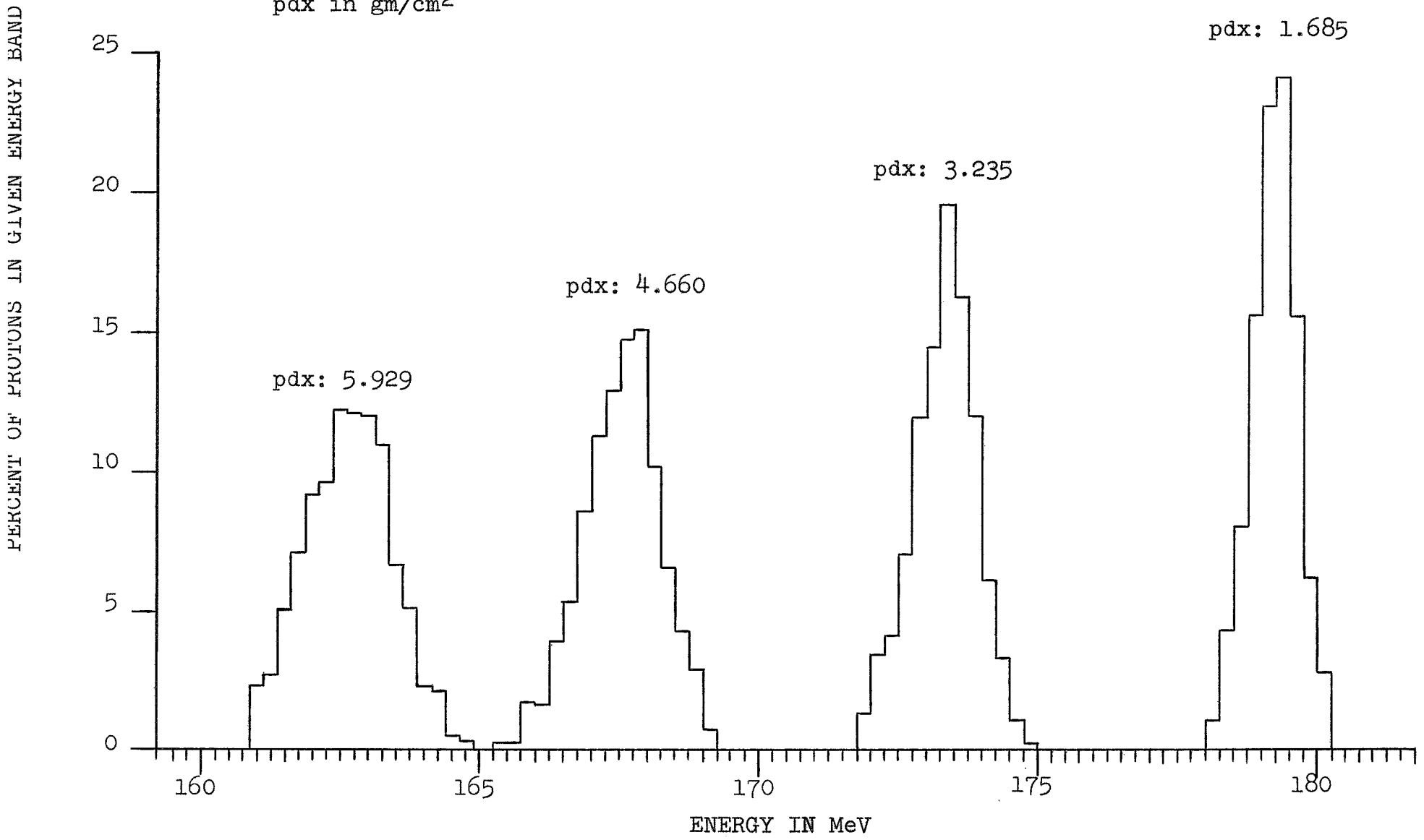

FIGURE 3-2: Multichannel Spectrum of 185.6 MeV Protons After Transmission Through Aluminum and Absorption in a Silicon Detector.
Channel Width: 0.50 MeV
pdx in gm/cm^2

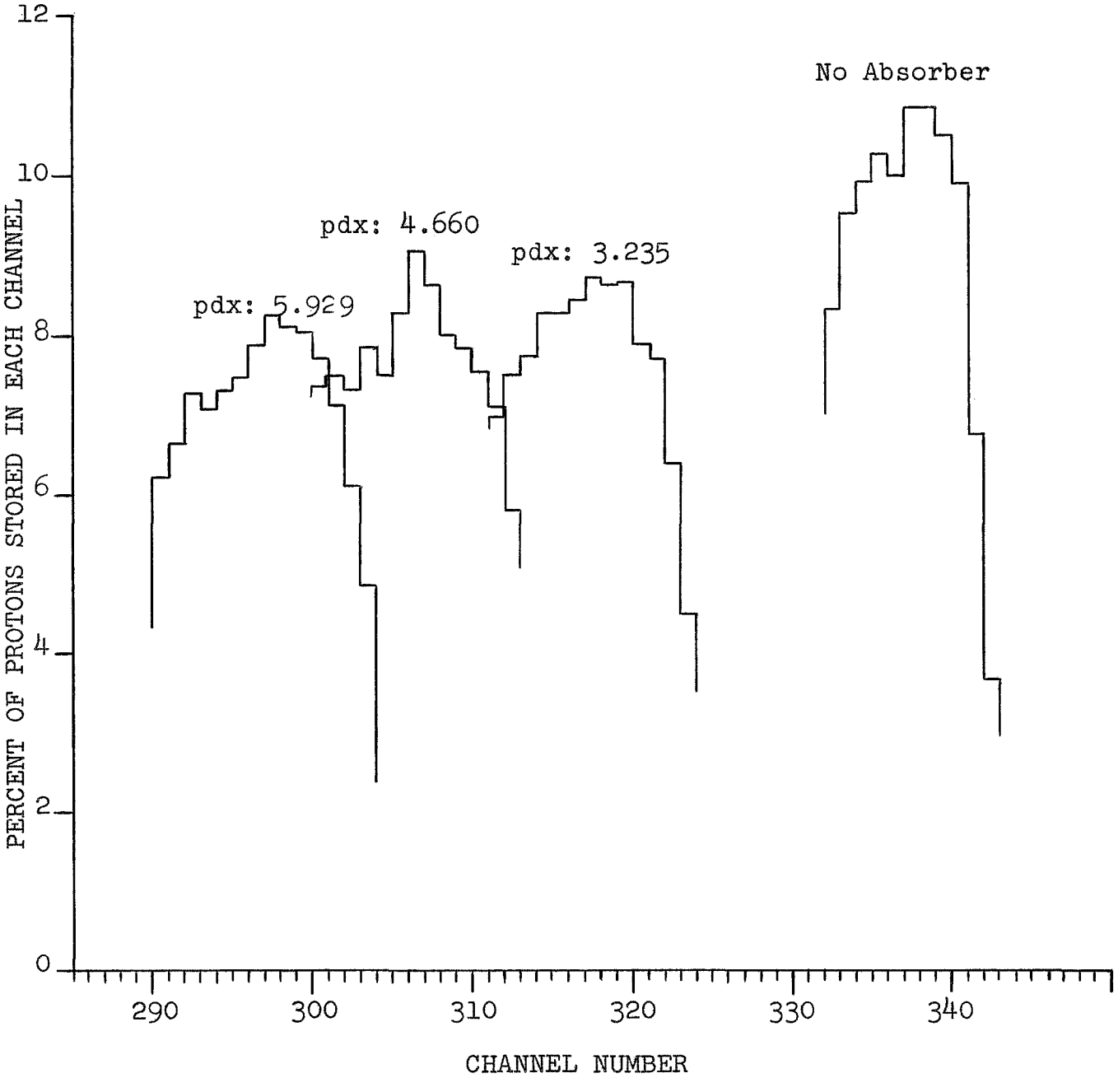

FIGURE 3_3: Monte Carlo Histogram of
159.8 MeV Protons After Transmission
Through Aluminum.
Channel Width: 0.50 MeV
pdx in gm/cm^2

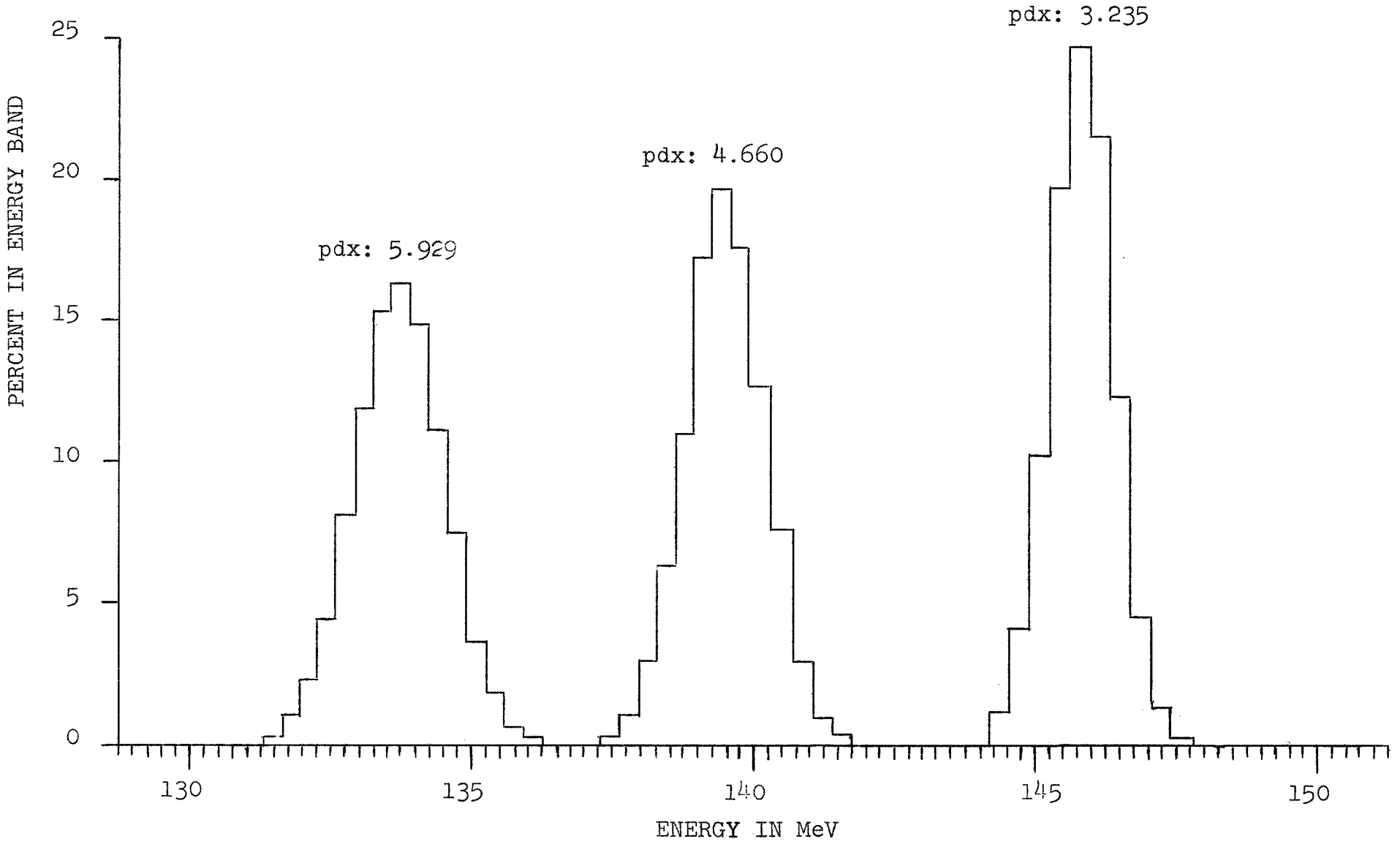

FIGURE 3-4: Multichannel Spectrum of 159.8 MeV Protons After Transmission Through Aluminum and Absorption in a Silicon Detector.
Channel Width: 0.50 MeV
pdx in gm/cm^2

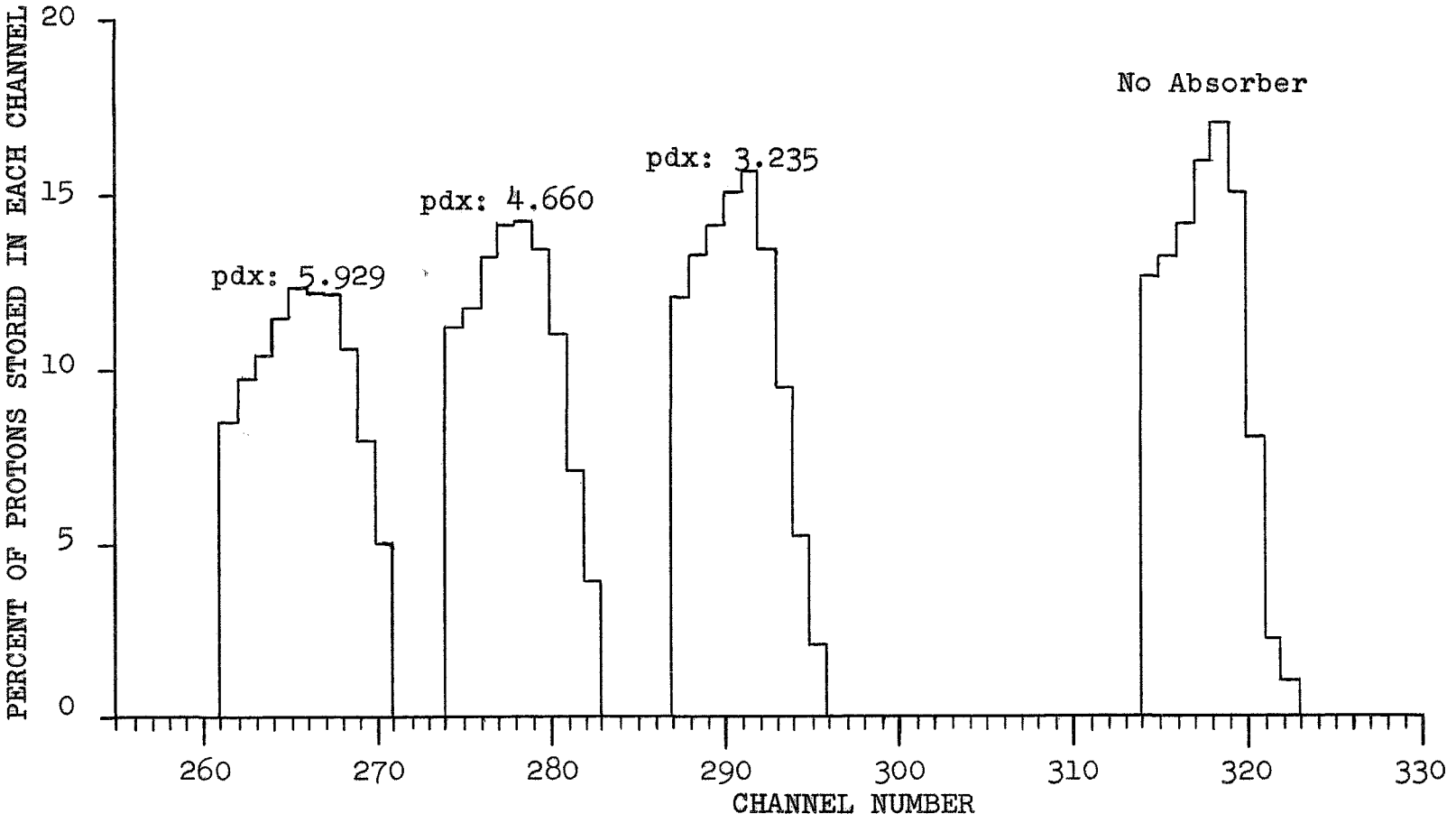

FIGURE 3-5: Monte Carlo Histogram of
99.9 MeV Protons After Transmission
Through Aluminum.
Channel Width: 0.54 MeV
pdx in gm/cm^2

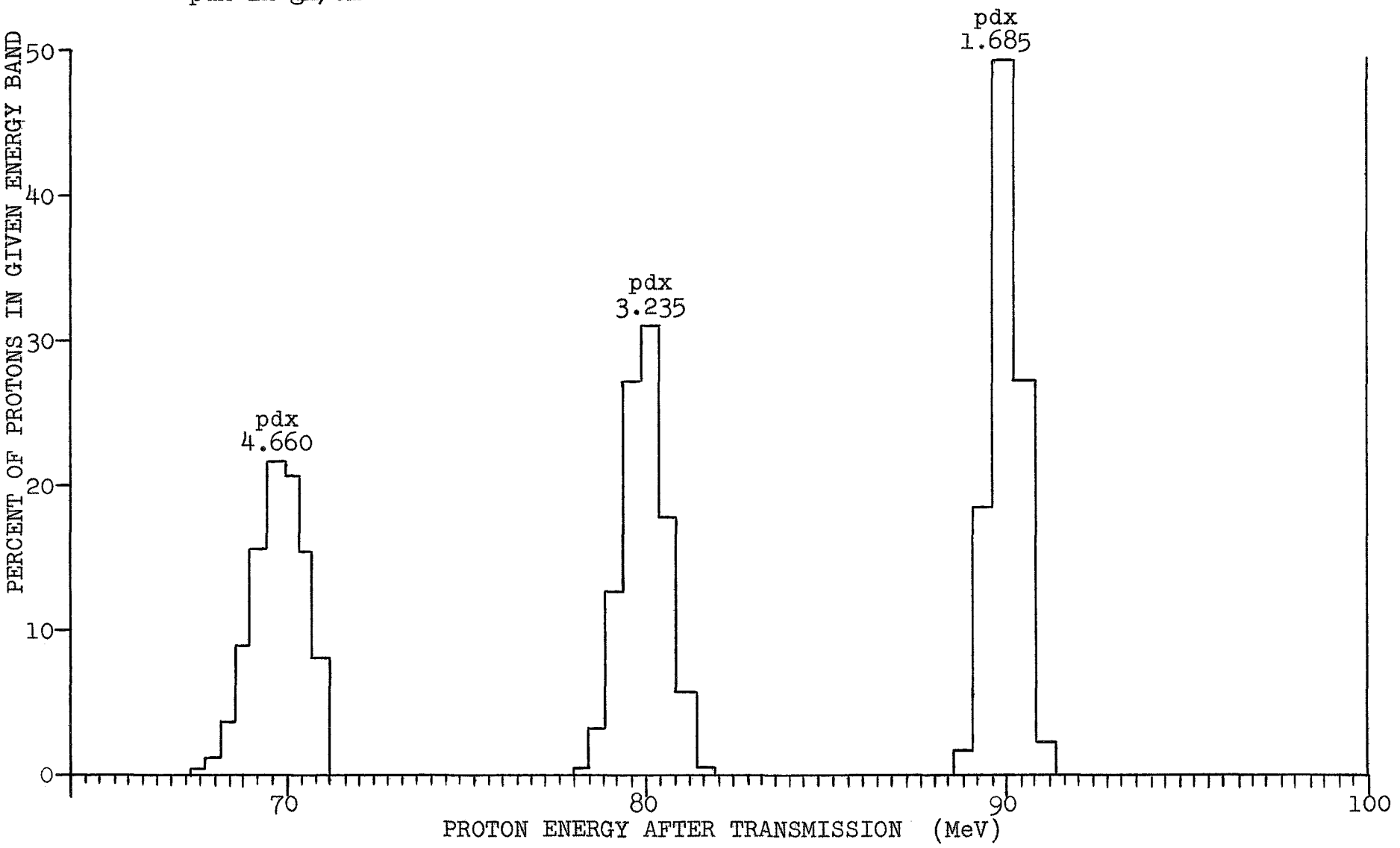

FIGURE 3-6 : Multichannel Spectrum of 99.9 MeV Protons After Transmission Through Aluminum and Absorption in a Silicon Detector.
Channel Width: 0.50 MeV
pdx in gm/cm^2

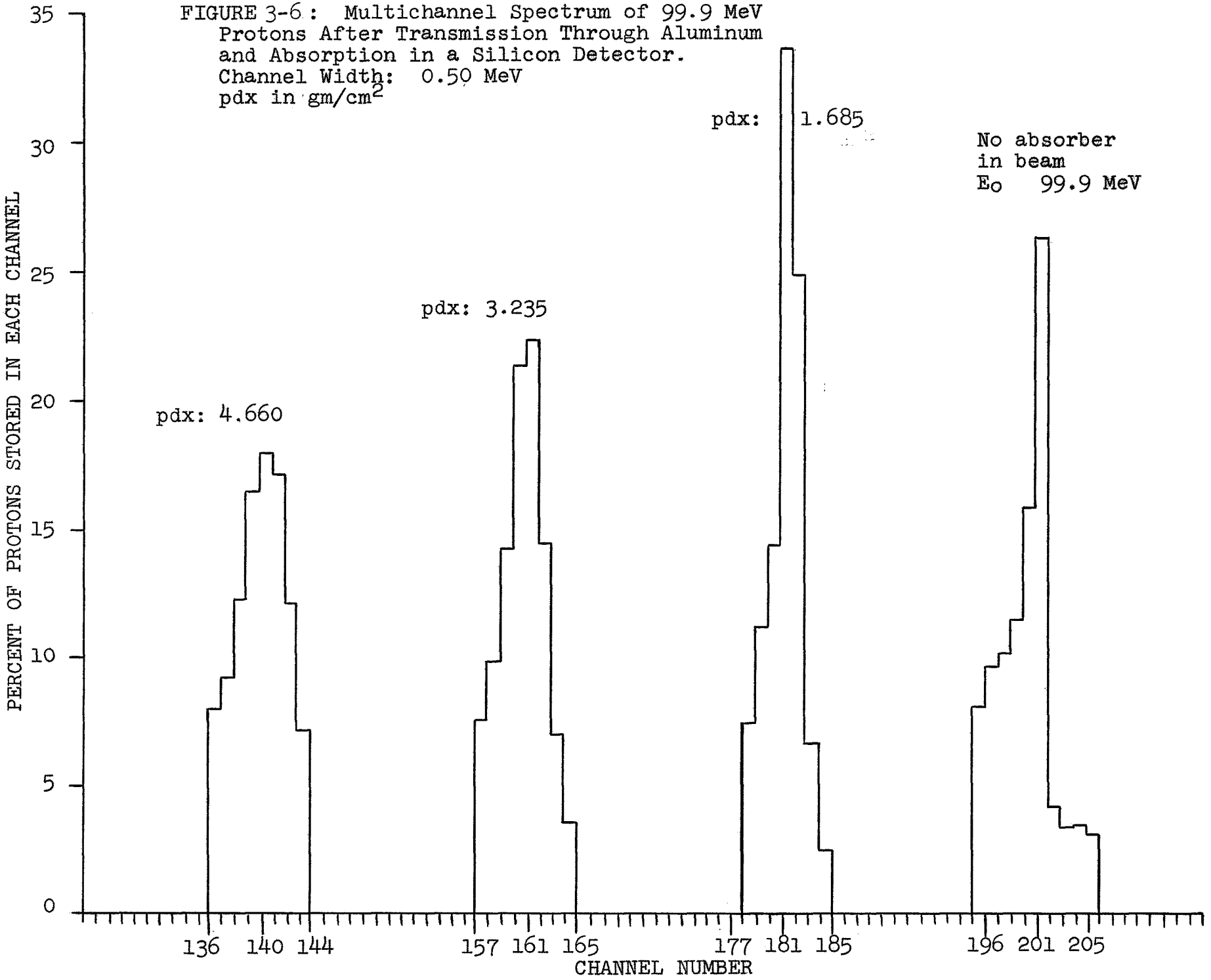

FIGURE 3-7: Monte Carlo Histogram of 36.1 MeV Protons after Transmission Through Aluminum.
Channel Width: 0.125 MeV
pdx in gm/cm^2

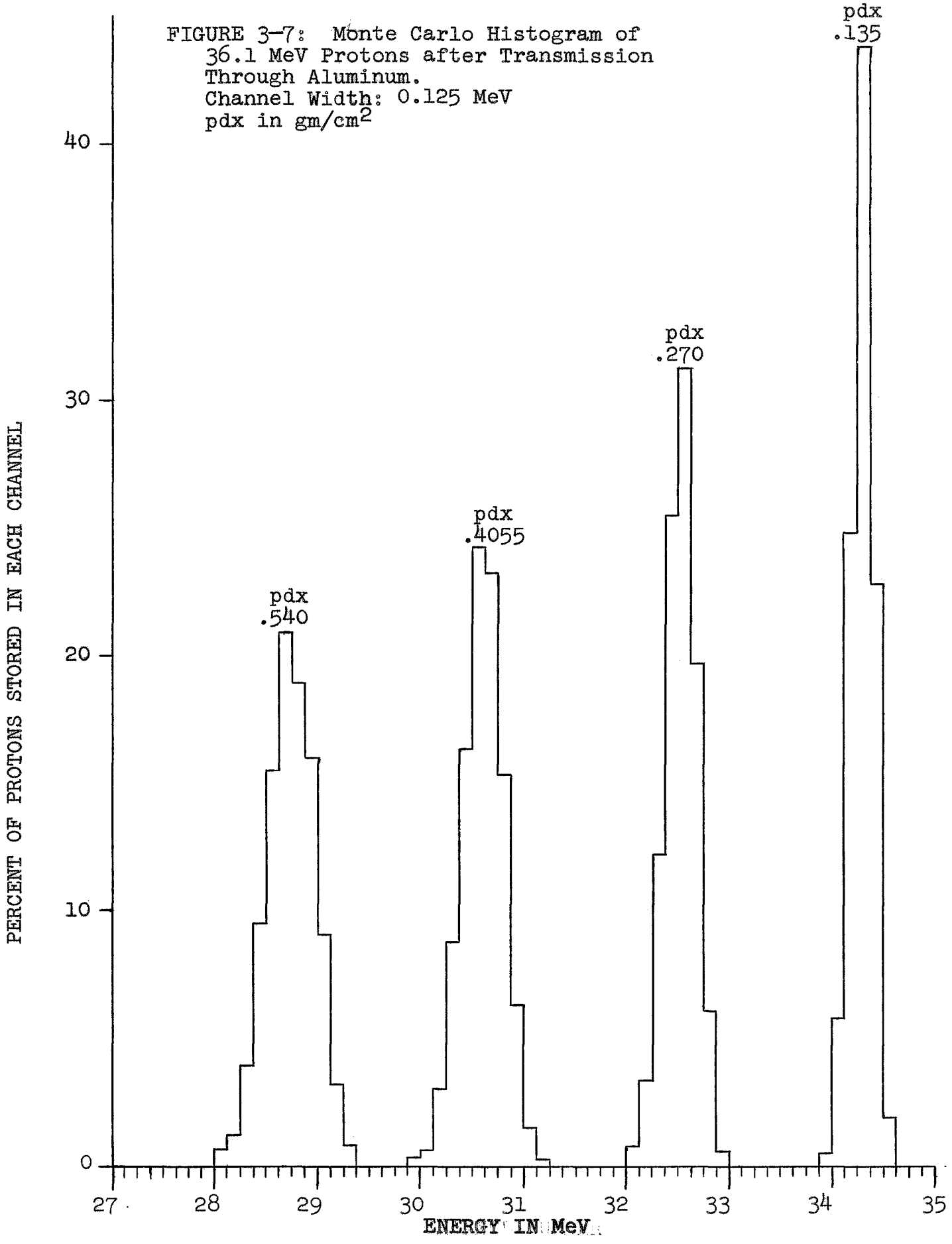

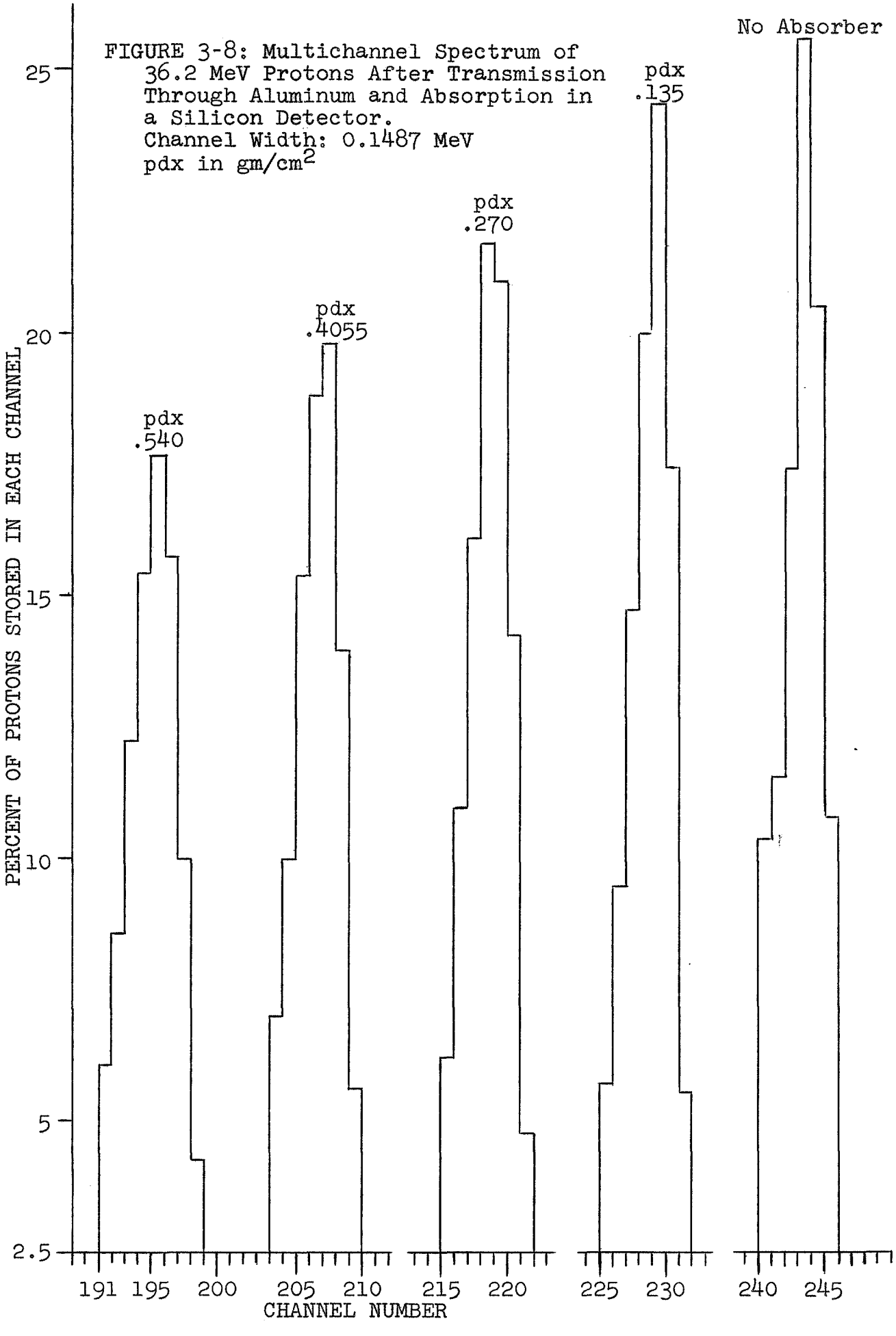

FIGURE 3-8: Multichannel Spectrum of 36.2 MeV Protons After Transmission Through Aluminum and Absorption in a Silicon Detector.
Channel Width: 0.1487 MeV
pdx in gm/cm^2

FIGURE 3-9: Multichannel Spectrum of 13.92 MeV Protons After Transmission Through Aluminum and Absorption in a Silicon Detector.
Channel Width: 0.0603 MeV. pdx in gm/cm^2.

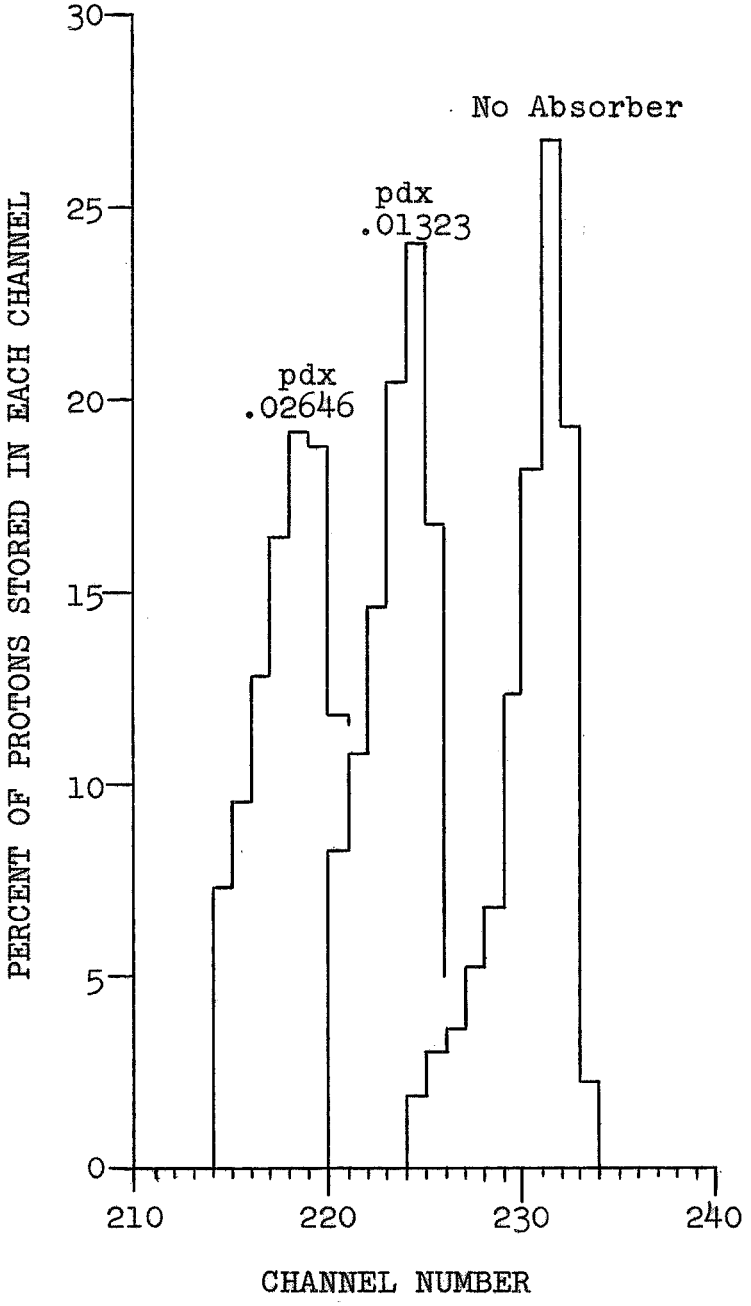

FIGURE 3-10: Multichannel Spectrum of 10.91 MeV Protons After Transmission Through Aluminum and Absorption in a Silicon Detector.
Channel Width: 0.0458 MeV
pdx in gm/cm^2

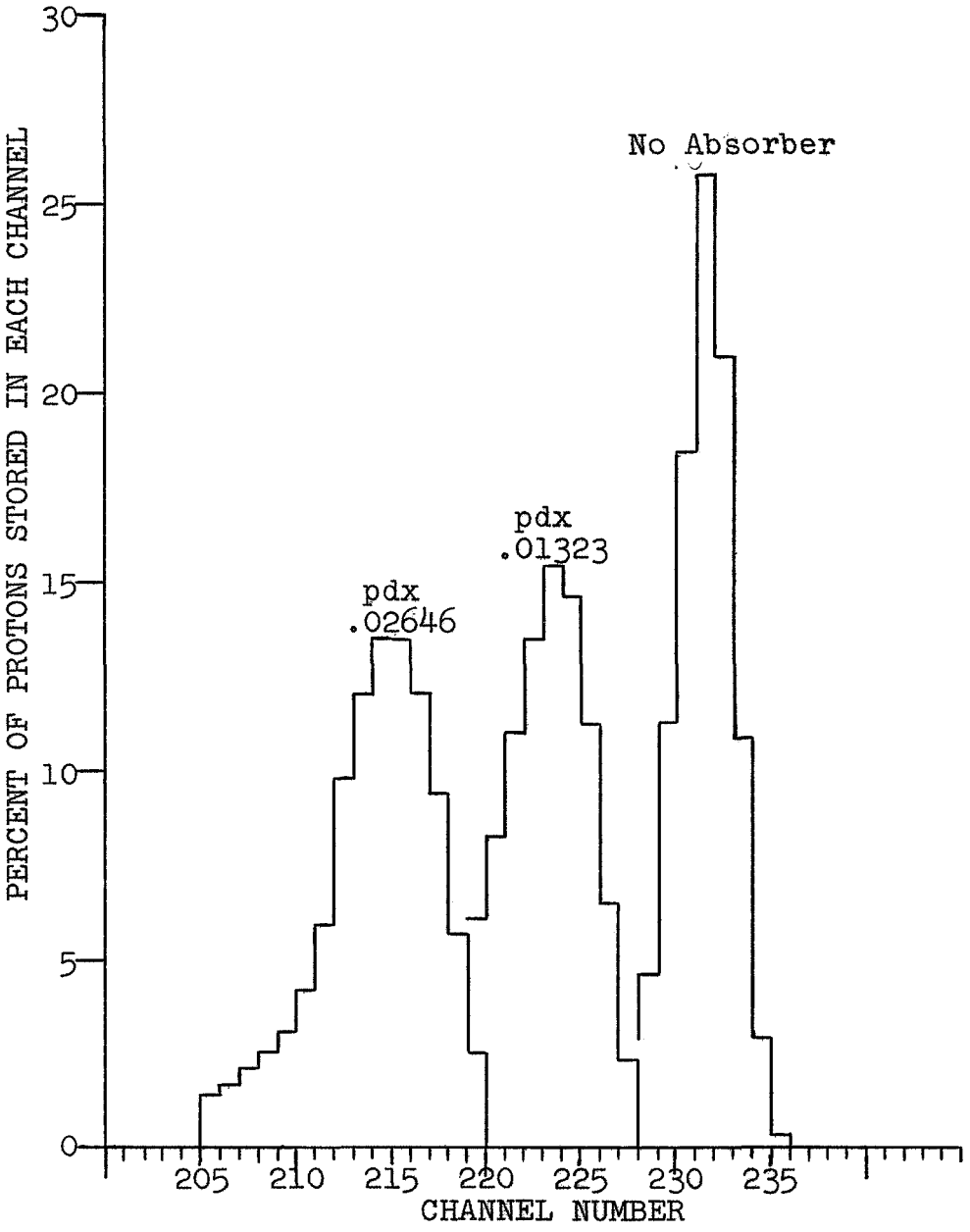

FIGURE 3-11: Multichannel Spectrum of 7.88 MeV Protons After Transmission Through Aluminum and Absorption in a Silicon Detector.
Channel Width: 0.03356 MeV
pdx in gm/cm^2

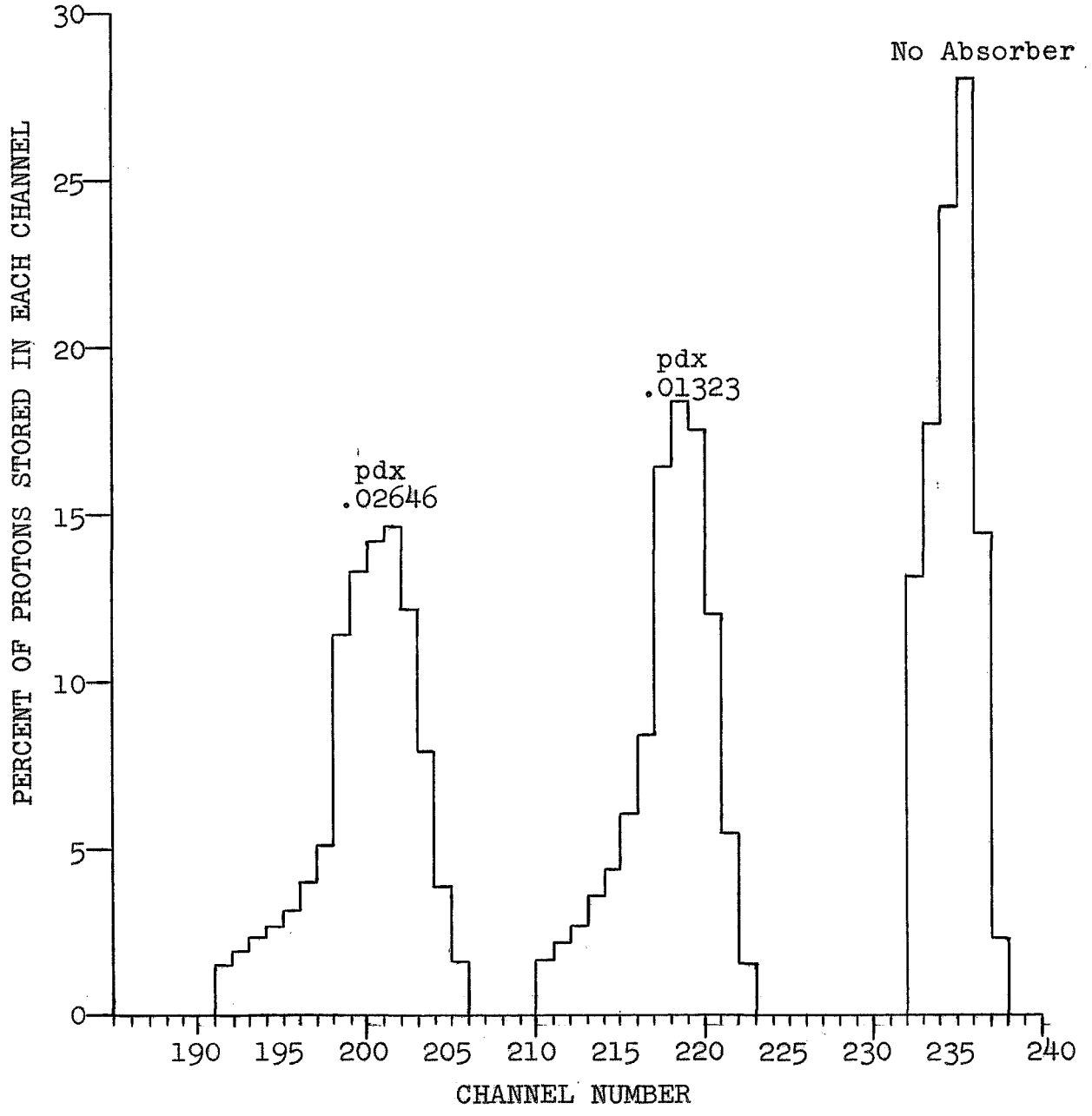

FIGURE 3-12: Multichannel Spectrum of Protons From van de Graaff Accelerator Absorbed in a Silicon Detector
Channel Width: 0.0603 MeV

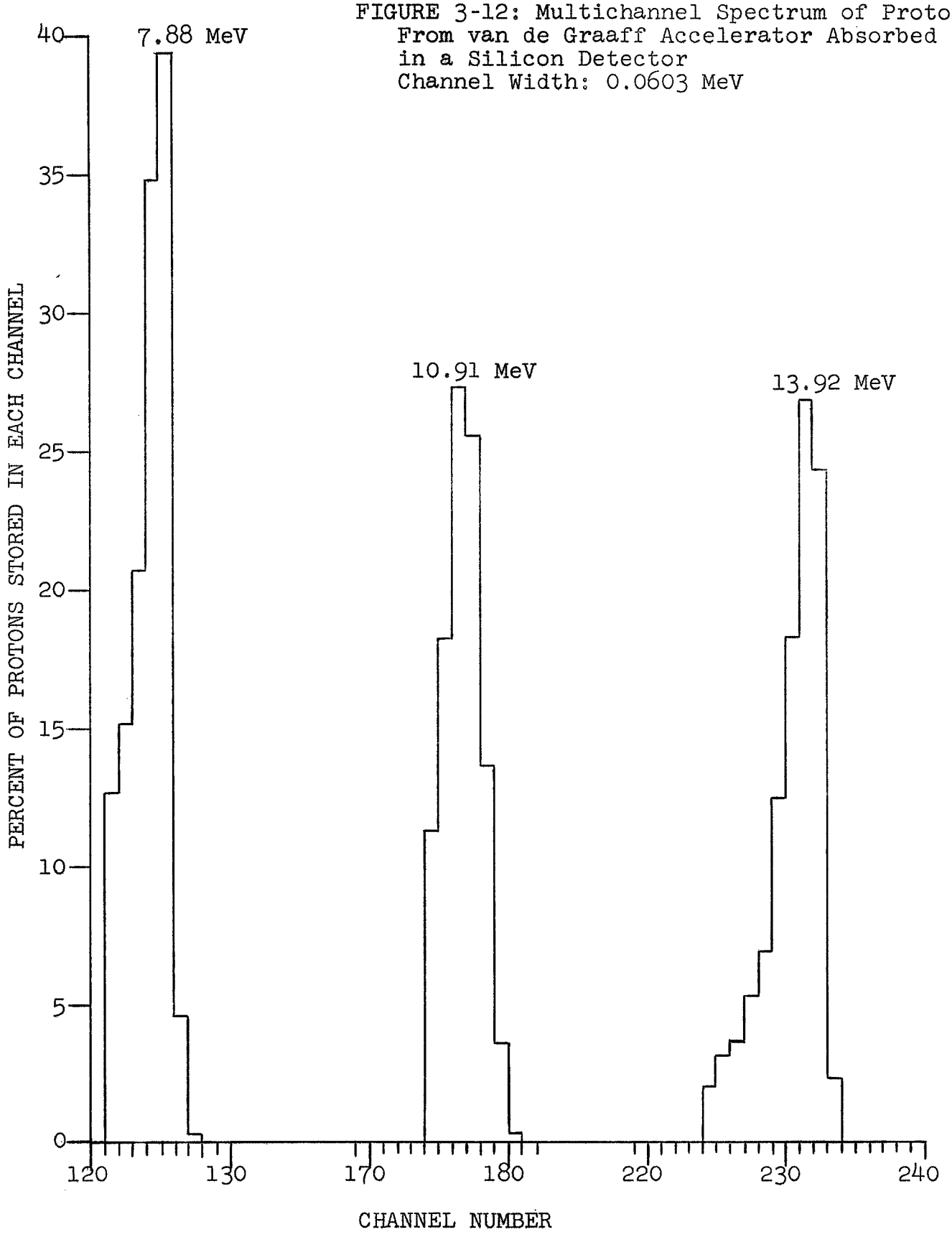

CHAPTER 4

PROTON STOPPING POWER MEASUREMENTS IN SEVEN ELEMENTS

by George W. Crawford, Stephen M. Curry, Danny R. Dixon, Patrick H. Hunt, Phillip L. Kehler and Daniel C. Nipper

Introduction

The purpose of this research is to contribute to the information available in the field of stopping power data, a reliable set of measurements from which the mean ionization potential of each of seven elements can be calculated. Additional data is reported in Chapter 5 of this volume (1). The values extracted from these data are reported in Chapter 6 (2).

A critical review of the experimental stopping power data previously available has been made by Bichsel (3). Turner (4) complements the work of Bichsel and regards the same data from the point of view of verification of the theory and determination of the parameters. As Turner and Bichsel report in their papers, no data is available on any of the seven elements reported herein covering the energy range from 30 to 265 MeV. Overlapping data is available at energies less than 30 MeV for aluminum and copper, and these data are analyzed by Bichsel to represent the same values for the mean ionization potential as reported for this work.

Design of the Experiment

It was desired to measure the energy lost, ΔE, by a proton of initial energy, E_o, in passing through an absorber of thickness X having a density, ρ. The measured quantities included the initial energy of the proton, the most probable energy of the unscattered proton, E_i, after leaving the absorber and the shortest possible distance, ρdx, through the absorber. The energies E_o and E_i were recorded as multichannel pulse height distributions of charge created in and collected from the active region of lithium-drifted silicon detectors. The detectors used were in each case large enough to totally absorb the entering proton beam. These detectors are described in Volume 68-1 of this report, with a full description of the total absorption technique given in Chapter 6 (5).

In order to obtain a single data point, 4 separate measurements were made using two detectors of different volumes and two nearly identical absorbers. The sequence was as follows. With detector number 1 operating at optimum bias and alignment (5), the histogram representing E_o was stored in the RIDL Nanolyzer. Absorber A was then intruded into the beam as exactly perpendicular to the beam as possible by a changer apparatus without breaking the vacuum and the histogram for $_1E_A$ was stored. Absorber A was replaced with absorber B and the histogram $_1E_B$ was stored. Precision pulse generator peaks were also stored with each proton peak. These were used to monitor the stability of the system. The typed record of one such histogram is given in Table 1, together with its companion E_o histogram. The pulse generator peaks are found in channels 144-5, 164-5 and 209 for both runs. Each histogram was analyzed using the new approach described in Chapter 1 (6). The analysis for each peak is given in Table 2. The program selects the most probable channel number, N, and determines the error in N.

DETECTOR G-3 BIAS 550 VOLTS: X8-1/16-662-376-ATT.IN: INPUT-1: E_o=100 MeV

Channel Number	Number Of Counts Stored In Each Channel									
	0	1	2	3	4	5	6	7	8	9
140	572	596	567	610	1220	759	598	540	556	543
150	548	523	526	534	461	489	494	503	468	476
160	462	448	442	466	910	1192	401	406	454	448
170	445	429	423	369	406	458	397	407	426	398
180	442	427	454	525	525	552	575	608	685	705
190	673	735	655	644	643	699	793	949	1251	3145
200	7773	1178	147	111	87	74	109	68	91	1050
210	59	86	74	74	70	84	68	78	72	61
	M*1-28 No Absorber									
140	827	840	823	883	1699	1025	855	811	819	741
150	814	784	824	791	806	803	856	894	911	939
160	952	932	1023	1100	1638	2323	1134	1104	1075	1078
170	1035	1007	950	917	938	1012	1142	1289	1684	3299
180	5483	5193	1765	427	250	257	201	202	205	180
190	186	179	185	184	178	143	164	169	159	160
200	167	150	170	160	144	154	141	150	387	1974
210	139	150	128	155	157	137	139	125	132	134
	M*1-29 AL(1.6778 g/cm^2) Absorber									

TABLE 1. TYPICAL MULTICHANNEL ANALYZER DATA HISTOGRAMS

Experimental Procedure

The electronic system had been carefully chosen and adjusted to give very linear, noise-free operation under the conditions existing at Southern Methodist University. Field trips to six different radiation facilities were made to obtain the data covering the range from 8 through 187 MeV. Essentially the same procedure was carried out at each laboratory. Any travel damage was located and corrected. Next a noise-free ground connection was established. As the operating conditions differed at each place, a thorough testing of the linearity of response and the noise level was made under the operating conditions of each laboratory. This test was repeated at intervals during the long continuous periods of operation. During certain periods of the early morning and early evening power transients, it was necessary to suspend data taking until the noise level returned to an acceptable level.

A very careful alignment of the detector in the beam was vital to the success of the experiment. The mounting of the detector permitted both translational and rotational motion with respect to all three axes. Fine adjustments continued until the proton beam entered one end (at the center of the active region of the detector) and remained in this region, traveling parallel to the length of the detector, until totally absorbed. This alignment produced both the maximum charge pulse and the sharpest peak histogram at the optimum bias voltage.

A series of histograms, each with the protons totally absorbed in the active region of the detector, were taken as a function of absorber

TABLE 2. DETERMINATION OF MOST PROBABLE CHANNEL

CHANNEL LIMITS: 196 197 198 199 200 201 202 203 204
COUNTS: 793 949 1251 3145 7773 1178 147 111

MEAN CHANNEL IS 199.3836 TOTAL COUNTS ARE 15357

K	A						
16463.	-.24572	.21027	-.04073	.08079			
16448.	-.23022	.21050	-.02815	.08090	.00101		
13891	-.23202	-.40445	-.00762	-.12468	.00308	-.01469	
14023.	-.42000	-.37547	-.16213	-.11722	.02464	-.01423	-.00110
24700.	-.38076	1.25470	-.20138	.55830	.03145	-.06379	-.00126 .00224

CHAN	EXP	4	5	6	7	8	CHAN
196.	793.	1171.53	1125.34	476.04	569.65	793.00	197.
197.	949.	811.40	818.60	1543.85	1417.13	949.00	198.
198.	1251.	609.90	636.72	592.70	705.93	1251.00	199.
199.	3145.	4150.03	4118.20	3844.85	3773.57	3145.00	200.
200.	7773.	6417.94	6426.63	7116.39	7142.30	7773.00	201.
201.	1178.	2325.94	2344.87	1839.62	1870.86	1178.00	202.
202.	147.	-694.32	-729.66	-436.17	-522.91	147.00	203.
203.	111.	66.25	73.92	606.54	740.92	111.00	204.
PROB. CH. NO.		200.34	200.35	200.36	200.39	200.41	

8 IS BEST N. AND GIVES CHAN = 200.41, ERROR IS .03 CHAN.

MONTREAL*1-28: E_o = 100 MeV: NO ABSORBER

CHANNEL LIMITS: 177 178 179 180 181 182 183 184 185
COUNTS: 1289 1684 3299 5483 5193 1765 427 250

MEAN CHANNEL IS 180.5242 TOTAL COUNTS ARE 19390

K	A						
20178.	-.22346	.12624	-.03763	.027544			
20180.	-.22536	.12636	-.03884	.027560	-.00012		
20430.	-.22488	.16124	-.04015	.038742	-.00026	.00073	
20408.	-.44855	.16821	-.20001	.039202	-.02837	.00067	-.00113

CHAN	EXP	4	5	6	7	CHAN
177.	1289	1201.99	1206.43	1238.84	1289.	178.
178.	1684	1820.61	1817.92	1766.99	1684.	179.
179.	3299	3165.06	3164.52	3198.68	3299.	180.
180.	5483	5608.22	5611.15	5589.30	5483.	181.
181.	5193	5090.44	5087.13	5080.12	5193.	182.
182.	1765	1852.71	1854.51	1878.65	1765.	183.
183.	427	369.14	371.02	321.07	427.	184.
184.	250	281.83	277.31	316.35	250.	185.
PROB. CH. NO.:		180.90	180.90	180.90	180.92	

7 IS BEST N AND GIVES CHAN = 180.92 ERROR IS .020 CHAN.

MONTREAL*1-29 AL (1.6778 ρdx) ABSORBER

TABLE 3

MEASUREMENTS FOR STOPPING POWER DETERMINATIONS
AT E_o = 159.75 (±.25) MeV

ρdx ($g.cm^2$) ±.001	Most Probable Channel	Error (Channels)	FWHM (Channels)	Average ΔE (MeV)	Error (MeV)
	BERYLLIUM: Z = 4, A = 9.012, ρ = 1.844				
None	322.50	±.02	2.05		
1.599	308.36	±.06	2.48	7.04	±.03
3.082	294.87	±.08	2.52	13.77	±.04
4.403	282.42	±.10	3.28	19.97	±.05
	CARBON: Z = 6, A = 12.011, ρ = 1.582				
None	322.24	±.02			
1.985	302.97	±.08	3.28	9.60	±.04
2.840	294.50	±.10	3.30	13.82	±.05
3.621	286.43	±.10	3.34	17.83	±.05
	ALUMINUM: Z = 13, A = 26.980, ρ = 2.702				
None	318.57	±.02	2.05		
1.685	304.46	±.04	3.26	7.03	±.02
3.235	291.14	±.06	3.29	13.67	±.03
4.660	278.46	±.06	3.42	19.98	±.03
5.929	266.89	±.08	3.43	25.76	±.04
	SILICON: Z = 14, A = 28.086, ρ = 2.328				
None	322.50	±.02	1.95		
2.328	302.40	±.04	2.58	10.00	±.02
3.503	292.10	±.04	3.24	15.15	±.02
4.656	281.40	±.06	3.38	20.48	±.03
6.984	258.84	±.10	3.36	31.72	±.05
9.335	234.72	±.10	3.42	43.74	±.05
	IRON: Z = 26, A = 55.847, ρ = 7.792				
None	322.35	±.02	2.00		
3.244	297.93	±.10	3.37	12.17	±.05
6.339	273.50	±.10	3.45	24.34	±.05
	COPPER: Z = 29, A = 63.540, ρ = 8.897				
None	318.55	±.02	2.10		
3.781	290.98	±.05	3.28	13.73	±.03
5.423	278.31	±.10	3.31	20.05	±.05
7.102	265.03	±.20	3.32	26.62	±.10
	LEAD: Z = 82, A = 207.190, ρ = 11.224				
None	318.40	±.02	2.20		
5.106	290.80	±.06	3.26	13.74	±.03
5.205	290.50	±.04	3.20	13.89	±.02
7.858	275.43	±.04	3.27	21.56	±.02

TABLE 4

MEASUREMENTS FOR STOPPING POWER DETERMINATIONS
AT E_o = 99.9 (±.1) MeV

ρdx (g/cm^2) ±.001	Most Probable Channel	Error (Channels)	FWHM (Channels)	Average ΔE (MeV)	Error (MeV)
	BERYLLIUM: Z = 4, A = 9.012, ρ = 1.844				
None	201.20	±.02	1.35		
1.599	181.53	±.05	2.47	10.10	±.02
3.082	161.93	±.05	2.47	20.16	±.04
4.403	142.04	±.06	2.66	30.38	±.05
	CARBON: Z = 6, A = 12.011, ρ = 1.582				
None	201.20	±.02	1.35		
1.037	187.48	±.04	2.10	7.03	±.02
1.985	174.28	±.06	2.38	13.82	±.03
2.856	160.10	±.10	2.69	20.43	±.05
3.636	149.26	±.20	2.90	26.68	±.10
	ALUMINUM: Z = 13, A = 26.980, ρ = 2.702				
None	201.21	±.02	1.25		
1.685	181.78	±.08	1.98	9.97	±.04
3.235	162.36	±.06	2.29	19.94	±.03
4.660	142.73	±.08	2.86	30.02	±.04
5.929	123.30	±.10	3.52	39.99	±.05
	IRON: Z = 26, A = 55.847, ρ = 7.792				
None	200.40	±.02	1.55		
1.666	183.05	±.04	2.08	8.65	±.02
3.244	165.46	±.08	2.62	17.41	±.04
6.304	126.62	±.10	3.54	36.78	±.05
	COPPER: Z = 29, A = 63.540, ρ = 8.897				
None	201.20	±.02	1.60		
1.974	181.09	±.04	1.88	10.00	±.02
3.781	161.21	±.06	2.30	19.93	±.03
5.423	141.10	±.05	3.04	29.95	±.02
	LEAD: Z = 82, A = 207.190, ρ = 11.224				
None	200.24	±.02	1.40		
2.680	180.99	±.10	2.43	9.94	±.05
2.723	180.73	±.04	2.55	10.11	±.02
5.205	162.00	±.08	3.02	20.08	±.04
7.893	140.81	±.06	3.75	31.89	±.03

TABLE 5

MEASUREMENTS FOR STOPPING POWER DETERMINATIONS

AT E_o = 36.2 (±.1) MeV

ρdx (g/cm^2) ±.001	Most Probable Channel	Error (Channels)	FWHM (Channels)	Average ΔE (MeV)	Error (MeV)
	ALUMINUM: Z = 13, A = 26.980, ρ = 2.702				
None	243.35	±.05	2.2		
0.135	232.00	.05	3.2	1.704	±.01
0.270	220.16	.05	4.6	3.477	.01
0.4055	207.87	.05	5.3	5.329	.02
0.540	194.88	.10	7.8	7.273	.02
	SILICON: Z = 14, A = 28.086, ρ = 2.328				
None	243.35	±.05	2.2		
0.3306	224.88	.10	5.1	4.42	±.03
0.6612	182.86	.10	6.4	9.38	.03
0.9941	143.75	.20	7.2	15.10	.05
	COPPER: Z = 29, A = 63.540, ρ = 8.897				
None	243.35	±.05	2.2		
0.106	236.89	.05	3.1	1.12	±.01
0.164	231.76	.05	3.8	1.74	.01
0.263	225.42	.05	4.3	2.84	.01
0.318	221.53	.10	4.7	3.44	.02
0.424	212.17	.10	5.1	4.68	.02

TABLE 6

MEASUREMENTS FOR STOPPING POWER DETERMINATIONS

AT E_o = 14. (±.05) MeV

	ALUMINUM: Z = 13, A = 26.980, ρ = 2.702				
None	231.52	±.05	2.6		
0.01323	225.72	.05	2.8	0.349	±.01
0.01981	222.72	.05	3.2	0.529	.01
0.02646	219.81	.05	3.5	0.704	.01
	SILICON: Z = 14, A = 28.086, ρ = 2.328				
None	231.52	±.05	2.6		
0.0856	189.90	.10	4.2	2.50	±.01
0.1676	143.36	.15	6.1	5.30	.01
	COPPER: Z = 29, A = 63.540, ρ = 8.897				
None	231.52	±.05	2.6		
0.0463	214.17	.05	2.8	1.04	±.01
0.09245	196.27	.05	3.7	2.12	.01
0.1112	187.70	.10	4.1	2.63	.01
0.1540	168.67	.10	4.6	3.78	.01

TABLE 7

MEASUREMENTS FOR STOPPING POWER DETERMINATIONS

AT E_o = 11. (±.05) MeV

ρdx (g/cm^2) ±.001	Most Probable Channel	Error (Channels)	FWHM (Channels)	Average ΔE (MeV)	Error (MeV)
	ALUMINUM: Z = 13, A = 26.980, ρ = 2.702				
None	232.32	±.05	2.2		
0.01323	223.45	.05	2.7	0.421	±.01
0.01981	218.92	.05	3.1	0.636	.01
0.02646	214.04	.05	3.6	0.868	.01
	SILICON: Z = 14, A = 28.086, ρ = 2.328				
None	232.32	±.05	2.2		
0.0856	166.21	.10	4.8	3.14	±.01
0.1676	72.1	.10	9.2	7.61	.01
	COPPER: Z = 29, A = 63.540, ρ = 8.897				
None	232.32	±.05	2.2		
0.0463	205.35	.05	3.9	1.281	±.01
0.09245	176.92	.05	4.3	2.635	.01
0.1112	162.97	.05	5.4	3.294	.01
0.1540	127.61	.05	7.1	4.974	.01

TABLE 8

MEASUREMENTS FOR STOPPING POWER DETERMINATIONS

AT E_o = 8. (±.05) MeV

	ALUMINUM: Z = 13, A = 26.980, ρ = 2.702				
None	234.7	±.10	2.1		
0.01323	218.4	.10	2.9	0.546	±.01
0.01981	209.9	.10	3.4	0.831	.01
0.02646	201.0	.10	3.9	1.128	.01
	SILICON: Z = 14, A = 28.086, ρ = 2.328				
None	234.7	±.10	2.1		
0.0856	97.3	.10	9.5	4.60	±.01
	COPPER: Z = 29, A = 63.540, ρ = 8.897				
None	234.7	±.10	2.1		
0.0463	183.8	.10	6.1	1.704	±.01
0.09245	121.6	.10	8.3	3.788	.01
0.1112	89.0	.10	9.8	4.880	.01

thickness. Examples are given in Figures 2, 4, 6, 8, 9, 10 and 11 of Chapter 3 (7), for aluminum. The data taken at 187 MeV was not accurate enough to be included. The 187 MeV data used for the stopping power measurements is that reported in Chapter 5 (1).

A series of data involving ten different absorbers could be taken without breaking the vacuum and entering the absorber changer. With each detector, one data point would be taken for each thickness by loading the holder with absorbers of the same material and increasing thickness. The second data point would be taken with absorbers of different materials but giving the same magnitude of ΔE. This was repeated with the second detector. Every effort was made to eliminate sytemmatic errors in the data taking procedure. This included a change of operator so that different persons took the four data points used to obtain the average values reported in Tables 3 - 8.

E_o was determined using three different ways. First was the calibrated value given by the laboratory group. This was checked by making a range measurement in aluminum. Data was taken as though it were a stopping power measurement with the aluminum absorber thickness increased until the energy of the badly scattered beam was less than 4 MeV. The remaining range was calculated and this was checked by inserting foils, each about 0.00662 g/cm^2 in thickness. Using I = 163 eV, the energy was determined using the Monte Carlo proton transport program described in SMU Report 68-2. The usual linear transport range calculation introduced considerable error. A third check was made using the $\Delta E/\Delta \rho dx$ measurements. The determined value and the accuracy with which E_o energy is known is given in the titles of Tables 3 - 8.

The values for the average ΔE for each ρdx as reported in Tables 3 - 8 and in Chapter 5 (1), were used in the determination of the mean ionization potential of the seven elements. These results are given in Chapter 6 (2).

Acknowledgments

We are grateful to Dr. A. M. Koehler of the Cyclotron Laboratory, Harvard University, Cambridge, Massachusetts; to Dr. R. E. Bell of the Foster Radiation Laboratory, McGill University, Montreal, Canada; to Dr. J. A. Auxier and Dr. A. Zucker, Oak Ridge National Laboratories, Oak Ridge, Tennessee; to Dr. R. N. Little of the Accelerator Laboratory, the University of Texas at Austin, Texas, for their support and interest in this experiment.

References

1. D. R. Dixon, et al, Chapter 5, SMU Report 68 - 3, 1968.
2. G. W. Crawford, et al, Chapter 6, SMU Report 68 - 3, 1968.
3. H. Bichsel, Chapter 2, Nuclear Science Series Report No. 39, 1964.
4. J. E. Turner, Chapter 3, Nuclear Science Series Report No. 39, 1964.
5. G. W. Crawford, et al, Chapter 6, SMU Report 68 - 1, 1968.
6. M. Leimdorfer, et al, Chapter 1, SMU Report 68 - 3, 1968.
7. M. Leimdorfer and G. W. Crawford, Editors, SMU Report 68 - 2, 1968.

CHAPTER 5

STOPPING POWER MEASUREMENTS USING A MAGNETIC SPECTROMETER

by Danny R. Dixon, Stephen M. Curry, Bo Jung and George W. Crawford

The 185 MeV protons from the synchrocyclotron of the Gustaf Werner Institute, the University of Uppsala, Uppsala, Sweden, have been used in a study of the energy lost by protons in traversing various metals and plastics. Data were taken using the double two-fold coincidence telescope system with six energy channels of the Gustaf Werner Nuclear Physics group.

Apparatus

A schematic drawing of the experimental set-up is shown in Fig. 1. The collimator inside the tank was a 10 mm thick brass piece with a circular aperture of 20 mm diameter. Its purpose was to reduce the geometrical cross-section of the beam. Photographic methods were used to determine the collimator shape. Neutrons and scattered protons produced at the collimator and in the magnetic channels inside the cyclotron were negligible due to the large distance from the detecting apparatus and the shields used.

The external, unpolarized proton beam of the 185 MeV synchrocyclotron passed two focusing magnets, two bending magnets and one adjusting magnet before striking the target. The focussing magnets consisted of two sets of quadrapole magnets. They were both necessary to handle the large astigmatism of the emerging beam. At optimum focusing the beam cross-section at the entrance of the apparatus was approximately circular with a diameter of 2.5 mm.

The bending magnets defined the direction of the beam. The photographic methods used allowed a determination of the beam position to at least $\pm$ 0.2 mm at the target position and of its angular deviation from the symmetry axis to $\pm$ 0.04^{o} (1).

The proton energies were analyzed in the magnetic spectrometer. The magnet has a bending angle of 135^{o} and accepts protons in a solid angle of 1.17×10^{-3} steradians (2). For this work, the spectrometer was positioned at zero degrees, since only those protons exiting parallel to the incident beam were of interest.

The incident beam was in vaccuum over the entire path of flight, until emerging from the magnetic spectrometer.

The magnetic field in the spectrometer was stable to about one part in 25000, corresponding to an uncertainty in the proton energy of 0.15 MeV out of 185 MeV. Consequently, the field fluctuations of the magnetic spectrometer did not contribute appreciably to the widths of the energy peaks (3).

The spectrometer field was measured with nuclear magnetic resonance equipment. The probe, containing lithium, was inserted and a field reading made before and after each measurement of the number of counts in the six energy channels. At the position of the probe, the field was thus known to a very high precision. However, due to a lack of knowledge of second order effects of the spectrometer there is assigned an uncertainity of approximately 0.5% to absolute energy values (3).

After bending, the protons were detected in a double two-fold coincidence telescope system with six energy channels. The light pulses from the scintillators were detected by photomultipliers. The photomultiplier pulses were fed into transistorized coincidence units and fast prescalers. The dead time of the circuits was sufficiently small (approximately 25 nsecs) for two protons from consecutive bursts of the cyclotron to be resolved (1). The beam intensity was reduced during the runs (to about 200 protons per second) in order to minimize pileup of the proton pulses.

Although the current in the cyclotron magnet was as stable as the spectrometer current, the cyclotron field, due to intermittent short circuits in the coils, occasionally "jumped", causing energy changes in the proton beam of 100 keV or more. This resulted in multiple-peaking, but the effect was so obvious that the data could always be adjusted appropriately.

Experimental Procedure

The size and position of the incident beam were frequently checked by photographing the beam using Polaroid type 57 3000 speed film. Fine position adjustments were performed using the adjusting magnet shown in Fig. 1.

The absorbers were mounted individually in a movable aluminum holder attached to the cover of the scattering chamber. The holder could be moved into the proton beam or out of the proton beam by remote control. When the holder was in the beam, the face of the absorber was perpendicular to the path of the incident protons. The beam was centered on the face of the absorber.

The elements studied were Al, Be, C, Cu, Fe, Pb and Si. The plastics studied were lucite, nylon, polyethylene and a tissue equivalent plastic. Each absorber was large compared to the beam diameter of 2.5 mm.

The energy loss, ΔE, is defined by the equation $\Delta E = E_o - E_i$, where E_o = the incident proton energy and E_i = the energy of the protons after passage through the absorber. E_o was determined experimentally in the following way:

With the proton beam turned off, the absorber was inserted into the aluminum holder. The cover was then placed on the scattering chamber, and the vacumm pump activated.

Next, the proton beam was turned on. With the holder out of the beam, the magnetic field strength was adjusted until scalers five and six were recording more counts than any of the other scalers. At this point, protons having energy slightly on the high side of the peak were then bent enough by the magnet to reach the detectors. Protons slightly on the low side of the peak were bent too much to reach the detectors.

Then the nuclear magnetic resonance probe was inserted, and the magnetic frequency read from the display unit. The probe was then removed and the scalers reset at zero.

Counts were then stored in the scalers until the data was valid statistically.

The probe was reinserted into the magnetic field. If there had been no significant change in the magnetic field strength, the number of counts in each of the six scalers was recorded. The six numbers representing the number of counts in each of the six energy channels and the average magnet frequency comprised one line of data.

Next the magnetic field strength was decreased until the peak had shifted about two channels. The probe was inserted, and the magnetic frequency determined. The probe was removed and the scalers reset to zero. Counts were stored. The magnetic frequency was rechecked and the counts recorded.

The field strength was again decreased until the peak had shifted another two channels. The magnetic frequency was determined, counts were stored, and the frequency checked. Then the third line of data was recorded.

Usually three lines of data were sufficient to determine the energy distribution of the incident protons. The incident proton energy peak ordinarily had only a 0.25 MeV FWHM, as compared to a 0.18 MeV channel width (approximate) for the scintillator detector system. Hence the full spectrum could be easily recorded in any three or four of the energy channels. Three lines of data therefore provided a very adequate description of the incident proton energy distribution.

The next step in the experimental procedure was the determination of E_i. The proton beam did not have to be turned off in order to place the absorber, since that process could be accomplished by remote control. This provided greater stability in the incident energy, E_o, and therefore better accuracy.

With the absorber in the beam, the procedure used for measuring E_o was repeated. However, the presence of the absorber in the beam caused the energy peak to broaden. The width of the peak dictated the number of lines of data required for adequate description. For the thicker absorbers, as many as six lines of data were required.

As soon as enough lines of data had been recorded to adequately describe the absorber peak, the absorber was removed from the beam by remote control. Then E_o was remeasured, using the same procedure previously described. The second measurement of E_o was necessary to insure that the incident proton energy had not fluctuated during the measurement of E_i. The most probable value of E_o was the average of the two measurements.

Δ E was then determined from $\Delta E = E_o - E_i$.

Data Analysis

Each line of data was analyzed using the CDC 3600 computer at the University of Uppsala. A program written especially for the analysis of data taken using the magnetic spectrometer and detector system at Uppsala was used. Knowing the NMR frequency and the number of counts recorded in each scaler, the computer tabulated the mean energy per channel, the channel width, the normalized number of counts per channel, and the standard deviation in the number of counts. The program corrected the data for the relative sensitivity of the six scintillator detectors.

As an example, the results of the computer analysis for Pb (pdx = 5.1050) are shown in Table 1. Note that channel three on every line of data shows 0.00 counts. The number three scintillator failed to function properly at any time during this experiment.

Figure 2 shows a plot of counts vs. energy for the data in Table 1. Through selection of the best multiplicative factors, the separate curves were all normalized relative to any one of the individual curves. The normalized curves are shown in Fig. 3.

To the extent that it was possible, a smooth curve was drawn through the various data points. The peak energy was then determined graphically for the position of maximum counts. The energy spread was determined at full width half maximum. For this example, the energy was determined to be 173.28 $\pm$ 0.05 MeV, and the spread to be 1.30 MeV.

This same procedure was used for the analysis of all the absorber peaks, as well as the incident proton energy spectra. Table 2 shows the computer print-out for a typical no-absorber run. Figure 4 shows a plot of counts vs. energy for the data in Table 2. A typical normalized curve is shown in Figure 5. Values for the mean

energy loss for the materials studied are listed in Table 3. Using these measured energy losses for the absorbers studied, the mean ionization potential for each material has been calculated. See Chapters 6 and 7.

We are grateful to Professor The Svedberg for his support and interest in this experiment. It is a pleasure to acknowledge our deep debt to Dr. Borje Larsson for his generous support in all phases of this work. We are very grateful to Dr. Arne Johansson and the other members of the Nuclear Physics group for permission to use the telescope system, the analyzing magnet, for their help in the data taking and for analyzing the data using their computer program.

References:

1. A. Johansson, U. Svanberg, and O. Sundberg, Arkiv for Fysik 19, 529, (1961).
2. D. Hasselgren, et al., Physics Letters 9, 166 (1964).
3. S. Dahlgren, et al., Nuclear Physics (Netherlands) 90A, 673 (1967).
4. Danny R. Dixon, Stopping Power Measurements of 185 MeV Protons in Various Metals, M.S. Thesis, Southern Methodist University (1966).

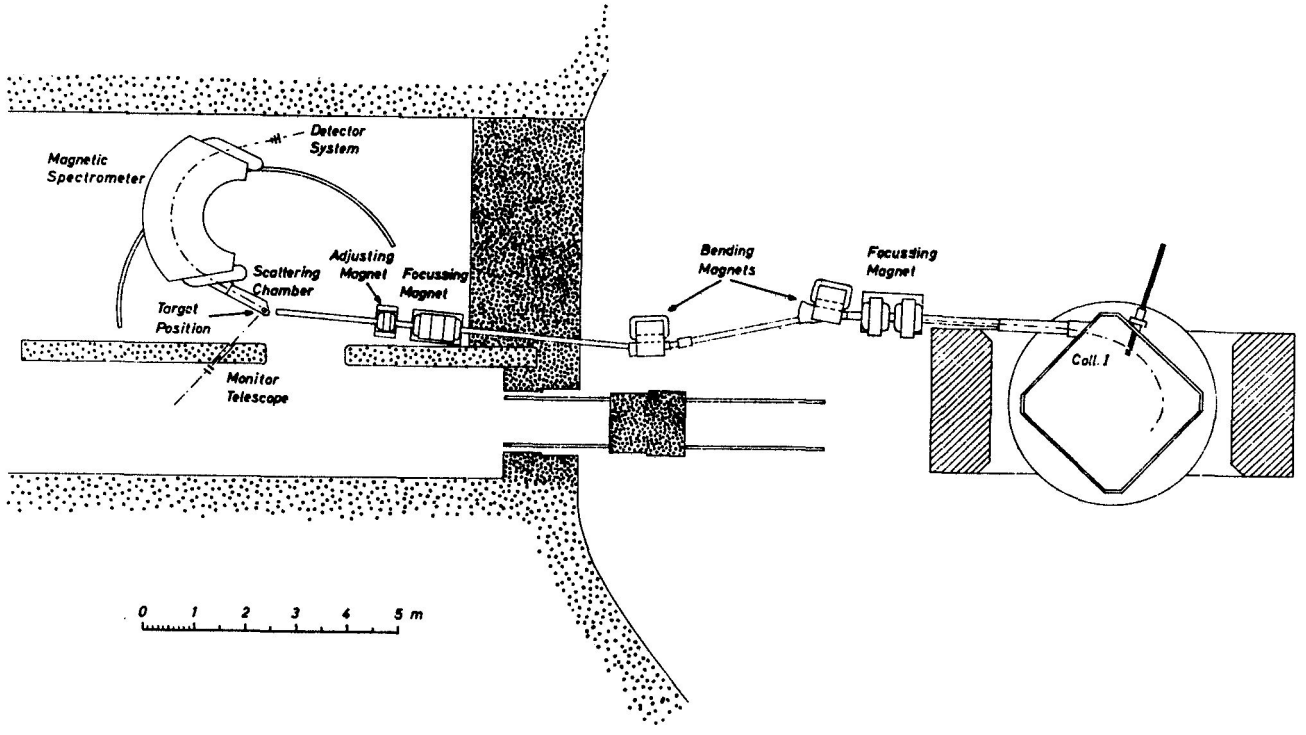

Figure 5-1

Schematic Drawing of the Experimental Area

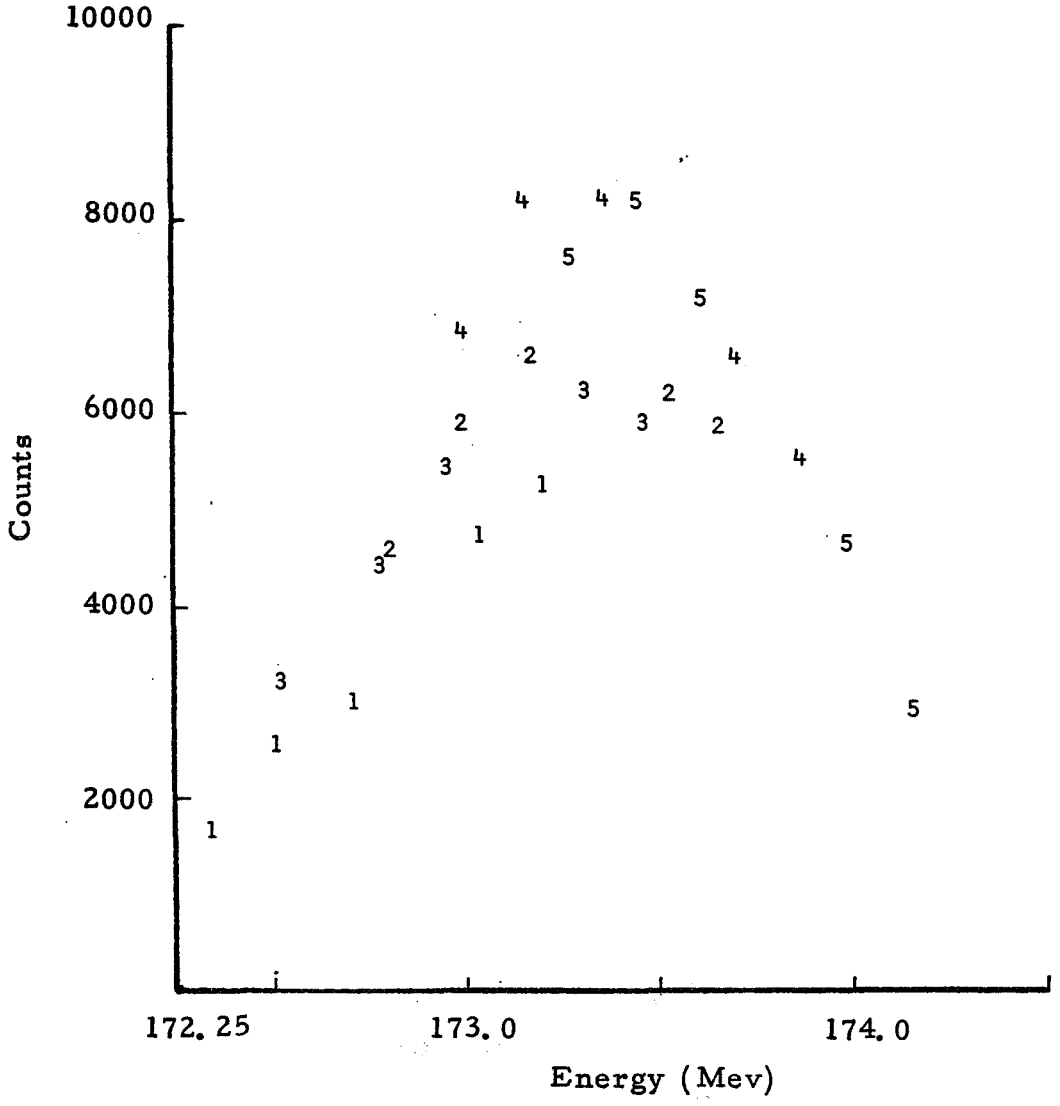

Figure 5-2

Counts as a Function of Energy after Computer Analysis for Pb ($\rho dx = 5.105$)

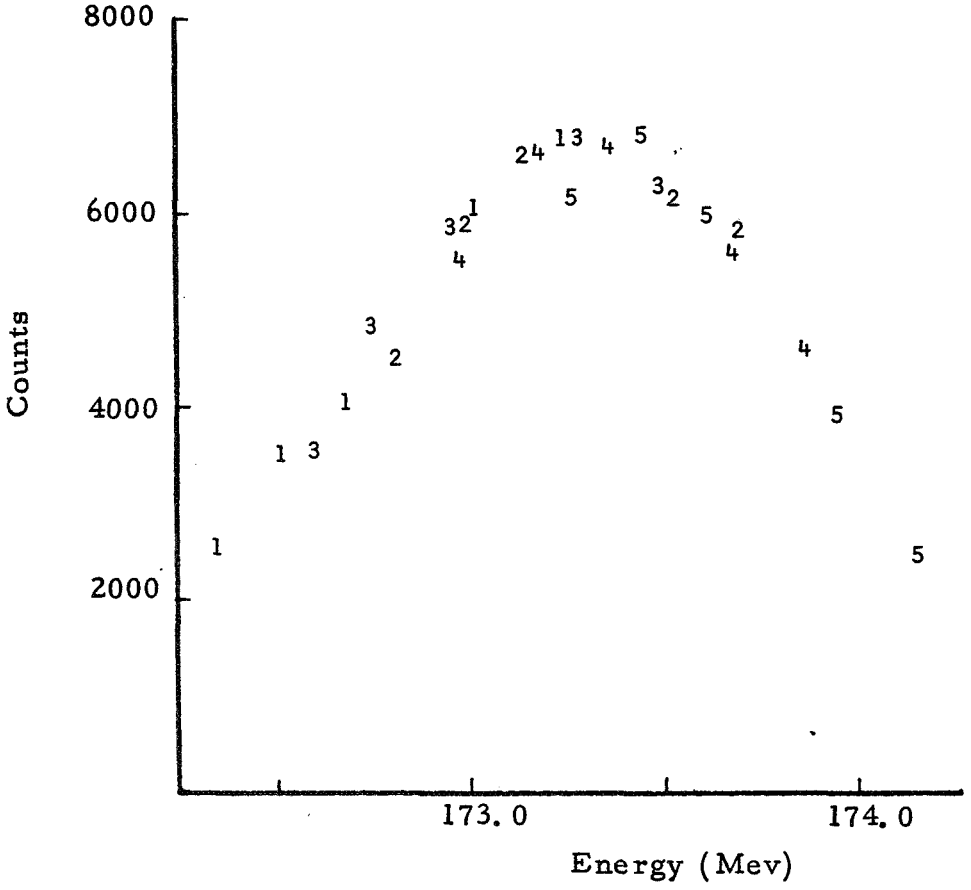

Figure 5-3

Normalized Curves for Pb ($\rho dx = 5.105$)

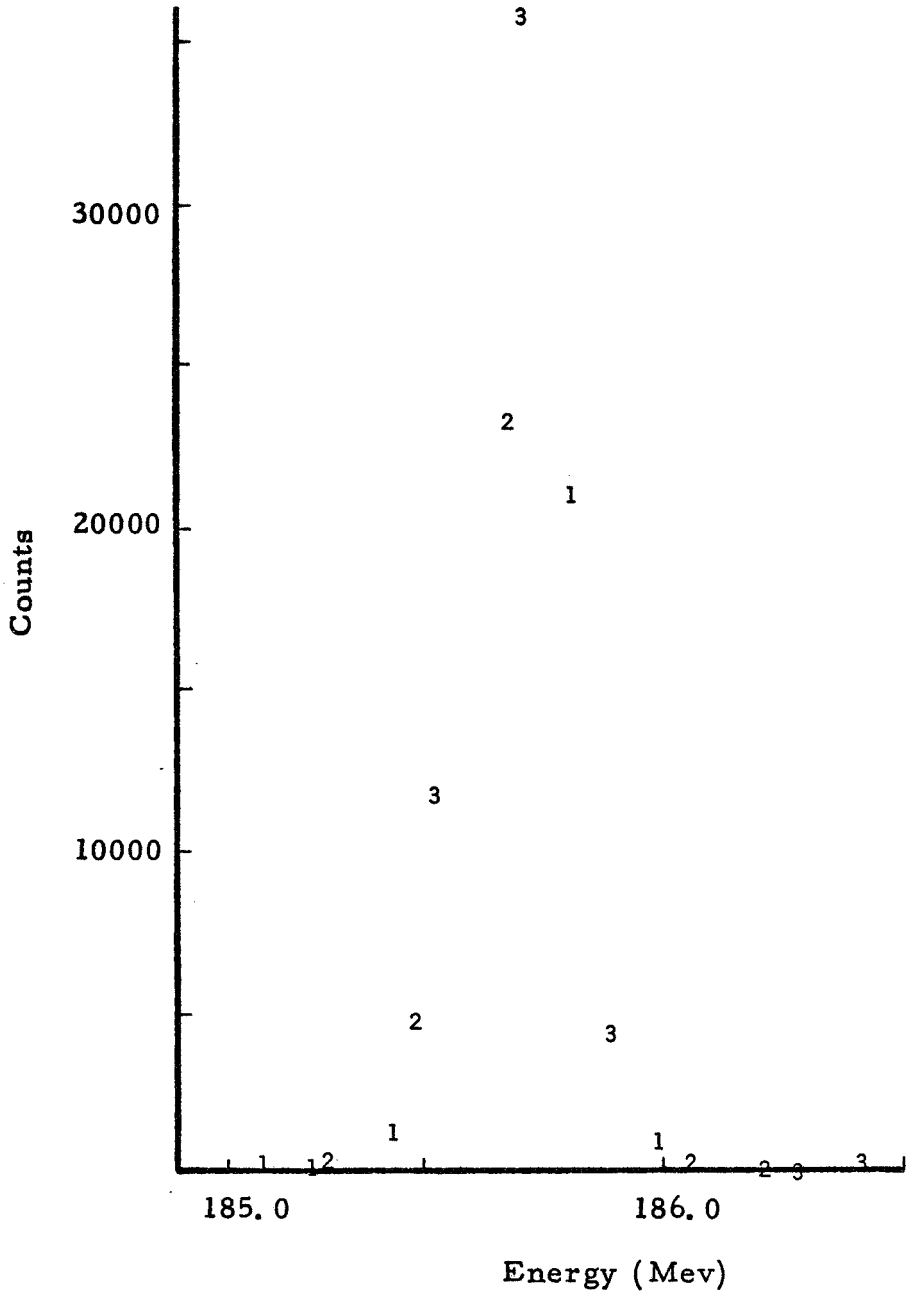

Figure 5-4

Counts as a Function of Energy After Computer Analysis for a Typical No-Absorber Run

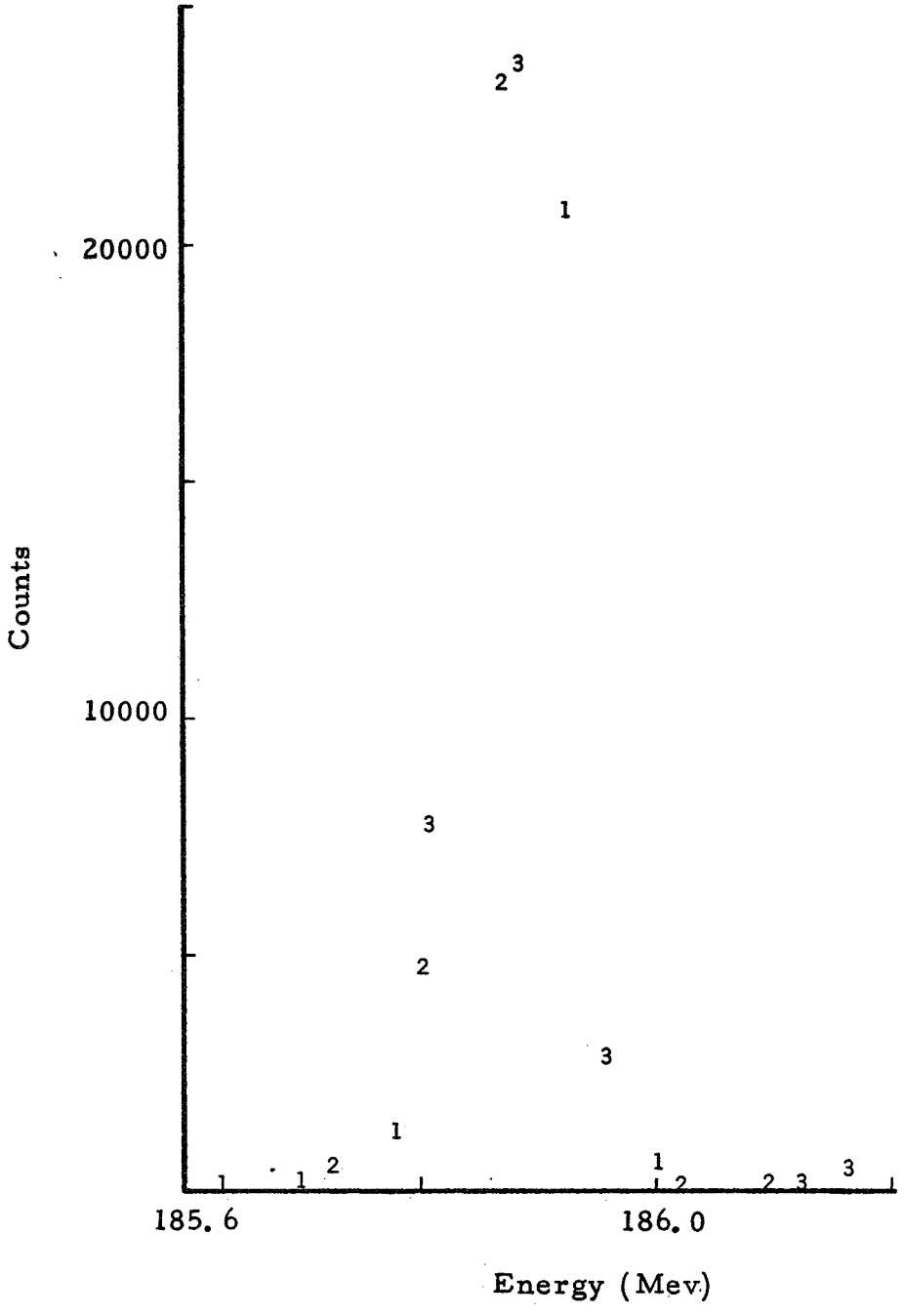

Figure 5-5

Normalized Curves for a Typical No-Absorber Run

TABLE 5-1

Results of the Uppsala Computer Analysis for Pb ($\rho\, dx = 5.105$)

Line No.	Ch. No.	Ch. Width	Energy	Counts	Stand. Dev.[a]	Max.[b]	Min.[c]
5	1	0.1737	174.130	2982.25	54.23	3036.48	2928.02
5	2	0.1732	173.956	4760.20	68.82	4829.02	4691.38
4	1	0.1734	173.851	5652.86	74.66	5727.52	5578.20
5	3	0.1727	173.783	0.00	0.00	0.00	0.00
4	2	0.1729	173.678	7028.86	83.63	7112.49	6945.23
2	1	0.1733	173.668	5822.49	75.78	5898.26	5746.71
5	4	0.1722	173.611	7289.87	85.51	7375.38	7204.36
4	3	0.1724	173.505	0.00	0.00	0.00	0.00
2	2	0.1728	173.495	6308.46	79.23	6387.69	6229.23
3	1	0.1731	173.454	5921.10	76.42	5997.52	5844.69
5	5	0.1717	173.438	8207.53	91.38	8298.90	8116.15
4	4	0.1719	173.333	8232.70	90.87	8323.57	8141.83
2	3	0.1723	173.322	0.00	0.00	0.00	0.00
3	2	0.1726	173.281	6232.84	78.75	6311.59	6154.08
5	6	0.1712	173.266	7576.42	87.00	7663.42	7489.42
1	1	0.1728	173.198	5272.16	72.12	5246.28	5202.04
4	5	0.1715	173.161	8146.49	91.04	8237.53	8055.46
2	4	0.1718	173.150	6595.79	81.34	6677.12	6514.45
3	3	0.1721	173.108	0.00	0.00	0.00	0.00
1	2	0.1723	173.025	4800.00	69.11	4869.11	4730.89
4	6	0.1710	172.989	6805.19	82.45	6887.65	6722.74
2	5	0.1713	172.978	5920.65	77.61	5998.26	5843.04
3	4	0.1716	172.936	5480.44	74.14	5554.58	5406.30
1	3	0.1718	172.853	0.00	0.00	0.00	0.00
2	6	0.1708	172.806	4563.44	67.52	4630.96	4495.92
3	5	0.1711	172.765	4455.75	67.33	4523.07	4388.42
1	4	0.1713	172.681	3217.65	56.81	3274.46	3160.84
3	6	0.1706	172.593	3392.61	58.22	3450.82	3334.39
1	5	0.1709	172.510	2669.38	52.11	2721.49	2617.27
1	6	0.1704	172.339	1806.19	42.48	1848.67	1763.72

[a] Standard Deviation in counts

[b] Maximum = Counts plus Standard Deviation

[c] Minimum = Counts minus Standard Deviation

TABLE 5-2

Results of the Uppsala Computer Analysis for a Typical No-Absorber Run

Line Number	Channel Number	Channel Width	Energy	Counts	Standard Deviation[a]	Maximum[b]	Minimum[c]
3	1	0.1850	186.436	607.50	24.48	631.97	583.02
3	2	0.1845	186.251	67.66	8.21	75.87	59.46
2	1	0.1848	186.225	311.64	17.53	329.17	294.11
3	3	0.1840	186.067	0.00	0.00	0.00	0.00
2	2	0.1843	186.040	238.81	15.41	254.22	223.39
1	1	0.1846	185.983	1001.97	31.43	1033.41	970.54
3	4	0.1835	185.883	4589.77	67.85	4657.62	4521.92
2	3	0.1838	185.856	0.00	0.00	0.00	0.00
1	2	0.1841	185.799	21106.47	144.92	21251.39	20961.55
3	5	0.1829	185.699	35947.10	191.23	36138.33	35755.87
2	4	0.1833	185.672	23835.51	154.62	23990.13	23680.89
1	3	0.1836	185.615	0.00	0.00	0.00	0.00
3	6	0.1824	185.516	11884.12	108.96	11993.08	11775.16
2	5	0.1827	185.489	4992.88	71.27	5064.15	4921.61
1	4	0.1830	185.431	1360.08	36.93	1397.01	1323.15
2	6	0.1822	185.306	575.42	23.98	599.40	551.45
1	5	0.1825	185.248	390.64	19.93	410.58	370.71
1	6	0.1820	185.066	247.75	15.73	263.48	232.02

[a]Standard Deviation in counts
[b]Maximum = Counts plus Standard Deviation
[c]Minimum = Counts minus Standard Deviation

TABLE 5-3

Mean Energy Lost by 185 MeV Protons
In Traversing Various Materials

Material	dx gm/cm^2	Mean Energy Loss (MeV)	FWHM (MeV)
Aluminum	1.685	6.35 ±.15	0.90 ±.06
	3.235	12.36 ±.05	1.29 ±.04
	4.660	17.92 ±.05	1.64 ±.05
	5.929	22.97 ±.11	1.79 ±.06
Beryllium	1.599	6.35 ±.05	0.83 ±.04
	3.082	12.43 ±.10	1.40 ±.05
	4.403	17.89 ±.10	1.54 ±.05
Carbon	1.985	8.59 ±.05	1.14 ±.05
	2.840	12.40 ±.05	1.28 ±.05
	2.856	12.50 ±.05	1.41 ±.05
Copper	3.781	12.46 ±.20	1.44 ±.05
	5.425	18.08 ±.20	1.50 ±.05
Iron	3.217	10.80 ±.05	1.13 ±.05
	3.244	10.91 ±.10	1.55 ±.05
	6.304	21.63 ±.10	1.85 ±.05
	6.339	21.79 ±.10	1.82 ±.05
Lead	5.106	12.43 ±.05	1.30 ±.05
	5.205	12.65 ±.05	1.39 ±.05
	7.858	19.30 ±.05	1.92 ±.05
	7.893	19.37 ±.05	1.79 ±.05
Silicon	0.233	0.82 ±.05	0.31 ±.05
	1.164	4.46 ±.05	0.82 ±.05
	2.328	9.03 ±.05	1.36 ±.05
	4.656	18.37 ±.10	1.60 ±.05
Lucite ($C_5H_8O_2$)	1.513	7.12 ±.10	1.07 ±.05
	2.260	10.42 ±.10	1.43 ±.05
	3.020	14.11 ±.10	1.43 ±.05
Nylon ($C_{12}H_{22}O_2N_2$)	1.450	6.92 ±.10	0.84 ±.05
	2.900	14.08 ±.10	1.44 ±.05
Polyethylene $(CH_2)^n$	1.199	6.16 ±.10	1.04 ±.05
	2.396	12.17 ±.10	1.28 ±.05
Tissue Equivalent ($C_{27}H_{21}ON$)	2.090	11.31 ±1.0	2.73 ±.10
	2.781	13.35 ±.20	1.46 ±.05

CHAPTER 6

MEAN IONIZATION POTENTIAL FOR MONTE CARLO PENETRATION OF CHARGED PARTICLES IN MATTER

by George W. Crawford

Introduction

The mean ionization potential, I, is defined as the mean value of the minimum energy transfer in an atomic collision which produces an ionization event. All of the atomic electrons are considered to participate in the collision process (1). It is treated here as a property of the material under consideration and not as a function of the kind or speed of the incident particle. I is the main parameter of the stopping power formula derived in Chapter 2 (1) based on the work of Bohr (2,3). A survey of the modifications and calculational methods used to determine charged particle energy degradation as a function of penetration depth in matter is given in Nuclear Science Series Report Number 39 (4). Tables of energy losses and ranges are given based on adjusted values of I determined from earlier stopping power or range measurements and assuming a "straight-ahead model." This model assumes that the incident particles lose energy by ionization losses with the removal of atomic electrons in the target material with no subsequent change in the incident particle direction.

This paper uses the latest form of the "straight-ahead" stopping power equation as part of a Monte Carlo nucleon transport program, PROTOS 3. This program is reported in detail in Volume 68-2 of this report (5). The incident particle is permitted to interact with the free and bound atomic electrons, to undergo small angle scattering from the electrons, to have large angle scattering from the nucleus and to create nuclear reactions. As nearly as possible, the program attempts to duplicat the actual path of any incident particle. As shown by Berger and Seltzer, (5), the "straight-ahead" model assumption that the path of the particle is the shortest distance from entrance to exit in a medium can be corrected in a number of ways. PROTOS 3 corrects for this by permitting multiple scattering. It further treats each particle penetration as an individual history, different from all others. A Monte Carlo histogram is compiled giving the distribution of emerging particles with respect to location, angle of emergence and energy of the particle as it emerges. A number of histograms are given in Chapter 3 (6). The evaluation of the most probable energy loss suffered by protons perpendicularly incident on plane parallel absorbers was carried out using the parametrization procedure derived in detail in Chapters 1 and 2 (7,8) of this report.

Procedure

Emerging energy histograms were calculated using PROTOS for each of the data points reported in Chapters 4 and 5 of this report (9,10). The value for I used for the initial run was that reported in Science Series Report Number 39 (4), for each element. The silicon value used was that provided by Bichsel (11). Bichsel also provided verification that the stopping power and shell correction program was correct. The value of I was then varied

TABLE 1

DETERMINATION OF MEAN IONIZATION POTENTIAL, I, OF BERYLLIUM

Absorber Thickness ρdx ±.001 (g/cm^2)	Measured ΔE (Mev)	Monte Carlo Calculated I = 53 eV ΔE (MeV)	The Change In ΔE Produced By A Change In: ρdx of .001 Δ(ΔE) (MeV)	I of 1 eV Δ(ΔE) (MeV)	E of .1 MeV Δ(ΔE) (MeV)	Most Probable Value Of I (eV)
		E_o = 185.6 MeV				
1.599	6.35±.05	6.35	.004	.014	.002	53.
3.082	12.43±.10	12.40	.004	.026	.004	51.8
4.403	17.89±.10	17.88	.004	.038	.006	52.7
		E_o = 159.75				
1.599	7.04±.03	7.05	.0045	.015	.002	53.7
3.082	13.77±.04	13.79	.0046	.029	.006	53.7
4.403	19.97±.05	19.99	.0048	.043	.008	53.4
		E_o = 99.9				
1.599	10.10±.02	10.12	.0065	.023	.007	53.7
3.082	20.16±.04	20.26	.0071	.066	.015	54.5
4.403	30.38±.05	30.42	.0080	.077	.030	53.6

TABLE 2

DETERMINATION OF MEAN IONIZATION POTENTIAL, I, OF CARBON

Absorber Thickness ρdx ±.001 (g/cm^2)	Measured ΔE (MeV)	Monte Carlo Calculated I = 72eV ΔE (MeV)	The Change In ΔE Produced By A Change In: ρdx of .001 Δ(ΔE) (MeV)	I of 1 eV Δ(ΔE) (MeV)	E of .1 MeV Δ(ΔE) (MeV)	Most Probable Value Of I (eV)
		E_o = 185.6 MeV				
1.985	8.59±.05	8.60	.0043	.011	.002	72.6
2.840	12.40±.10	12.41	.0045	.021	.003	72.5
2.856	12.50±.14	12.49	.0045	.030	.003	71.5
		E_o = 159.75 MeV				
1.985	9.60±.04	9.57	.005	.016	.002	70.8
2.840	13.82±.05	13.81	.005	.024	.005	71.7
3.621	17.83±.05	17.78	.005	.031	.006	70.6
		E_o = 99.9 MeV				
1.037	7.03±.02	7.03	.007	.013	.006	72.
1.985	13.82±.03	13.86	.007	.026	.009	73.5
2.856	20.43±.05	20.45	.007	.040	.012	72.5
3.636	26.68±.10	26.80	.007	.068	.026	73.7

TABLE 3

DETERMINATION OF MEAN IONIZATION POTENTIAL, I, OF ALUMINUM

Absorber Thickness ρdx ±.001 (g/cm^2)	Measured ΔE (MeV)	Monte Carlo Calculated I=163 eV ΔE (MeV)	The Change In ΔE Produced By A Change In ρdx of .001 Δ(ΔE) (MeV)	The Change In ΔE Produced By A Change In I of 1 eV Δ(ΔE) (MeV)	The Change In ΔE Produced By A Change In Eo of .1 MeV Δ(ΔE) (MeV)	Most Probable Value Of I (eV)
	E_o = 185.6 MeV					
1.685	6.35±.15	6.344	.0038	.005	.002	161.8
3.235	12.26±.05	12.297	.0039	.010	.004	166.2
4.660	17.92±.05	17.894	.0040	.015	.006	161.3
5.929	22.97±.11	22.984	.0041	.020	.009	163.7
	E_o = 159.75 MeV (Range = 22.607±.001 g/cm^2)					
1.685	7.03±.02	7.024	.0042	.006	.002	162.
3.235	13.67±.03	13.672	.0044	.013	.006	163.1
4.660	19.98±.03	19.993	.0046	.021	.008	163.6
5.929	25.76±.04	25.756	.0046	.030	.010	162.9
	E_o = 99.9 MeV (Range = 9.935±.001 g/cm^2)					
1.685	9.97±.02	9.98	.0061	.009	.008	163.9
3.235	19.94±.03	19.95	.0068	.019	.018	163.5
4.660	30.02±.04	30.02	.0074	.031	.031	163.
5.929	39.99±.05	39.99	.0084	.044	.047	163.
	E_o = 36.2 MeV (Range = 1.645±.001 g/cm^2)					
.135	1.704±.01	1.710	.0013	.0016	.005	166.6
.270	3.477±.01	3.486	.0013	.0037	.010	164.6
.4055	5.329±.02	5.342	.0014	.006	.015	164.5
.540	7.273±.02	7.288	.0015	.008	.020	163.8
	E_o = 14 MeV					
.01323	.349±.01	.3508	.027	.00034	.002	168.
.01981	.529±.01	.5287	.027	.00051	.004	162.
.02646	.704±.01	.7083	.028	.00069	.005	168.
	E_o = 11 MeV					
.01323	.421±.01	.424	.032	.00041	.002	170.
.01981	.636±.01	.638	.033	.0009	.005	165.
.02646	.868±.01	.860	.034	.0011	.006	156.
	E_o = 8 MeV					
.01323	.546±.01	.545	.043	.00063	.006	161.
.01981	.831±.01	.830	.044	.00098	.007	162.
.02646	1.128±.01	1.124	.045	.00017	.013	160.

TABLE 4

DETERMINATION OF MEAN IONIZATION POTENTIAL, I, OF SILICON

Absorber Thickness ρdx ±.001 (g/cm^2)	Measured ΔE (MeV)	Monte Carlo Calculated I=172.5eV ΔE (MeV)	The Change In ΔE Produced By A Change In ρdx of .001 Δ(ΔE) (MeV)	The Change In ΔE Produced By A Change In I of 1 eV Δ(ΔE) (MeV)	The Change In ΔE Produced By A Change In E of .1 MeV Δ(ΔE) (MeV)	Most Probable Value Of I (eV)
		E_o = 185.6 MeV				
0.233	0.82±.05	.814	.0038	.002	.002	169.5
1.164	4.46±.15	4.485	.0039	.004	.002	178.7
2.328	9.03±.10	9.038	.0039	.007	.003	173.6
4.656	18.37±.10	18.374	.0041	.015	.004	172.8
		E_o = 159.75 MeV				
2.328	10.00±.02	10.005	.0044	.009	.004	172.9
3.503	15.15±.02	15.134	.0046	.014	.006	171.4
4.656	20.48±.02	20.495	.0047	.020	.007	173.3
6.984	31.72±.05	31.585	.0049	.039	.012	169.1
9.335	43.74±.05	43.63	.0053	.058	.023	170.6
		E_o = 36.2 MeV				
.3306	4.42±.03	4.409	.013	.0043	.004	170.
.6612	9.38±.03	9.353	.014	.0102	.006	169.5
.9941	15.10±.05	15.195	.022	.0184	.081	178.
		E_o = 14 MeV				
.0856	2.50±.01	2.484	.031	.0034	.017	168.
.1676	5.30±.01	5.353	.040	.0073	.108	179.
		E_o = 11 MeV				
.0856	3.14±.01	3.129	.042	.003	.029	170.
.1676	7.61±.01	7.606	.081	.017	.140	170.
		E_o = 8 MeV				
.0856	4.60±.01	4.669	.083	.0092	.096	173.

TABLE 5

DETERMINATION OF MEAN IONIZATION POTENTIAL, I, OF COPPER

Absorber Thickness ρdx ±.001 (g/cm^2)	Measured ΔE (MeV)	Monte Carlo Calculated I=314 eV ΔE (MeV)	The Change In ΔE Produced By A Change In ρdx of .001 Δ(ΔE) (MeV)	I of 1 eV Δ(ΔE) (MeV)	E of .1 MeV Δ(ΔE) (MeV)	Most Probable Value Of I (eV)
		E_o = 185.6 MeV				
3.781	12.44±.20	12.46	.003	.006	.006	317.2
5.423	18.05±.20	18.02	.0033	.007	.009	312.1
		E_o = 159.75 MeV				
3.781	13.73±.03	13.75	.0037	.006	.008	317.2
5.423	20.05±.05	20.03	.0038	.009	.013	312.1
7.102	26.62±.10	26.64	.0040	.013	.022	315.5
		E_o = 99.9 MeV				
1.974	10.00±.02	10.01	.0046	.005	.005	316.
3.781	19.93±.03	19.97	.0058	.011	.012	317.4
5.423	29.95±.02	29.95	.0063	.018	.023	314.
		E_o = 36.2 MeV				
.106	1.12±.01	1.121	.011	.0007	.003	314.
.164	1.74±.01	1.747	.011	.0011	.004	320.
.263	2.84±.01	2.835	.011	.0017	.007	311.
.318	3.44±.02	3.451	.011	.0021	.008	319.
.424	4.68±.02	4.666	.011	.0029	.011	309.
		E_o = 14 MeV				
.0463	1.04±.01	1.040	.023	.0007	.003	314.
.09245	2.12±.01	2.132	.025	.0017	.007	321.
.1112	2.63±.01	2.619	.027	.0020	.009	309.
.1540	3.78±.01	3.759	.030	.0031	.014	307.
		E_o = 11 MeV				
.0463	1.281±.01	1.274	.0286	.0010	.005	307.
.09245	2.635±.01	2.659	.0322	.0023	.012	324.
.1112	3.294±.01	3.289	.0345	.0030	.015	312.
.1540	4.974±.01	4.958	.0372	.0040	.018	310.
		E_o = 8 MeV				
.0463	1.704±.01	1.691	.041	.0013	.019	304.
.09245	3.788±.01	3.782	.056	.0042	.061	316.
.1112	4.880±.01	4.887	.071	.0065	.101	313.

TABLE 6

DETERMINATION OF MEAN IONIZATION POTENTIAL, I, OF IRON

Absorber Thickness ρdx ±.001 (g/cm^2)	Measured ΔE (MeV)	Monte Carlo Calculated I = 302 eV ΔE (MeV)	The Change In ΔE Produced By A Change In: ρdx of .001 Δ(ΔE) (MeV)	I of 1 eV Δ(ΔE) (MeV)	E of .1 MeV Δ(ΔE) (MeV)	Most Probable Value Of I (eV)
		E_o = 185.6 MeV				
3.217	10.80±.10	10.805	.0035	.005	.005	303.
3.244	10.91±.10	10.91	.0036	.005	.005	302.
6.304	21.63±.10	21.61	.0036	.011	.012	300.2
6.339	21.79±.10	21.73	.0036	.011	.012	296.6
		E_o = 159.75 MeV				
3.244	12.17±.05	12.12	.0038	.007	.008	295.
6.339	24.34±.05	24.30	.0039	.013	.019	299.1
		E_o = 99.9 MeV				
1.666	8.65±.02	8.66	.0054	.005	.004	304.
3.244	17.41±.04	17.44	.0058	.010	.010	305.
6.304	36.78±.05	36.80	.0070	.020	.026	303.

TABLE 7

DETERMINATION OF MEAN IONIZATION POTENTIAL, I, OF LEAD

Absorber Thickness ρdx ±.001 (g/cm^2)	Measured ΔE (MeV)	Monte Carlo Calculated I = 840 eV ΔE (MeV)	The Change In ΔE Produced By A Change In: ρdx of .001 Δ(ΔE) (MeV)	I of 1 eV Δ(ΔE) (MeV)	E of .1 MeV Δ(ΔE) (MeV)	Most Probable Value Of I (eV)
		E_o = 185.6 MeV				
5.106	12.43±.05	12.426	.0025	.0025	.009	838.4
5.205	12.65±.05	12.647	.0025	.0025	.009	838.8
7.858	19.30±.05	19.296	.0025	.0040	.016	841.
7.893	19.37±.05	19.381	.0025	.0040	.017	842.8
		E_o = 159.75 MeV				
5.106	13.74±.03	13.703	.0027	.0030	.012	827.5
5.205	13.89±.02	13.925	.0028	.0031	.013	851.3
7.858	21.56±.02	21.555	.0029	.0047	.022	839.5
		E_o = 99.9 MeV				
2.680	9.94±.05	9.943	.0036	.0030	.006	841.
2.723	10.11±.02	10.105	.0036	.0030	.006	838.3
5.205	20.08±.04	20.084	.0038	.0048	.016	840.8
7.893	31.89±.03	31.896	.0038	.0076	.028	840.8

until the calculated ΔE for the given absorber and ρdx was the same as that measured. The many values of I, each duplicating a data point, are given in seven tables, one for each element. Each table also contains the ρdx, E_o, measured ΔE, value of ΔE calculated using the nearest whole value for I, the experimental value for I and the effects of errors in I, E_o and ρdx on the calculated ΔE value. The tables are numbered 1 through 7 and arranged in increasing values of Z, for Be, C, Al, Si, Fe, Cu and Pb.

Consider the case of the aluminum absorber having a ρdx of 5.929 g/cm^2 (see Table 3). The average of four measurements of ΔE at E_o = 185.6 MeV was 22.97 ±.11 using the magnetic spectrometer. Assuming a value of I = 163.0 eV, the Monte Carlo calculated ΔE was 22.984 MeV. The LINEAR calculated ΔE was 22.946 MeV. If the shell correction and density factors were removed from the program, both calculated ΔE's were increased by 0.015 MeV. A change of 1 eV in the value of I produced a change of 0.020 in the calculated value of ΔE. Thus the difference between LINEAR and MONTE CARLO transport calculations represented a difference of 1.9 eV in the determination of I. The shell correction represented a difference of only 0.75 eV in I.

If an error of 0.1 MeV had been made in measuring E_o, then ΔE was in error by 0.009 MeV. The magnetic field in the spectrometer was stable to about one part in 25000, corresponding to an uncertainty in E_o of 0.15 MeV, or an error in ΔE of 0.014 and in I of .7 eV.

An error of 0.001 g/cm^2 in the ρdx measurement causes a change of 0.0041 MeV in the calculated ΔE. The material used was the purest available, 99.96 %, and the measurements had been made with great care and precision. The many absorbers had been checked for internal holes. Handling was done to minimize damage. Positioning was done within 1 degree in the holder and the holder in the beam. This is the major error in the ρdx value used. Thus the error in I caused by the ρdx measurement was not greater than 0.2 eV.

The combined errors in determining I from the measured values of E_o, ρdx and ΔE gave a maximum uncertainty of 5 eV. The difference between Linear and Monte Carlo determinations is roughly half that. The most probable value of I to use in the Monte Carlo program is 163.7 eV, for this data point.

The average of four measurements of ΔE at E_o = 159.75 MeV for the same set of absorbers was 25.76 ± .04 MeV, using silicon detectors to totally absorb the protons emerging from the absorbers in the straight ahead direction as described in Chapter 4 (9). Assuming a value of I = 163.0 eV, the Monte Carlo calculated ΔE was 25.756 MeV. The LINEAR calculated ΔE was 25.721. Using both programs to match the measured ΔE, the most probable value for the Monte Carlo calculation of I was 162.86 as compared to the linear calculation of I = 161.7. The maximum possible error from a ρdx or E_o measurement would change I by 1.5 eV. Removal of the shell corrections and density factors caused an increase of .04 MeV in ΔE. For the same set of absorbers, at E_o = 99.9 MeV, the removal of the corrections gave an increase of .12 MeV in ΔE. The average measured ΔE was 39.99 MeV. Using I = 163.0, the Monte Carlo ΔE was 39.991 MeV, and the Linear ΔE was 39.958. The best linear I would be 162.9.

Using LINEAR calculation technics, the data reported here would give a value for I of 161.1 eV. The Monte Carlo average value based on the 25 average ΔE measurements at seven different energies is 163.8 eV. The greatest variation in the values for I occurred in the low energies. The standard deviation for the 25 data points is 3.7 and the probable error is 2.0 eV.

TABLE 8

MONTE CARLO STOPPING POWER, RANGE AND ENERGY LOSS VALUES FOR PROTONS

IN BERYLLIUM: I = 53.34 eV, Z = 4, A = 9.012, ρ = 1.844

Energy	Stopping Power	Range	Range	Most Probable Energy Loss		
				in 1 mm	in 5 mm	in 10 mm
(MeV)	(MeV cm^2/g)	(g/cm^2)	(cm)	(MeV)	(MeV)	(MeV)
2.0	136.87541	0.008	0.004	2.	2.	2.
3.0	101.00023	0.017	0.009	3.	3.	3.
4.0	80.83231	0.028	0.015	4.	4.	4.
5.0	67.79744	0.041	0.022	5.	5.	5.
6.0	58.62854	0.057	0.031	6.	6.	6.
7.0	51.80132	0.075	0.041	7.	7.	7.
8.0	46.50525	0.096	0.052	8.	8.	8.
9.0	42.26816	0.118	0.064	9.	9.	9.
10.0	38.79544	0.143	0.077	10.	10.	10.
12.0	33.42961	0.199	0.108	9.262	12.	12.
14.0	29.46494	0.262	0.142	6.867	14.	14.
16.0	26.40779	0.334	0.181	5.743	16.	16.
18.0	23.97363	0.414	0.224	5.011	18.	18.
20.0	21.98665	0.501	0.271	4.478	20.	20.
24.0	18.93118	0.697	0.378	3.737	24.	24.
28.0	16.68556	0.922	0.500	3.236	28.	28.
32.0	14.96136	1.176	0.637	2.868	18.264	32.
36.0	13.59349	1.456	0.789	2.586	15.276	36.
40.0	12.48031	1.763	0.956	2.361	13.387	40.
45.0	11.34856	2.183	1.184	2.137	11.738	28.868
50.0	10.42842	2.643	1.433	1.956	10.532	24.134
55.0	9.66487	3.140	1.703	1.808	9.600	21.229
60.0	9.02059	3.676	1.993	1.684	8.852	19.150
65.0	8.46932	4.247	2.303	1.579	8.234	17.552
70.0	7.99205	4.855	2.632	1.488	7.714	16.269
75.0	7.57464	5.497	2.981	1.409	7.269	15.208
80.0	7.20637	6.173	3.347	1.339	6.883	14.312
85.0	6.87895	6.882	3.732	1.277	6.545	13.541
90.0	6.58590	7.624	4.135	1.222	6.246	12.871
95.0	6.32199	8.399	4.554	1.173	5.979	12.281
100.0	6.08303	9.204	4.991	1.128	5.740	11.757
110.0	5.66704	10.907	5.914	1.050	5.327	10.864
120.0	5.31703	12.727	6.902	0.985	4.984	10.132
130.0	5.01839	14.662	7.951	0.929	4.694	9.518
140.0	4.76052	16.707	9.060	0.881	4.445	8.996
150.0	4.53561	18.857	10.226	0.839	4.229	8.545
160.0	4.33769	21.110	11.448	0.802	4.039	8.152
170.0	4.16218	23.461	12.723	0.770	3.872	7.807
180.0	4.00547	25.908	14.050	0.741	3.723	7.500
190.0	3.86472	28.447	15.427	0.715	3.590	7.266
200.0	3.73762	31.076	16.852	0.691	3.470	6.980
220.0	3.51715	36.590	19.843	0.650	3.262	6.555

TABLE 8 (Continued)

MONTE CARLO STOPPING POWER, RANGE AND ENERGY LOSS VALUES FOR PROTONS

IN BERYLLIUM: $I = 53.34$ eV, $Z = 4$, $A = 9.012$, $\rho = 1.844$

Energy	Stopping Power	Shielding Range in		Most Probable Energy Loss		
				in 1 mm	in 5 mm	in 10 mm
(MeV)	(MeV cm^2/g)	(g/cm^2)	(cm)	(MeV)	(MeV)	(MeV)
240.0	3.33260	42.429	23.009	0.616	3.089	6.202
260.0	3.17594	48.573	26.341	0.587	2.942	5.903
280.0	3.04137	55.004	29.828	0.562	2.816	5.648
300.0	2.92461	61.705	33.462	0.541	2.707	5.427
320.0	2.82242	68.661	37.234	0.521	2.612	5.234
340.0	2.73229	75.857	41.137	0.505	2.527	5.064
360.0	2.65226	83.280	45.162	0.490	2.453	4.914
380.0	2.58079	90.918	49.304	0.477	2.386	4.780
400.0	2.51661	98.758	53.556	0.465	2.327	4.659
425.0	2.44511	108.828	59.017	0.452	2.260	4.525
450.0	2.38184	119.179	64.631	0.440	2.201	4.407
475.0	2.32551	129.792	70.386	0.430	2.149	4.302
500.0	2.27510	140.651	76.275	0.421	2.102	4.208
525.0	2.22979	151.741	82.289	0.412	2.060	4.123
550.0	2.18888	163.047	88.420	0.404	2.002	4.047
575.0	2.15180	174.556	94.661	0.398	1.988	3.978
600.0	2.11809	186.255	101.006	0.391	1.957	3.915
625.0	2.08734	198.134	107.448	0.385	1.928	3.857
650.0	2.05921	210.181	113.981	0.380	1.902	3.805
675.0	2.03341	222.386	120.600	0.376	1.878	3.757
700.0	2.00969	234.742	127.300	0.371	1.856	3.713
725.0	1.98784	247.238	134.077	0.367	1.836	3.673
750.0	1.96766	259.866	140.925	0.363	1.817	3.635
775.0	1.94901	272.620	147.841	0.360	1.800	3.600
800.0	1.93172	285.492	154.822	0.357	1.784	3.568
825.0	1.91568	298.475	161.863	0.354	1.769	3.539
850.0	1.90077	311.564	168.961	0.351	1.755	3.511
875.0	1.88690	324.752	176.112	0.349	1.742	3.485
900.0	1.87397	338.034	183.315	0.346	1.730	3.461
925.0	1.86191	351.405	190.566	0.344	1.719	3.439
950.0	1.85065	364.859	197.863	0.342	1.709	3.418
975.0	1.84013	378.394	205.202	0.340	1.699	3.398
1000.0	1.83028	392.003	212.583	0.338	1.690	3.380
1100.0	1.79672	447.114	242.469	0.333	1.659	3.318
1200.0	1.77066	503.141	272.853	0.328	1.635	3.271
1300.0	1.75028	559.903	303.635	0.326	1.617	3.232
1400.0	1.73428	617.255	334.737	0.320	1.602	3.203
1500.0	1.72174	675.079	366.095	0.320	1.591	3.180
1600.0	1.71192	733.278	397.656	0.318	1.581	3.162
1700.0	1.70431	791.773	429.377	0.315	1.573	3.148
1800.0	1.69849	850.498	461.224	0.315	1.568	3.135
1900.0	1.69413	909.399	493.166	0.315	1.565	3.128
2000.0	1.69099	968.430	525.179	0.313	1.563	3.123

TABLE 9

MONTE CARLO STOPPING POWER, RANGE AND ENERGY LOSS VALUES FOR PROTONS

IN CARBON: I = 72.14 eV, Z = 6, A = 12.011, ρ = 1.582

Energy	Stopping Power	Range	Range	Most Probable Energy Loss		
				in 1 mm	in 5 mm	in 10 mm
(MeV)	(MeV cm^2/g)	(g/cm^2)	(cm)	(MeV)	(MeV)	(MeV)
2.0	143.12657	0.008	0.005	2.	2.	2.
3.0	106.12961	0.016	0.010	3.	3.	3.
4.0	85.27849	0.027	0.017	4.	4.	4.
5.0	71.49788	0.040	0.025	5.	5.	5.
6.0	62.03261	0.055	0.034	6.	6.	6.
7.0	54.94438	0.072	0.045	7.	7.	7.
8.0	49.42262	0.091	0.057	8.	8.	8.
9.0	44.99054	0.112	0.071	9.	9.	9.
10.0	41.34846	0.135	0.085	10.	10.	10.
12.0	35.70401	0.187	0.118	7.80	12.	12.
14.0	31.52017	0.247	0.156	6.107	14.	14.
16.0	28.28621	0.314	0.198	5.179	16.	16.
18.0	25.70627	0.388	0.245	4.550	18.	18.
20.0	23.59694	0.469	0.296	4.084	20.	20.
24.0	20.34734	0.652	0.412	3.426	24.	24.
28.0	17.95422	0.861	0.544	2.975	21.083	28.
32.0	16.11388	1.096	0.693	2.643	16.244	32.
36.0	14.65200	1.356	0.857	2.386	13.817	36.
40.0	13.46108	1.641	1.037	2.182	12.201	33.726
45.0	12.24908	2.030	1.283	1.976	10.756	25.498
50.0	11.26276	2.456	1.552	1.811	9.683	21.777
55.0	10.44365	2.916	1.843	1.675	8.846	19.328
60.0	9.75200	3.411	2.156	1.562	8.170	17.525
65.0	9.15985	3.940	2.490	1.465	7.610	16.116
70.0	8.64690	4.501	2.845	1.381	7.137	14.974
75.0	8.19806	5.094	3.220	1.308	6.731	14.023
80.0	7.80190	5.718	3.614	1.244	6.378	13.215
85.0	7.44956	6.373	4.028	1.187	6.609	12.518
90.0	7.13408	7.058	4.461	1.136	5.795	11.910
95.0	6.84988	7.772	4.913	1.090	5.550	11.373
100.0	6.59247	8.515	5.382	1.049	5.330	10.895
110.0	6.14417	10.085	6.375	0.977	4.951	10.079
120.0	5.76681	11.764	7.436	0.916	4.634	9.408
130.0	5.44469	13.546	8.563	0.865	4.366	8.845
140.0	5.16644	15.430	9.753	0.821	4.136	8.364
150.0	4.92368	17.410	11.005	0.782	3.937	7.949
160.0	4.70999	19.484	12.316	0.748	3.762	7.587
170.0	4.52044	21.649	13.684	0.717	3.607	7.268
180.0	4.35117	23.901	15.108	0.690	3.470	6.985
190.0	4.19910	26.237	16.585	0.666	3.346	6.732
200.0	4.06175	28.655	18.113	0.644	3.235	6.504
220.0	3.82344	33.726	21.319	0.607	3.042	6.111

TABLE 9 (Continued)

MONTE CARLO STOPPING POWER, RANGE AND ENERGY LOSS VALUES FOR PROTONS

IN CARBON: I = 72.14 eV, Z = 6, A = 12.011, ρ = 1.582

Energy	Stopping Power	Shielding in	Range	Most Probable Energy Loss		
				in 1 mm	in 5 mm	in 10 mm
(MeV)	(MeV cm^2/g)	(g/cm^2)	(cm)	(MeV)	(MeV)	(MeV)
240.0	3.62391	39.095	24.712	0.575	2.882	5.784
260.0	3.45449	44.742	28.282	0.548	2.745	5.508
280.0	3.30895	50.651	32.017	0.525	2.629	5.271
300.0	3.18264	56.807	35.908	0.505	2.528	5.067
320.0	3.07208	63.196	39.947	0.487	2.439	4.888
340.0	2.97456	69.804	44.124	0.472	2.361	4.730
360.0	2.88796	76.620	48.432	0.458	2.292	4.591
380.0	2.81062	83.631	52.864	0.446	2.230	4.466
400.0	2.74117	90.827	57.413	0.435	2.175	4.355
425.0	2.66381	100.068	63.254	0.423	2.113	4.230
450.0	2.59534	109.565	69.257	0.412	2.059	4.121
475.0	2.53439	119.301	75.411	0.402	2.010	4.023
500.0	2.47986	129.261	81.707	0.393	1.966	3.936
525.0	2.43084	139.430	88.135	0.385	1.927	3.857
550.0	2.38658	149.797	94.688	0.378	1.892	3.787
575.0	2.34649	160.347	101.357	0.373	1.860	3.722
600.0	2.31003	171.070	108.136	0.367	1.832	3.664
625.0	2.27679	181.959	115.018	0.361	1.805	3.611
650.0	2.24638	192.999	121.997	0.356	1.781	3.562
675.0	2.21850	204.183	129.066	0.352	1.759	3.518
700.0	2.19288	215.503	136.222	0.348	1.738	3.477
725.0	2.16928	226.951	143.458	0.344	1.719	3.439
750.0	2.14749	238.519	150.770	0.341	1.702	3.404
775.0	2.12735	250.200	158.154	0.337	1.686	3.373
800.0	2.10870	261.988	165.605	0.335	1.671	3.343
825.0	2.09139	273.877	173.121	0.332	1.658	3.315
850.0	2.07531	285.862	180.696	0.329	1.645	3.290
875.0	2.06036	297.936	188.328	0.327	1.633	3.266
900.0	2.04643	310.095	196.014	0.324	1.622	3.244
925.0	2.03345	322.334	203.751	0.322	1.611	3.223
950.0	2.02132	334.650	211.536	0.320	1.602	3.204
975.0	2.01000	347.036	219.365	0.319	1.593	3.186
1000.0	1.99941	359.491	227.238	0.317	1.584	3.169
1100.0	1.96336	409.916	259.112	0.313	1.557	3.112
1200.0	1.93544	461.164	291.507	0.307	1.534	3.068
1300.0	1.91367	513.070	324.317	0.305	1.518	3.034
1400.0	1.89666	565.502	357.460	0.302	1.503	3.005
1500.0	1.88338	618.353	390.867	0.300	1.492	2.984
1600.0	1.87306	671.535	424.484	0.297	1.484	2.969
1700.0	1.86512	724.976	458.265	0.297	1.479	2.956
1800.0	1.85911	778.616	492.172	0.297	1.474	2.945
1900.0	1.85468	832.407	526.174	0.294	1.471	2.940
2000.0	1.85157	886.307	560.244	0.294	1.469	2.935

TABLE 10

MONTE CARLO STOPPING POWER, RANGE AND ENERGY LOSS VALUES FOR PROTONS

IN ALUMINUM: I = 163. eV, Z = 13, A = 26.980, ρ = 2.702

Energy	Stopping Power	Range	Range	Most Probable Energy Loss		
				in 1mm	in 5 mm	in 10 mm
(MeV)	(MeV cm^2/g)	(g/cm^2)	(cm)	(MeV)	(MeV)	(MeV)
2.0	112.40285	0.0114	0.004	2.	2.	2.
3.0	83.96190	0.0217	0.008	3.	3.	3.
4.0	67.96378	0.0350	0.013	4.	4.	4.
5.0	57.55107	0.0510	0.018	5.	5.	5.
6.0	49.91376	0.0697	0.025	6.	6.	6.
7.0	44.46603	0.0909	0.033	7.	7.	7.
8.0	40.19299	0.1145	0.042	8.	8.	8.
9.0	36.74388	0.1405	0.052	9.	9.	9.
10.0	33.89330	0.1688	0.062	10.	10.	10.
12.0	29.44807	0.2321	0.085	12.	12.	12.
14.0	26.12646	0.3042	0.112	10.068	14.	14.
16.0	23.54118	0.3848	0.142	7.995	16.	16.
18.0	21.46654	0.4737	0.175	6.869	18.	18.
20.0	19.73187	0.5707	0.211	6.097	20.	20.
24.0	17.10208	0.7887	0.291	5.056	24.	24.
28.0	15.15052	1.0373	0.383	4.373	28.	28.
32.0	13.64088	1.3154	0.486	3.879	32.	32.
36.0	12.43610	1.6224	0.600	3.501	22.882	36.
40.0	11.45084	1.9573	0.724	3.201	19.306	40.
45.0	10.44458	2.4143	0.893	2.900	16.607	45.
50.0	9.62295	2.9127	1.078	2.660	14.763	38.647
55.0	8.93868	3.4513	1.277	2.462	13.385	31.683
60.0	8.35951	4.0291	1.491	2.296	12.302	27.840
65.0	7.86259	4.6452	1.719	2.155	11.421	25.162
70.0	7.43135	5.2986	1.961	2.034	10.686	23.123
75.0	7.05339	5.9884	2.216	1.928	10.062	21.493
80.0	6.71929	6.7137	2.484	1.834	9.524	20.146
85.0	6.42174	7.4739	2.766	1.751	9.054	19.008
90.0	6.15501	8.2682	3.060	1.677	8.639	18.029
95.0	5.91445	9.0958	3.366	1.611	8.271	17.176
100.0	5.69636	9.9561	3.684	1.550	7.941	16.423
110.0	5.31601	11.7720	4.356	1.446	7.373	15.153
120.0	4.99533	13.7108	5.074	1.357	6.901	14.119
130.0	4.72122	15.7680	5.835	1.282	6.503	13.258
140.0	4.48415	17.9392	6.639	1.217	6.162	12.528
150.0	4.27709	20.2201	7.483	1.161	5.866	11.900
160.0	4.09466	22.6070	8.366	1.111	5.607	11.354
170.0	3.93270	25.0961	9.288	1.066	5.378	10.875
180.0	3.78796	27.6839	10.245	1.027	5.174	10.450
190.0	3.65784	30.3671	11.238	0.992	4.991	10.071
200.0	3.54024	33.1426	12.266	0.960	4.827	9.731
220.0	3.33604	38.9583	14.418	0.904	4.543	9.145

TABLE 10 (Continued)

MONTE CARLO STOPPING POWER, RANGE AND ENERGY LOSS VALUES FOR PROTONS

IN ALUMINUM: I = 163. eV, Z = 13, A = 26.980, ρ = 2.702

Energy	Stopping Power	Shielding	Range in	Most Probable Energy Loss		
				in 1 mm	in 5 mm	in 10 mm
(MeV)	(MeV cm^2/g)	(g/cm^2)	(cm)	(MeV)	(MeV)	(MeV)
240.0	3.16491	45.108	16.694	0.857	4.305	8.658
260.0	3.01951	51.572	19.086	0.818	4.104	8.247
280.0	2.89452	58.331	21.588	0.784	3.932	7.896
300.0	2.78600	65.366	24.192	0.755	3.782	7.591
320.0	2.69097	72.663	26.892	0.729	3.652	7.326
340.0	2.60713	80.206	29.684	0.706	3.537	7.093
360.0	2.53267	87.980	32.561	0.686	3.435	6.886
380.0	2.46616	95.974	35.519	0.668	3.344	6.702
400.0	2.40643	104.174	38.554	0.652	3.262	6.537
425.0	2.33989	114.698	42.449	0.634	3.171	6.353
450.0	2.28102	125.507	46.450	0.618	3.091	6.191
475.0	2.22862	136.583	50.549	0.604	3.020	6.046
500.0	2.18174	147.908	54.740	0.591	2.955	5.917
525.0	2.13962	159.465	59.017	0.580	2.898	5.802
550.0	2.10161	171.241	63.375	0.569	2.846	5.697
575.0	2.06718	183.221	67.809	0.560	2.800	5.603
600.0	2.03590	195.393	72.314	0.552	2.757	5.518
625.0	2.00739	207.745	76.885	0.544	2.718	5.439
650.0	1.98133	220.266	81.519	0.537	2.682	5.368
675.0	1.95745	232.945	86.212	0.530	2.650	5.303
700.0	1.93553	245.774	90.960	0.524	2.620	5.243
725.0	1.91535	258.742	95.759	0.519	2.593	5.187
750.0	1.89673	271.843	100.608	0.514	2.567	5.137
775.0	1.87954	285.068	105.502	0.509	2.544	5.090
800.0	1.86364	298.409	110.440	0.505	2.522	5.046
825.0	1.84890	311.861	115.418	0.501	2.502	5.006
850.0	1.83522	325.417	120.435	0.497	2.484	4.969
875.0	1.82252	339.070	125.488	0.494	2.466	4.934
900.0	1.81070	352.815	130.575	0.490	2.451	4.902
925.0	1.79969	366.648	135.695	0.487	2.436	4.872
950.0	1.78944	380.562	140.844	0.484	2.421	4.844
975.0	1.77987	394.554	146.023	0.482	2.408	4.818
1000.0	1.77093	408.618	151.228	0.479	2.396	4.794
1100.0	1.74066	465.527	172.289	0.471	2.357	4.711
1200.0	1.71740	523.312	193.675	0.466	2.326	4.648
1300.0	1.69947	581.789	215.318	0.461	2.300	4.599
1400.0	1.68563	640.814	237.162	0.458	2.281	4.562
1500.0	1.67500	700.266	259.166	0.453	2.268	4.534
1600.0	1.66693	760.050	281.291	0.453	2.255	4.510
1700.0	1.66090	820.087	303.511	0.451	2.248	4.495
1800.0	1.65653	880.311	325.799	0.451	2.242	4.482
1900.0	1.65351	940.669	348.138	0.448	2.237	4.474
2000.0	1.65160	1001.117	370.509	0.448	2.234	4.469

TABLE 11

MONTE CARLO STOPPING POWER, RANGE AND ENERGY LOSS VALUES FOR PROTONS

IN SILICON: I = 172.3, Z = 14, A = 28.086, ρ = 2.328

Energy	Stopping Power	Range	Range	Most Probable Energy Loss		
				in 1 mm	in 5 mm	in 10 mm
(MeV)	(MeV cm^2/g)	(g/cm^2)	(cm)	(MeV)	(MeV)	(MeV)
2.0	114.41418	0.012	0.005	2.	2.	2.
3.0	85.78734	0.022	0.009	3.	3.	3.
4.0	69.44820	0.035	0.015	4.	4.	4.
5.0	58.81833	0.050	0.021	5.	5.	5.
6.0	51.28148	0.068	0.029	6.	6.	6.
7.0	45.63120	0.089	0.038	7.	7.	7.
8.0	41.03139	0.112	0.048	8.	8.	8.
9.0	37.52287	0.138	0.059	9.	9.	9.
10.0	34.62308	0.165	0.071	10.	10.	10.
12.0	30.09547	0.227	0.097	12.	12.	12.
14.0	26.71164	0.298	0.128	8.187	14.	14.
16.0	24.07713	0.376	0.161	6.777	16.	16.
18.0	21.96254	0.463	0.199	5.904	18.	18.
20.0	20.22415	0.558	0.239	5.279	20.	20.
24.0	17.50618	0.770	0.331	4.415	24.	24.
28.0	15.51462	1.013	0.435	3.830	28.	28.
32.0	13.97303	1.284	0.551	3.405	23.670	32.
36.0	12.74212	1.584	0.680	3.078	18.980	36.
40.0	11.73507	1.910	0.820	2.817	16.428	40.
45.0	10.70617	2.356	1.012	2.556	14.319	41.507
50.0	9.86578	2.841	1.220	2.346	12.817	30.919
55.0	9.16567	3.366	1.446	2.172	11.670	26.608
60.0	8.57296	3.929	1.688	2.027	10.757	23.774
65.0	8.06432	4.530	1.945	1.903	10.007	21.679
70.0	7.62282	5.166	2.219	1.796	9.378	20.034
75.0	7.23581	5.838	2.507	1.703	8.841	18.693
80.0	6.89366	6.544	2.811	1.621	8.376	17.570
85.0	6.58891	7.285	3.129	1.548	7.969	16.613
90.0	6.31569	8.058	3.461	1.483	7.609	15.784
95.0	6.06926	8.864	3.807	1.424	7.289	15.057
100.0	5.84581	9.702	4.167	1.371	7.001	14.414
110.0	5.45609	11.470	4.927	1.279	6.505	13.322
120.0	5.12746	13.357	5.738	1.201	6.093	12.428
130.0	4.84651	15.360	6.598	1.134	5.743	11.681
140.0	4.60351	17.473	7.506	1.077	5.444	11.046
150.0	4.39124	19.694	8.549	1.027	5.184	10.498
160.0	4.20420	22.017	9.457	0.983	4.956	10.022
170.0	4.03815	24.439	10.498	0.944	4.755	9.603
180.0	3.88973	26.957	11.579	0.909	4.576	9.231
190.0	3.75630	29.569	12.701	0.878	4.415	8.899
200.0	3.64570	32.269	13.861	0.849	4.270	8.600
220.0	3.42628	37.928	16.292	0.801	4.020	8.085

TABLE 11 (Continued)

MONTE CARLO STOPPING POWER, RANGE AND ENERGY LOSS VALUES FOR PROTONS

IN SILICON: I = 172.3, Z = 14, A = 28.086, ρ = 2.328

Energy	Stopping Power	Shielding Range in		Most Probable Energy Loss in		
(MeV)	(MeV cm^2/g)	(g/cm^2)	(cm)	1 mm (MeV)	5 mm (MeV)	10 mm (MeV)
240.0	3.25077	43.912	18.862	0.759	3.810	7.657
260.0	3.10163	50.201	21.564	0.725	3.633	7.296
280.0	2.97342	56.776	24.388	0.694	3.481	6.986
300.0	2.86210	63.620	27.328	0.668	3.349	6.718
320.0	2.76462	70.717	30.377	0.646	3.233	6.484
340.0	2.67861	78.054	33.528	0.626	3.132	6.279
360.0	2.60222	85.616	36.776	0.607	3.042	6.096
380.0	2.53399	93.391	40.116	0.592	2.962	5.934
400.0	2.47271	101.366	43.542	0.577	2.889	5.788
425.0	2.40446	111.601	47.938	0.561	2.809	5.626
450.0	2.34405	122.113	52.454	0.548	2.738	5.482
475.0	2.29030	132.884	57.080	0.535	2.675	5.355
500.0	2.24221	143.896	61.811	0.523	2.618	5.242
525.0	2.19900	155.135	66.638	0.513	2.567	5.139
550.0	2.16001	166.585	71.557	0.504	2.521	5.048
575.0	2.12469	178.234	76.561	0.496	2.480	4.964
600.0	2.09261	190.069	81.645	0.488	2.443	4.888
625.0	2.06337	202.079	86.803	0.482	2.408	4.819
650.0	2.03664	214.252	92.032	0.475	2.377	4.757
675.0	2.01215	226.579	97.328	0.469	2.348	4.699
700.0	1.98966	239.051	102.685	0.464	2.322	4.646
725.0	1.96897	251.659	108.101	0.460	2.298	4.597
750.0	1.94989	264.395	113.572	0.455	2.275	4.552
775.0	1.93226	277.251	119.094	0.451	2.255	4.510
800.0	1.91595	290.221	124.665	0.447	2.236	4.472
825.0	1.90084	303.298	130.282	0.444	2.218	4.437
850.0	1.88683	316.475	135.943	0.440	2.201	4.404
875.0	1.87380	329.746	141.643	0.438	2.186	4.373
900.0	1.86169	343.107	147.383	0.434	2.172	4.344
925.0	1.85041	356.553	153.158	0.432	2.159	4.318
950.0	1.83990	370.078	158.968	0.430	2.146	4.294
975.0	1.83010	383.677	164.810	0.427	2.135	4.270
1000.0	1.82095	397.348	170.682	0.425	2.125	4.249
1100.0	1.78994	452.659	194.441	0.419	2.089	4.177
1200.0	1.76615	508.818	218.564	0.414	2.060	4.123
1300.0	1.74781	565.648	242.976	0.409	2.039	4.078
1400.0	1.73367	623.006	267.614	0.406	2.023	4.044
1500.0	1.72284	680.777	292.429	0.404	2.010	4.018
1600.0	1.71461	738.867	317.382	0.401	2.000	4.000
1700.0	1.70849	797.200	342.440	0.398	1.992	3.984
1800.0	1.70407	855.714	367.574	0.398	1.987	3.974
1900.0	1.70103	914.355	392.764	0.398	1.984	3.969
2000.0	1.69914	973.081	417.990	0.398	1.982	3.964

TABLE 12

MONTE CARLO STOPPING POWER, RANGE AND ENERGY LOSS VALUES FOR PROTONS

IN IRON: I = 300.9 eV, Z = 26, A = 55.847, ρ = 7.792

Energy	Stopping Power	Range	Range	Most Probable Energy Loss		
				in 1 mm	in 5 mm	in 10 mm
(MeV)	(MeV cm^2/g)	(g/cm^2)	(cm)	(MeV)	(MeV)	(MeV)
2.0	88.83200	0.015	0.002	2.	2.	2.
3.0	68.39137	0.028	0.004	3.	3.	3.
4.0	56.20445	0.044	0.006	4.	4.	4.
5.0	48.03178	0.063	0.008	5.	5.	5.
6.0	42.13054	0.085	0.011	6.	6.	6.
7.0	37.64806	0.110	0.014	7.	7.	7.
8.0	34.11525	0.138	0.017	8.	8.	8.
9.0	31.22868	0.168	0.021	9.	9.	9.
10.0	28.83948	0.202	0.025	10.	10.	10.
12.0	25.10947	0.276	0.035	12.	12.	12.
14.0	22.32050	0.360	0.046	14.	14.	14.
16.0	20.14899	0.455	0.058	16.	16.	16.
18.0	18.40541	0.558	0.071	18.	18.	18.
20.0	16.97198	0.671	0.086	20.	20.	20.
24.0	14.74782	0.924	0.118	15.760	24.	24.
28.0	13.09584	1.212	0.155	12.488	28.	28.
32.0	11.81591	1.533	0.196	10.629	32.	32.
36.0	10.75110	1.887	0.242	9.389	36.	36.
40.0	9.92165	2.274	0.291	8.456	40.	40.
45.0	9.07187	2.800	0.359	7.577	45.	45.
50.0	8.37567	3.373	0.433	6.907	50.	50.
55.0	7.79413	3.991	0.512	6.368	48.573	55.
60.0	7.30069	4.654	0.597	5.923	38.578	60.
65.0	6.87637	5.358	0.687	5.548	33.855	65.
70.0	6.50747	6.104	0.783	5.228	30.662	70.
75.0	6.18354	6.891	0.884	4.950	28.259	75.
80.0	5.89354	7.717	0.990	4.706	26.339	80.
85.0	5.63824	8.583	1.101	4.489	24.750	63.031
90.0	5.40902	9.487	1.217	4.298	23.406	56.123
95.0	5.20202	10.428	1.338	4.127	22.248	51.515
100.0	5.01410	11.405	1.463	3.972	21.237	48.016
110.0	4.68585	13.466	1.728	3.703	19.553	42.848
120.0	4.40855	15.663	2.010	3.477	18.194	39.097
130.0	4.17113	17.992	2.309	3.285	17.070	36.195
140.0	3.96550	20.447	2.624	3.120	16.121	33.855
150.0	3.78566	23.024	2.954	2.975	15.309	31.915
160.0	3.62705	25.718	3.300	2.848	14.605	30.273
170.0	3.48610	28.526	3.661	2.736	13.988	28.862
180.0	3.36002	31.443	4.035	2.636	13.442	27.633
190.0	3.24659	24.466	4.423	2.545	12.955	26.551
200.0	3.14400	37.591	4.824	2.464	12.519	25.591
220.0	2.96571	44.134	5.664	2.323	11.768	23.960

TABLE 12 (Continued)

MONTE CARLO STOPPING POWER, RANGE AND ENERGY LOSS VALUES FOR PROTONS

IN IRON: I = 300.9 eV, Z = 26, A = 55.847, ρ = 7.792

Energy (MeV)	Stopping Power (MeV cm^2/g)	Shielding (g/cm^2)	Range in (cm)	Most Probable Energy Loss in 1 mm (MeV)	in 5 mm (MeV)	in 10 mm (MeV)
240.0	2.81615	51.046	6.551	2.205	11.145	22.624
260.0	2.68896	58.304	7.482	2.104	10.620	21.508
280.0	2.57955	65.888	8.455	2.018	10.171	20.562
300.0	2.48452	73.777	9.468	1.943	9.783	19.750
320.0	2.40126	81.954	10.517	1.878	9.445	19.044
340.0	2.32778	90.401	11.401	1.820	9.148	18.427
360.0	2.26250	99.103	12.718	1.768	8.885	17.882
380.0	2.20418	108.045	13.866	1.722	8.650	17.397
400.0	2.15181	117.214	15.043	1.681	8.440	16.965
425.0	2.09347	128.976	16.552	1.635	8.206	16.485
450.0	2.04184	141.051	18.102	1.595	8.000	16.062
475.0	1.99589	153.416	19.689	1.559	7.816	15.687
500.0	1.95480	166.054	21.310	1.527	7.652	15.353
525.0	1.91789	178.946	22.965	1.498	7.505	15.053
550.0	1.88459	192.076	24.650	1.472	7.373	14.784
575.0	1.85444	205.429	26.364	1.449	7.253	14.541
600.0	1.82706	218.990	28.104	1.427	7.145	14.319
625.0	1.80212	232.746	29.870	1.408	7.046	14.119
650.0	1.77934	246.686	31.659	1.389	6.956	13.936
675.0	1.75848	260.798	33.470	1.373	6.873	13.768
700.0	1.73933	275.071	35.301	1.358	6.798	13.615
725.0	1.72172	289.495	37.152	1.344	6.728	13.473
750.0	1.70550	304.062	39.022	1.332	6.664	13.344
775.0	1.69053	318.763	40.909	1.320	6.604	13.224
800.0	1.67669	333.589	42.811	1.309	6.550	13.113
825.0	1.66388	348.534	44.729	1.299	6.500	13.011
850.0	1.65200	363.590	46.662	1.290	6.453	12.916
875.0	1.64098	378.751	48.607	1.281	6.409	12.828
900.0	1.63074	394.010	50.566	1.273	6.369	12.747
925.0	1.62122	409.362	52.536	1.266	6.331	12.671
950.0	1.61236	424.802	54.517	1.259	6.296	12.600
975.0	1.60411	440.323	56.509	1.253	6.264	12.535
1000.0	1.59641	455.922	58.511	1.246	6.233	12.473
1100.0	1.57045	519.006	66.607	1.227	6.133	12.268
1200.0	1.55066	583.009	74.821	1.211	6.055	12.109
1300.0	1.53557	647.731	83.127	1.201	5.995	11.990
1400.0	1.52407	713.014	91.506	1.190	5.948	11.898
1500.0	1.51541	778.729	99.939	1.185	5.914	11.831
1600.0	1.50898	844.770	108.415	1.180	5.888	11.779
1700.0	1.50434	911.053	116.921	1.175	5.870	11.742
1800.0	1.50115	977.509	125.450	1.172	5.859	11.716
1900.0	1.49915	1044.080	133.993	1.172	5.852	11.701
2000.0	1.49812	1110.718	142.545	1.169	5.846	11.690

TABLE 13

MONTE CARLO STOPPING POWER, RANGE AND ENERGY LOSS VALUES FOR PROTONS

IN COPPER: I = 313.8 eV, Z = 29, A = 63.54, ρ = 8.897

Energy	Stopping Power	Range	Range	Most Probable Energy Loss		
				in 1 mm	in 5 mm	in 10 mm
(MeV)	(MeV cm^2/g)	(g/cm^2)	(cm)	(MeV)	(MeV)	(MeV)
2.0	83.22719	0.0162	0.0018	2.	2.	2.
3.0	64.73953	0.0295	0.0033	3.	3.	3.
4.0	52.62654	0.0462	0.0052	4.	4.	4.
5.0	44.66743	0.0660	0.0074	5.	5.	5.
6.0	38.99442	0.0889	0.0100	6.	6.	6.
7.0	35.07007	0.1148	0.0129	7.	7.	7.
8.0	31.65868	0.1435	0.0161	8.	8.	8.
9.0	29.37289	0.1750	0.0197	9.	9.	9.
10.0	27.42743	0.2092	0.0235	10.	10.	10.
12.0	23.96626	0.2856	0.0321	12.	12.	12.
14.0	21.36069	0.3724	0.0419	14.	14.	14.
16.0	19.41222	0.4692	0.0527	16.	16.	16.
18.0	17.75064	0.5758	0.0647	18.	18.	18.
20.0	16.38200	0.6920	0.0778	20.	20.	20.
24.0	14.25314	0.9520	0.1070	19.177	24.	24.
28.0	12.66833	1.2478	0.1403	14.313	28.	28.
32.0	11.43869	1.5781	0.1774	12.059	32.	32.
36.0	10.45452	1.9418	0.2183	10.592	36.	36.
40.0	9.68537	2.3380	0.2628	9.524	40.	40.
45.0	8.85178	2.8775	0.3234	8.519	45.	45.
50.0	8.14362	3.4668	0.3897	7.729	50.	50.
55.0	7.57969	4.1023	0.4611	7.108	55.	55.
60.0	7.10098	4.7829	0.5376	6.606	46.846	60.
65.0	6.68921	5.5073	0.6190	6.185	39.500	65.
70.0	6.33111	6.2745	0.7052	5.825	35.236	70.
75.0	6.01662	7.0833	0.7962	5.514	32.194	75.
80.0	5.73813	7.9329	0.8916	5.242	29.856	80.
85.0	5.48979	8.8223	0.9916	5.002	27.966	85.
90.0	5.26681	9.7506	1.0959	4.788	26.386	67.449
95.0	5.06544	10.7170	1.2046	4.596	25.038	60.300
100.0	4.88045	11.7209	1.3174	4.422	23.866	55.477
110.0	4.56166	13.8380	1.5554	4.121	21.921	48.883
120.0	4.29228	16.0952	1.8091	3.870	20.364	44.310
130.0	4.06158	18.4871	2.0779	3.656	19.086	40.850
140.0	3.86174	21.0087	2.3613	3.471	18.012	38.102
150.0	3.68695	23.6552	2.6588	3.311	17.095	35.849
160.0	3.53275	26.4220	2.9698	3.170	16.301	33.957
170.0	3.39571	29.3049	3.2938	3.044	15.606	32.338
180.0	3.27311	32.3000	3.6304	2.933	14.992	30.933
190.0	3.16281	35.4033	3.9792	2.832	14.446	29.702
200.0	3.06304	38.6112	4.3398	2.742	13.957	28.611
220.0	2.88963	45.3272	5.0947	2.585	13.116	26.764

TABLE 13 (COntinued)

MONTE CARLO STOPPING POWER, RANGE AND ENERGY LOSS VALUES FOR PROTONS

IN COPPER: I = 313.8 eV, Z = 29, A = 63.54, ρ = 8.897

Energy	Stopping Power	Shielding Range		Most Probable Energy Loss		
		in		in 1 mm	in 5 mm	in 10 mm
(MeV)	(MeV cm^2/g)	(g/cm^2)	(cm)	(MeV)	(MeV)	(MeV)
240.0	2.74413	52.421	5.892	2.543	12.419	25.255
260.0	2.62040	59.871	6.729	2.342	11.832	23.998
280.0	2.51395	67.654	7.604	2.246	11.330	22.935
300.0	2.42148	75.749	8.514	2.163	10.897	22.022
320.0	2.34046	84.139	9.457	2.090	10.520	21.231
340.0	2.26896	92.806	10.431	2.026	10.188	20.540
360.0	2.20544	101.734	11.434	1.968	9.894	19.929
380.0	2.14868	110.909	12.465	1.917	9.633	19.388
400.0	2.09771	120.316	13.523	1.872	9.398	18.903
425.0	2.04093	132.382	14.879	1.821	9.138	18.367
450.0	1.99068	144.768	16.271	1.776	8.908	17.895
475.0	1.94597	157.453	17.697	1.736	8.704	17.475
500.0	1.90598	170.416	19.154	1.700	8.521	17.102
525.0	1.87005	183.639	20.640	1.668	8.358	16.768
550.0	1.83765	197.106	22.154	1.639	8.210	16.468
575.0	1.80831	210.801	23.693	1.613	8.078	16.196
600.0	1.78166	224.709	25.256	1.589	7.957	15.950
625.0	1.75739	238.818	26.842	1.567	7.846	15.726
650.0	1.73522	253.114	28.449	1.547	7.746	15.521
675.0	1.71492	267.585	30.075	1.529	7.654	15.335
700.0	1.69629	282.222	31.721	1.512	7.570	15.164
725.0	1.67916	297.014	33.383	1.497	7.492	15.007
750.0	1.66338	311.951	35.062	1.483	7.421	14.862
775.0	1.64882	327.025	36.756	1.470	7.355	14.729
800.0	1.63535	342.228	38.465	1.458	7.294	14.605
825.0	1.62289	357.552	40.188	1.447	7.238	14.492
850.0	1.61134	372.989	41.923	1.436	7.186	14.386
875.0	1.60063	388.534	43.670	1.427	7.138	14.289
900.0	1.59067	404.180	45.428	1.418	7.093	14.198
925.0	1.58141	419.920	47.198	1.410	7.051	14.113
950.0	1.57280	435.749	48.977	1.402	7.012	14.035
975.0	1.56477	451.663	50.765	1.395	6.976	13.962
1000.0	1.55730	467.655	52.563	1.388	6.942	13.893
1100.0	1.53206	532.327	59.832	1.367	6.831	13.664
1200.0	1.51286	597.937	67.206	1.349	6.742	13.490
1300.0	1.49821	664.282	74.663	1.336	6.677	13.357
1400.0	1.48707	731.197	82.184	1.326	6.628	13.255
1500.0	1.47868	798.551	89.755	1.318	6.589	13.180
1600.0	1.47247	866.237	97.362	1.312	6.560	13.123
1700.0	1.46801	934.168	104.998	1.310	6.542	13.081
1800.0	1.46496	1002.273	112.653	1.307	6.526	13.055
1900.0	1.46305	1070.493	120.320	1.305	6.518	13.037
2000.0	1.46210	1138.780	127.996	1.305	6.513	13.026

TABLE 14

MONTE CARLO STOPPING POWER, RANGE AND ENERGY LOSS VALUES FOR PROTONS

IN LEAD: I = 840. eV, Z = 82, A = 207.19, ρ = 11.224

Energy (MeV)	Stopping Power ($MeV\ cm^2/g$)	Range (g/cm^2)	Range (cm)	Most Probable Energy Loss in 1 mm (MeV)	in 5 mm (MeV)	in 10 mm (MeV)
2.0	44.69257	0.033	0.003	2.	2.	2.
3.0	37.55753	0.057	0.005	3.	3.	3.
4.0	32.31839	0.085	0.007	4.	4.	4.
5.0	28.44336	0.117	0.010	5.	5.	5.
6.0	25.47507	0.154	0.013	6.	6.	6.
7.0	23.12759	0.194	0.017	7.	7.	7.
8.0	21.22166	0.239	0.021	8.	8.	8.
9.0	19.64079	0.287	0.025	9.	9.	9.
10.0	18.30627	0.339	0.030	10.	10.	10.
12.0	16.17175	0.454	0.040	12.	12.	12.
14.0	14.53462	0.582	0.051	14.	14.	14.
16.0	13.23496	0.725	0.064	16.	16.	16.
18.0	12.17552	0.880	0.078	18.	18.	18.
20.0	11.29363	1.049	0.093	20.	20.	20.
24.0	9.90564	1.423	0.126	14.736	24.	24.
28.0	8.85917	1.845	0.164	12.024	28.	28.
32.0	8.03932	2.314	0.206	10.407	32.	32.
36.0	7.37811	2.828	0.252	9.274	36.	36.
40.0	6.83254	3.385	0.301	8.418	40.	40.
45.0	6.27060	4.141	0.369	7.593	45.	45.
50.0	5.80803	4.962	0.442	6.948	50.	50.
55.0	5.42009	5.844	0.520	6.425	47.151	55.
60.0	5.08973	6.786	0.604	5.992	38.595	60.
65.0	4.80477	7.787	0.693	5.627	34.144	65.
70.0	4.55628	8.845	0.788	5.313	31.060	70.
75.0	4.33756	9.959	0.887	5.040	28.709	75.
80.0	4.14346	11.127	0.991	4.801	26.823	80.
85.0	3.96953	12.348	1.100	4.588	25.258	64.146
90.0	3.81317	13.621	1.213	4.398	23.930	57.330
95.0	3.67180	14.945	1.331	4.228	22.783	52.729
100.0	3.54331	16.318	1.453	4.074	21.778	49.228
110.0	3.31852	19.208	1.711	3.809	20.095	44.048
120.0	3.12825	22.285	1.985	3.581	18.735	40.278
130.0	2.96506	25.540	2.275	3.386	17.608	37.353
140.0	2.82350	28.966	2.580	3.223	16.657	34.992
150.0	2.69954	32.556	2.900	3.074	15.841	33.034
160.0	2.59006	36.305	3.234	2.951	15.132	31.376
170.0	2.49266	40.207	3.582	2.834	14.510	29.950
180.0	2.40546	44.256	3.943	2.737	13.960	28.708
190.0	2.32693	48.447	4.316	2.643	13.470	27.614
200.0	2.25586	52.774	4.702	2.564	13.030	26.642
220.0	2.13220	61.822	5.508	2.422	12.272	24.991

TABLE 14 (Continued)

MONTE CARLO STOPPING POWER, RANGE AND ENERGY LOSS VALUES FOR PROTONS

IN LEAD: I = 840. eV, Z = 82, A = 207.19, ρ = 11.224

Energy (MeV)	Stopping Power ($MeV\ cm^2/g$)	Shielding (g/cm^2 in)	Range (cm)	Most Probable Energy Loss in 1 mm (MeV)	in 5 mm (MeV)	in 10 mm (MeV)
240.0	2.02833	71.363	6.358	2.303	11.642	23.637
260.0	1.93992	81.366	7.249	2.201	11.110	22.506
280.0	1.86380	91.801	8.179	2.114	10.656	21.546
300.0	1.79764	102.642	9.144	2.038	10.264	20.721
320.0	1.73965	113.863	10.144	1.972	9.921	20.006
340.0	1.68846	125.441	11.176	1.914	9.619	19.379
360.0	1.64298	137.356	12.237	1.862	9.353	18.826
380.0	1.60913	149.581	13.326	1.823	9.125	18.344
400.0	1.57256	162.057	14.438	1.781	8.940	17.972
425.0	1.53183	178.043	15.862	1.734	8.703	17.484
450.0	1.49579	194.434	17.323	1.693	8.493	17.054
475.0	1.46373	211.203	18.817	1.657	8.307	16.673
500.0	1.43507	228.324	20.342	1.625	8.141	16.333
525.0	1.40934	245.773	21.897	1.595	7.992	16.029
550.0	1.38615	263.527	23.478	1.568	7.858	15.757
575.0	1.36517	281.567	25.086	1.545	7.737	15.510
600.0	1.34614	299.873	26.717	1.523	7.627	15.287
625.0	1.32865	318.429	28.370	1.503	7.527	15.083
650.0	1.31287	337.220	30.044	1.485	7.436	14.896
675.0	1.29845	356.229	31.738	1.469	7.352	14.728
700.0	1.28523	375.442	33.450	1.454	7.276	14.574
725.0	1.27309	394.846	35.178	1.440	7.207	14.432
750.0	1.26193	414.429	36.923	1.427	7.143	14.302
775.0	1.25166	434.179	38.683	1.416	7.083	14.182
800.0	1.24218	454.087	40.456	1.405	7.029	14.072
825.0	1.23342	474.142	42.243	1.395	6.979	13.970
850.0	1.22533	494.334	44.042	1.385	6.932	13.876
875.0	1.21784	514.656	45.853	1.377	6.889	13.789
900.0	1.21090	535.099	47.674	1.369	6.849	13.708
925.0	1.20447	555.656	49.506	1.362	6.812	13.634
950.0	1.19851	576.319	51.347	1.355	6.778	13.564
975.0	1.19297	597.083	53.197	1.349	6.746	13.500
1000.0	1.18783	617.939	55.055	1.343	6.716	13.440
1100.0	1.17066	702.191	62.561	1.326	6.620	13.242
1200.0	1.15785	787.527	70.164	1.310	6.544	13.094
1300.0	1.14834	873.691	77.841	1.300	6.490	12.982
1400.0	1.14137	960.477	85.573	1.292	6.451	12.901
1500.0	1.13638	1047.723	93.346	1.284	6.422	12.841
1600.0	1.13296	1135.295	101.148	1.281	6.401	12.802
1700.0	1.13079	1223.088	108.970	1.279	6.388	12.776
1800.0	1.12962	1311.014	116.804	1.276	6.380	12.760
1900.0	1.12928	1399.003	124.643	1.276	6.378	12.755
2000.0	1.12960	1486.997	132.483	1.276	6.380	12.758

Results

The average of the most probable value of the mean ionization potential for each of the seven materials is given in Table 15. The variance and probable error of each value is given. These are compared to values of I used by Barkas and Berger (4,12) and Berger and Seltzer (13) from the two emperical equations

$$I_{adj}/Z = 12 + 7/Z \text{ eV}, \qquad I_{adj} \quad 163 \text{ eV} \tag{17a}$$

$$I_{adj}/Z = 9.76 + 58.8\, Z^{-1.19} \text{ eV}, \qquad I_{adj} \quad 163 \text{ eV} \tag{17b}$$

Equation 17b is due to Sternheimer (private communication to Barkas and Berger). Dixon (14) used his measured values for Al, Si, Fe, and Pb and found that equation 17b should be

$$I/Z = 9.81 + 35.5/Z \tag{17c}$$

Values reported by Bichsel (15) are also listed.

TABLE 15

VALUES OF I

Element	Z	Bichsel (eV)	Barkas Berger (eV)	Crawford (eV)	Variance (eV)	Probable Error (eV)
Be	4	64	60.	53.3	.78	.5
C	6	78	78	72.1	.98	.7
Al	13	166	163	163.8	2.9	2.0
Si	14	175.6	172.0	172.3	3.7	2.5
Fe	26		285	300.9	3.2	2.2
Cu	29	320	314	313.8	4.9	3.3
Pb	82	820	826	840	5.2	3.5

Rather than merely find another mathematical equation which fits the new values of I, this report proposes a new model. This model is based on the lowest (Class 1) ionization potential as reported in the Handbook of Chemistry and Physics (16). Assume that the lowest ionization potential indicates the magnitude of the difference between two adjacent elements. Thus the proposed emperical relationship which can be used to determine the correct value of I to be used in the Monte Carlo transport calculation is given in Table 16. This system gives values for the first two shells well within the experimental value error. Each step in the first ten elements fills another position in the spd system of identifying electron configuration. Beginning with hydrogen with its one electron, only one electron can be involved in a collision. The lowest ionization potential value of 13.53 eV and the x-ray K edge ionization potential of 14 eV are in close agreement. Thus the mean ionization potential is really one electron and should be the same with I = 13.5 eV.

The ionization potential is defined as the work (expressed in electron volts) required to remove a given electron from its atomic orbit and place it at rest at an infinite distance. The mean ionization parameter, I, is defined to be the mean value of the minimum energy transfer in a proton-atomic electron collision which produces an ionization event. All of the atomic electrons are considered to participate in the collision process.

Fano (4) has derived a definition for I based on the Thomas-Fermi statistical model, namely that it is the logarithmic average over the excitation energies weighted by the oscillator strengths. I depends only upon the ground and excited state wave functions of a stopping material. The determination of I from this definition presents serious difficulties since the oscillator strengths are not generally well known in the desired energy range. Theoretical values for I for the first four elements are reported by Fano to be 15. for hydrogen; 41.8 for helium; 45, 38.8 for lithium and 60, 66 eV for Be. The model proposed here is a numerical correlation which may lead to new insight with a possible relationship between the lowest ionization potential and the oscillator strengths.

Helium with two electrons has a lowest ionization potential of 24.46 eV, with an x-ray K edge ionization potential of 25 eV. Using this emperical model, I for helium should be 37.99 eV. Both electrons would be involved in the nucleon - electron collision process. The Class 2 ionization potential of helium is 54.14 eV. The sum of the two is 78.6 eV. If the mean value, I, involves both with equal weight then I would be equal to $\frac{1}{2}$ (24.46 + 54.14) = 39.3 eV. Thus the possible I value would be between 38 and 39.3, Fano on page 311 of NSS Report No. 39 (4), lists values of 15.0 and 42 ± 3 eV for H and He, as compared to 13.5 and 38. for this model.

The problem becomes more complex in stepping from the first period to the second period. Three electrons are now involved in the collision process. However, if one assumes that the change in the MEAN value is indicated by the lowest ionization potential, then I for lithium is about 43.35 eV. The I for beryllium becomes 52.63 and this compares favorably with the measured value of 53.3 eV. Continuing on, the model gives a value for carbon of I = 72.11 which is that measured for carbon. Values for the value of I for the rest of the second period are obtained by adding in turn the lowest ionization potential of each element.

The values for I for higher Z elements can be obtained using two assumptions. First, that within a given period, the Class 1 ionization potential represents the difference in mean ionization potential, I, between any two adjacent elements. Second, that the correct value for I is known for at least one element in the period. Thus the values for I in the third period listed in Table 16 are valid if the I-value for aluminum is 163.0 eV. Those listed in the fourth period are based on I_{Cu} = 314.0 eV. The baseline values used in each of the periods, two, three and four, agree closely with those measured in this research effort using protons having energies as low as 8 MeV and as high as 185.6 MeV.

TABLE 16

SUGGESTED VALUES FOR I

Element	Z	Electron Configuration	Lowest Ionization Potential	Values of I in eV: Summing Column 3	Crawford	Barkas Berger	Fano	Anderson
H	1	s^1	13.53	13.53		18.7	15	
He	2	s^2	24.46	37.99		42.	42±3	
Li	3	$s^2 2s^1$	5.36	43.35			40,38	
Be	4	$s^2 2s^2$	9.28	52.63	53.3	60.0	64	
B	5	" $2p^1$	8.26	60.89				
C	6	" $2p^2$	11.22	72.11	72.1	78.0	81	
N	7	" $2p^3$	14.48	86.59			88	
O	8	" $2p^4$	13.55	100.14			101	
F	9	" $2p^5$	17.34	117.48				
Ne	10	" $2p^6$	21.47	138.95		131.		
Na	11	" $3s^1$	5.12	149.4				
Mg	12	" $3s^2$	7.61	157.0				
Al	13	" " $3p^1$	5.96	163.0	163.8	163.0	163	
Si	14	" " $3p^2$	8.12	171.1	172.3	172.0		
P	15	" " $3p^3$	10.9	182.0				
S	16	" " $3p^4$	10.30	192.3				
Cl	17	" " $3p^5$	12.95	205.3				
Ar	18	" " $3p^6$	15.68	221.0		210.	190	
K	19	(Ar)$4s^1$	4.32	242.7				
Ca	20	" $4s^2$	6.09	248.8				194.8±3.4
Sc	21	" $3d^1 4s^2$	6.7	255.5				216.8±3.6
Ti	22	" $3d^2 4s^2$	6.81	262.3				229.8±2.6
V	23	" $3d^3 4s^2$	6.71	269.0				239.2±2.8
Cr	24	" $3d^5 4s^1$	6.74	275.7				258.0±4.4
Mn	25	" $3d^5 4s^2$	7.41	283.1				273.2±5.4
Fe	26	" $3d^6 4s^2$	7.83	290.9	300.9	285	273	280.6±3.1
Co	27	" $3d^7 4s^2$	7.81	298.7				298.8±3.7
Ni	28	" $3d^8 4s^2$	7.61	306.3		304		303.2±3.7
Cu	29	" $3d^{10} 4s^1$	7.68	314.0	313.8	314	315	320.8±3.8
Zn	30	" " $4s^2$	9.36	323.4				323.1±3.8
Ga	31	" " " $4p^1$	5.97	329.4				
Ge	32	" " " $4p^2$	8.09	337.5		343.0		
As	33	" " " $4p^3$	10.5	348.0				
Se	34	" " " $4p^4$	9.70	375.7				
Br	35	" " " $4p^5$	11.80	369.5				
Kr	36	" " " $4p^6$	13.93	383.4		381.	360	

Anderson, Sorensen and Vajda (17) obtained a value of 320.8 ± 3.8 eV from "smoothed stopping power values" and a linear transport calculation. Dalton and Turner (18) report a "new average value for I_{Cu}" calculated from the data of nine experiments that measured absolute stopping power, relative stopping power, or range. The experiments reviewed were those of Bakker and Segre (19); Thompson (20); Sachs and Richardson (21); Brolley and Ribe (22); Burkig and MacKenzie (23); Zrelov and Stoletov (24); Nielsen (25); Barkas and von Friesen (26); and Nakano, MacKenzie and Bichsel (27). They describe their procedure as follows: "The older data have been analyzed with insufficient allowance for the contribution of shell corrections, and new shell corrections (C/Z) for the entire atom, as described by Fano (28), have been included in this analysis. I-values obtained from relative stopping power measurements have been normalized to I = 163 eV for aluminum and I = 314 for copper." Their results are given in Table 17. The standard error reported for the new average values "is about 2% for the elements considered, which is consistent with the accuracy of the experimental measurements."(17)

The 25 average values for I_{Al} given in Table 3 represent 100 different measurements. The 24 average values for I_{Cu} in Table 5 represent 96 different measurements. The average values reported in Table 15 are in experimental agreement with the "new average values, for aluminum and copper but not for the other five elements.

The value obtained for I from a given measurement, whether of stopping power or of range, is determined as much by the method of evaluation (smoothed, linear, Monte Carlo, etc.) as by the measurement. The equations used for shell and density corrections also play a vital role in the value of I. The changes in the I-values as reported and as modified in the Dalton and Turner (18) paper are ample evidence of this. As an example, Nielsen's values (25) were reduced due to C/Z correction as follows:

	I	Reduction	New Value	Crawford (Theory)
4-Be	56 eV	3.6%	55.6 eV	52.63 eV
13-Al	179	10.7	163.	163.
28-Ni	371	18.5	308.	306.3
29-Cu	376	18.4	315.	314.
47-Ag	577	25.2	461.	461.
79-Au	942	21.2	777.	816.

Copied from Table 8, page 29, reference 18. For protons of 1 to 5 MeV energy.

Burkig and MacKenzie's values (23) reduced due to C/Z correction as follows:

26-Fe	328.8	289.5	290.0
29-Cu	366.0	318.6	314.
47-Ag	587.0	459.6	461.
79-Au	997.	719.6	816.
82-Pb	1070	774.	840.

Copied from Table 2, page 17, reference 18. For protons of 19.8 MeV energy.

Thompson's values (20) were raised by C/Z corrections as follows:

1-H_2	18.2	21.9	
H-saturated	15.5	18.6	
H-unsaturated	13.0	15.7	13.53
6-C	70.2	82.2	72.11
C-saturated	69.3	80.0	
C-unsaturated	67.2	78.7	
7-N_2	76.3	89.1	
N-in ring	68.8	80.6	86.59
8-O_2	88.3	102.8	100.1

Copied from Table 5, page 23, reference 18. For 270-MeV protons

Bakker and Segre (19) performed an experiment similar to the one reported here in that they measured the amount of material necessary to obtain a fairly large amount of energy loss from the incident 340 MeV proton, reporting their results in terms of relative absorption of copper. They found the mass stopping power relative to copper by dividing the number of g/cm^2 of copper by the equivalent number of g/cm^2 of the element being studied. Dalton and Turner "treated Bakker and Segre's values of stopping powers per electron relative to aluminum as the raw data. Bakker and Segre's results were corrected by using 163 eV instead of 150 eV for the I-value of aluminum." (18). Their values for the mass stopping power relative to copper are compared to the Monte Carlo values and to the results of Zrelov and Stoletov (24) in the following compilation.

Element	Mass Stopping Power Relative to Copper 340 MeV		660 MeV		Mean Ionization Potential, eV				
	Bakker	Crawford	Zrelov	Crawford	Bakker	Dalton	Craw-Ford	Zrelov	Dalton
1-H	3.010*	3.088	3.016*	3.022	15.6	17.5	13.5	15±4	13.6
3-Li	1.214	1.199			34.	37.4	43.4		
4-Be	1.171	1.205	1.167	1.188	60.4	66.6	52.6	61±6	61.7
6-C	1.285	1.310	1.268	1.294	76.4	83.5	72.1	85±8	86.2
13-Al	1.143	1.148			150.	163.	163.		
26-Fe	1.036	1.030	1.034	1.029	243.	266.	290.	273±22	276.
29-Cu	1.	1.	1.	1.	279.	297.	314.	305±10	307.
47-Ag	0.902	0.904			428.	444.	462.		
48-Cd			0.887	0.888			470.	468±35	461.
50-Sn	0.858	0.868			479.	491.	483.		
82-Pb	0.754	0.752			758.	742.	840.		

*Both Bakker and Zrelov measured H as part of CH_2. "The stopping power of hydrogen was determined from the CH_2 - C difference. For hydrogen the accuracy of the mass stopping power is about 5% and that of I_H is about 50%." according to Zrelov (24). It is apparent that the chemical binding of the hydrogen in polyethylene has considerable influence on the stopping power and I-value. (20).

The only direct data given by either group is the range in copper. Bakker and Segre (19) report a range of 92.4 g/cm^2 Cu. The Monte Carlo range for a 340 MeV proton in copper is 92.806 for I = 313.8 eV. An error of 1 MeV in the energy of the proton represents an error of 0.434 g/cm^2 Cu, so the measured range is within the range for a 339 MeV proton in copper. Zrelov and Stoletov report a range of 257.6 ± 0.3 g/cm^2 Cu for protons having an energy of 658 ± 2 MeV. The Monte Carlo calculation using I = 314 eV gives a range of 257.75 g/cm^2 Cu for 658 MeV protons. It is quite apparent that the Monte Carlo calculation which includes the latest shell and density corrections gives results in complete agreement with the reported data for copper whereas a simple linear recalculation does not.

This superiority of the Monte Carlo determination is also shown in the following comparison of the reported ranges of protons in aluminum. Data covering a range of energies from 6 to 18. MeV were taken by Bichsel, Mozley and Aron (30); at 18 MeV by Hubbard and MacKenzie (31); at 36.2 and 99.9 MeV by Crawford; at 100 MeV by Portner and Moore (29); at 159.75 MeV by Crawford; at 340 MeV by Mather and Segre (32); and at 752 MeV by Barkas and von Friesen (26). The corresponding Monte Carlo range for I=163 eV is given for each data point.

The shell corrections decrease in value as the proton energy increases, producing very small changes at energies above 100 MeV. The magnitude of the change with proton energy is clearly shown in the examples given.

When the I-value is obtained from a range measurement, a new variable must be considered. This variable is the difference between the range calculated from the linear or "straight ahead" concept and that calculated by a Monte Carlo transport program which permits small and large angle scattering as well as nuclear interaction in addition to the usual linear movement of the proton between these events.

Range

The range of a heavy particle is well defined only when the particle loses energy solely by many, small energy losses to electrons without scattering. The straight ahead model uses this continuous slowing down approximation. This c.s.d.a. range is calculated from the equation

$$R = R_{E_o} + \int_{E_o}^{E} dE/(dE/\rho dx)$$

where R_o is the range at some low energy, E_o, and must be measured. In this report, the values of R_o at E_o = 2 MeV were taken from the Barkas and Berger range tables in SSR Report No. 39 (4). For proton energies above 25 MeV, R_o represents less than 1% of the range of the proton. Thus any error in this measurement has very little effect on the range calculated for high proton energies and a large effect on range values at low energies. This represents a maximum straight line travel and may be correlated with the perpendicular distance between the faces of an absorber. Scattering spreads the beam of protons, resulting in a shortened perpendicular path. The value given for the range in Tables 8 through 14 were obtained from a Monte Carlo penetration and represent this shortened perpendicular path. At energies below 200 MeV, the percentage of protons removed from the beam by large angle scattering and by nuclear reactions is sufficiently low to continue to use the concept of range in giving the depth of penetration. At higher energies, the percentage of protons remaining in the original beam decreases rapidly as the proton energy increases. Thus the term "Shielding Range" is used rather than the Monte Carlo range. Some do penetrate this far but most of the beam does not.

The linear method of determining I from a range measurement is to estimate the probable I-value of the absorber and then to numerically integrate over the energy interval E_o to E. The pre-determined value of R_{E_o} is added to the result of the numerical intergration. The value of I is adjusted until a value of I is found which gives the measured range. In the Monte Carlo calculation, the same basic game of varying the value of I is played, but for the same value of I and the same shell and density corrections, the Monte Carlo range is always shorter than the c.s.d.a. range. The Monte Carlo value for I is always larger than the c.s.d.a. I-value for the same range, if the same stopping power tables are used. Dalton and Turner (18) used the same range c.s.d.a. equation but different stopping power tables to obtain "new values of I" from the following data. The same range measurements, when compared to the Monte Carlo ranges reported in Tables 8 - 14, are in agreement within experimental error. Many of the large differences in I-values which appear in comparing results of different experimenters disappear when the Monte Carlo evaluation of I is made using the same data.

TABLE 17

Comparison of Measured Ranges in Aluminum to Monte Carlo Ranges

Source	Proton Energy (MeV)		Measured Range (g/cm^2)		Monte Carlo Range I = 163 eV	Change in Range if Energy Wrong by 1 MeV (g/cm^2)
30	6.15	±.010	0.07301	±.0002	0.0729	
30	11.820	±.015	0.22633	"	0.2264	
30	14.971	±.020	0.34263	"	0.3432	
30	17.836	±.025	0.46692	±.0003	0.4666	
31	18.00	±.02	0.4770	±.0005	0.4737	.045
	36.2	±.1	1.645	±.001	1.640	.077
	99.9	±.1	9.935	±.001	9.939	
29	99.58	±.08	9.768	±.010	9.884	.017
29	99.88	±.08	9.940	±.009	9.936	
	159.75	±.25	22.607	±.001	22.550	.036
32	338.5	±1.40	78.63	±.92	79.540	.118
32	339.7	±1.84	79.42	±1.04	80.093	
26	752.2		273.29		273.170	.536
	752.7				273.29	

Thus the range predicted for Monte Carlo transport of the proton through the absorber using a value of I = 163 eV gives a value within the experimental accuracy of the experiments when one considers both the range uncertainity and the energy uncertainity.

Comparison of Measured Ranges in Copper to Monte Carlo Ranges

					I = 314 eV	
32	337.9	±1.44	91.84	±.92	91.896	.433
32	338.5	±1.89	91.77	±.92	92.156	
19	340.	±2.	92.4		92.806	
24	658.	±2.	257.6	±.3	257.748	.571
26	752.2		314.91		313.46	.603
	754.9				314.9	

Comparison of Measured Ranges in Lead to Monte Carlo Ranges

					I = 840 eV	
	335.5				122.76	
32	338.5	±2.25	122.76	±1.84	124.00	.579
32	339.7	±2.32	124.37	±1.90	125.26	
26	752.2		415.62		416.009	.790
	751.7				415.62	

Comparison of Measured Range in Carbon to Monte Carlo Range

					I = 72.11 eV	
32	339.7	±1.83	70.03	±.88	69.705	.330
19	340.	±2.	70.9		69.804	
	343.3				70.9	

Again the Monte Carlo calculated ranges using the I-values measured in this research effort are in agreement within experimental error with the reported ranges.

TABLE 18

New Average Values of I (Dalton and Turner)

Element	Average Value of I (eV)	References
1 - H	18.2	19, 20, 22, 24
2 - He	44.3	22
3 - Li	37.4	19
4 - Be	61.7	19, 23, 24, 25, 27
6 - C	81.2	19, 20, 22, 24
7 - N	89.6	20, 22
8 - O	101	20, 22
10 - Ne	132	22
13 - Al	163	25
17 - Cl	176	20
18 - Ar	189	22
20 - Ca	187	23
22 - Ti	224	23, 27
23 - V	250	23, 27
26 - Fe	277	19, 23, 24
27 - Co	290	27
28 - Ni	312	23, 25, 27
29 - Cu	316	19, 23, 24, 25, 26, 27
30 - Zn	319	23
36 - Kr	350	22
41 - Nb	407	23
42 - Mo	422	23
45 - Rh	440	23
46 - Pd	456	23
47 - Ag	466	19, 23, 25, 27
48 - Cd	462	23, 24
49 - In	481	23
50 - Sn	486	19, 23
54 - Xe	480	22
73 - Ta	692	23, 27
74 - W	704	19, 23, 24, 27
77 - Ir	730	23, 27, 25
78 - Pt	711	23
79 - Au	760	23, 25, 27
82 - Pb	767	19, 23, 26
90 - Th	698	23
92 - U	856	19, 26

Acknowledgements

Dr. Hans Bichsel made invaluable contributions to the development of this research. His great assistance in the verification of the shell and density corrections were vital to the success of the Monte Carlo program. The parametrization of experimental results reported in Chapter 1 of this volume was developed thanks to his help in analyzing the early data. We wish to thank Dr. Bichsel for his help.

References

1. M. L. Leimdorfer and G. W. Crawford, SMU Phys. Res. Rep. 68-2 (1968)
2. N. Bohr, Phil. Mag. 25, 10 (1913)
3. N. Bohr, Phil. Mag. 30, 581 (1915)
4. Studies in Penetration of Charged Particles in Matter Publication 1133 National Academy of Sciences-National Research Council, Nuclear Science Series Report Number 39, Washington, D.C. (1964).
5. M. J. Berger and S. M. Seltzer, ibid.
6. A. Bergstrom, et al, SMU Phys, Res. Rep. 69-1, Chap. 3 (1969)
7. M. Leimdorfer, et al, SMU Phys. Res. Rep. 69-1, Chap 1 (1969)
8. M. Leimdorfer, et al, SMU Phys. Res. Rep. 69-1, Chap 2 (1969)
9. G. W. Crawford, et al, SMU Phys. Res. Rep. 69-1 Chap 4 (1969)
10. D. R. Dixon, et al, SMU Phys. Res. Rep. 69-1, Chap. 5 (1969)
11. H. Bichsel and C. Tschalser, Nucl. Data Sect. A 3: 343-360, UCRL-17663
12. W. H. Barkas and M. J. Berger, NASA SP-3013 (1964)
13. M. J. Berger and S. M. Seltzer, NASA SP-3036 (1966)
14. D. R. Dixon, Stopping Power Measurements of 185 MeV Protons in Various Metals, M.S. Thesis, SMU (1967).
15. H. Bichsel, USC-136-150 (1969)
16. Handbook of Chem. And Phys., Chem. Rubber Co., 48, E-69 (1968-69)
17. H. H. Anderson, H. Sorensen, and P. Vajda, Phys Rev. 180, No. 2 (1969)
18. P. Dalton and J. E. Turner, ORNL - TM - 1777 (1967).
19. C. J. Bakker and E. Segre, Phys. Rev. 81, 489 (1951).
20. T. J. Thompson, Effect of Chemical Structure on Stopping Powers for High-Energy Protons. Thesis, USAEC Report UCRL-1910 (1952).
21. D. C. Sachs and J. R. Richardson, Phys. Rev. 89, 1163 (1953).
22. J. E. Brolley, Jr. and F. L. Ribe, Phys. Rev. 98, 1112 (1955).
23. V. C. Burkig and K. R. MacKenzie, Phy. Rev. 106, 848 (1957).
24. V. P. Zrelov and G. D. Stoletov, Soviet Phys. JETP 9, 461 (1959).
25. L. P. Nielsen, Mat. Fys. Medd. Dan. Vid. Selsk. 33, No. 6 (1961).
26. W. H. Barkas and S. von Friesen, Nuovo Cimento Suppl., Ser. 10, 19, 41 (1961).
27. G. H. Nakano, K. R. MacKenzie and H. Bichsel, Phys. Rev. 132, 291 (1963).
28. U. Fano, Annual Reviews of Nuclear Science, E. Segre, Ed. 13, 1 (1963).
29. P. M. Portner and R. B. Moore, Canadian J. Phys. 43, 1904 (1965).
30. H. Bichsel, R. F. Mozley, and W. A. Aron, Phys. Rev. 105, 1788 (1957).
31. E. L. Hubbard and K. R. MacKenzie, Phys. Rev. 85, 107 (1952).
32. R. Mather and E. Segre, Phys. Rev. 84, 191 (1951).

Periodic Table of the Elements

1a	2a	3b	4b	5b	6b	7b	8			1b	2b	3a	4a	5a	6a	7a	0
1 H 1.008 13.53 13.53																	2 He 4.003 24.46 37.99
3 Li 6.939 5.36 43.35	4 Be 9.101 9.28 52.63											5 B 10.81 8.26 60.89	6 C* 12.01 11.22 72.11	7 N 14.01 14.48 86.59	8 O 15.999 13.55 100.1	9 F 18.998 17.34 117.5	10 Ne 20.18 21.47 138.9
11 Na 22.99 5.12 149.4	12 Mg 24.31 7.61 157.0											13 Al* 26.98 5.96 163.0	14 Si 28.09 8.12 171.1	15 P 30.97 10.9 182.0	16 S 32.06 10.3 192.3	17 Cl 35.45 12.95 205.3	18 Ar 39.95 15.68 221.0
19 K 39.10 4.32 242.7	20 Ca 40.08 6.09 248.8	21 Sc 44.96 6.7 255.5	22 Ti 47.90 6.81 262.3	23 V 50.94 6.71 269.0	24 Cr 51.99 6.74 275.7	25 Mn 54.94 7.41 283.1	26 Fe 55.85 7.83 290.0	27 Co 58.93 7.81 298.7	28 Ni 58.71 7.61 306.3	29 Cu* 63.55 7.68 314.0	30 Zn 65.37 9.36 323.4	31 Ga 69.72 5.97 329.4	32 Ge 72.59 8.09 337.5	33 As 74.92 10.5 348.0	34 Se 78.96 9.70 357.7	35 Br 79.90 11.80 369.5	36 Kr 83.80 13.93 383.4
37 Rb 85.47 4.16 388.	38 Sr 87.62 5.67 393.	39 Y 88.91 6.5 400.	40 Zr 91.22 6.92 407.	41 Nb 92.91 7.2 415.	42 Mo* 95.94 7.35 422.	43 Tc 7.7 430.	44 Ru 101.1 7.7 438.	45 Rh 102.9 7.7 445.	46 Pd 106.4 8.3 454.	47 Ag 107.9 7.54 461.	48 Cd 112.4 8.96 470.	49 In 114.8 5.76 476.	50 Sn 118.7 7.30 483.	51 Sb 121.7 8.5 492.	52 Te 127.6 8.96 501.	53 I 126.9 10.6 511.	54 Xe 131.3 12.1 523.
55 Cs 132.9 3.87 527.	56 Ba 137.3 5.19 532.	57 La 138.9 5.6 538.	72 Hf 178.5	73 Ta 180.9	74 W 183.8	75 Re 186.2	76 Os 190.2 8.7	77 Ir 192.2 798.	78 Pt 195.1 8.88 807.	79 Au 197. 9.18 816.	80 Hg 200.6 10.39 827.	81 Tl 204.4 6.07 833.	82 Pb* 207.2 7.38 840.	83 Bi 209. 8.0 848.	84 Po 210 8 856.	85 At 209 9 865.	86 Rn 222 10.70 876.
		58 Ce 140.1 6.54 545.	59 Pr 140.9 5.8 550.	60 Nd 144.2 6.3 557.	61 Pm 145	62 Sm 150.3 6.6	63 Eu 151.9 5.64	64 Gd 157.2 6.7	65 Tb 158.9 6.7	66 Dy 162.5 6.8	67 Ho 164.9 7	68 Er 167.2 7	69 Tm 168.9 7	70 Yb 173.1 7.1	71 Lu 174.9 8		

KEY TO CHART

Atomic Number 24
Symbol Cr
Atomic Weight 51.99
6.74 Class I Ionization Potential, volts.
275.7 Mean Ionization Potential, eV.

*Note: The values for the Mean Ionization Potential, I, of each element is based on the theory that the Class I Ionization Potential represents the difference in the I-value between any two adjacent elements. Thus if one value for I is known in any one period, the remainder may be calculated. The key elements used in this report are Carbon, Aluminum, Copper, Molybdenum, and lead.

CHAPTER 7

MEAN IONIZATION POTENTIAL VALUES FOR MIXTURES AND COMPOUNDS

by George W. Crawford

Introduction

As part of the stopping power measurements in seven elements described in Chapter 4 of this report, data was taken using lucite, nylon, polyethylene and a tissue equivalent plastics. The plastics were inserted in the beam in sequence with the elements and data was taken and processed for them in exactly the same way as for the elements. In order to obtain a single data point, 4 separate measurements were made using two detectors of different volumes and two nearly identical absorbers.

Description of the Plastics

LUCITE ($C_5H_8O_2$) = 1.1892 gm/cm^2

Carbon: Z = 6, A = 12.01115
Hydrogen: Z = 1, A = 1.00797
Oxygen: Z = 8, A = 15.9994

Gram Molecule = 100.1188 grams contain 6.023×10^{23} molecules

Density of Carbon = .713242 gm/cc
Density of Hydrogen = .0957678 "
Density of Oxygen = .380028 "

NYLON ($C_{12}H_{22}O_2N_2$) = 1.1399 gm/cc

Carbon: Z = 6, A = 12.01115
Hydrogen: Z = 1, A = 1.00797
Oxygen: Z = 8, A = 15.9994
Nitrogen: Z = 7, A = 14.0067

Gram Molecule = 226.309 grams

Density of Carbon: = .7260 gm/cc
Density of Hydrogen: = .1117 "
Density of Oxygen: = .1611 "
Density of Nitrogen: = .1411 "

POLYETHYLENE $(CH_2)^n$ = .94582 gm/cc

Carbon: Z = 6, A = 12.01115
Hydrogen: Z = 1, A = 1.00797

Gram Molecule = 14.02709 grams

Density of Carbon = .80990 gm/cc
Density of Hydrogen = .13592 "

TISSUE EQUIVALENT ($C_{27}H_{21}ON$) ρ = 1.0999 gm/cc

Carbon: Z = 6, A = 12.01115
Hydrogen: Z = 1, A = 1.00797
Oxygen: Z = 8, A = 15.9994
Nitrogen: Z = 7, A = 14.0067

Gram Molecule = 375.4745 grams

Density of Carbon: = .95003
Density of Hydrogen: = .06210
Density of Oxygen: = .04687
Density of Nitrogen: = .04103

Bragg's Rule (1)

It is assumed that Bragg's rule gives the correct proceedure for determining the proper value for Z/A, I, and shell corrections to be used in the Monte Carlo calculations.

$$Z/A = (1/\rho) \Sigma (Z_i/A_i)\rho_i$$

$$\log I = A/Z \ (1/\rho) \Sigma (Z_i/A_i)\rho_i \log I_i$$

$$C/Z = A/Z \ (1/\rho) \Sigma (Z_i/A_i)\rho_i \ (C_i/A_i)$$

The values obtained for the four plastics are as follows:

Name	Z/A	I(theory)	I(measured)	I(i)
Lucite	.53990	61.9	63.89	68.1
Nylon	.54860	57.0	57.55	63.4
Polyethylene	.57137	47.4	46.58	54.5
Tissue Equiv.	.52776	61.5	61.50	

Values for I are measured in electron Volts.

Reference

1. Studies in Penetration of Charged Particles in Matter Publication 1133 National Academy of Sciences-National Research Council, Nuclear Science Series Report Number 39, Washington, D/C/ (1964).

TABLE 1

DETERMINATION OF MEAN IONIZATION POTENTIAL, I, OF LUCITE

Absorber Thickness $\rho\Delta x$ ±.001 (g/cm^2)	Measured ΔE (MeV)	Monte Carlo Calculated I = 61.9 eV ΔE (MeV)	The Change in ΔE Produced By A Change In: $\rho\Delta x$ of .001 $\Delta(\Delta E)$ (MeV)	I of 1 eV $\Delta(\Delta E)$ (MeV)	E_o of .1 MeV $\Delta(\Delta E)$ (MeV)	Most Probable Value Of I (eV)
			E_o = 185.6 MeV			
1.510	7.17 ±.05	7.172	.005	.012	.002	62.51
2.263	10.82 ±.05	10.820	.005	.021	.003	61.93
			E_o = 159.75 MeV			
1.510	7.95 ±.03	7.966	.005	.015	.002	63.00
2.263	12.00 ±.04	12.046	.005	.023	.003	63.85
3.009	16.19 ±.05	16.226	.005	.032	.003	63.06
			E_o = 99.9 MeV			
0.754	5.58 ±.05	5.593	.007	.011	.006	63.11
1.510	11.47 ±.03	11.467	.007	.024	.009	61.81
					Average Value =	62.89

Lucite: $(C_5 H_8 O_2)$.
ρ = 1.1892 g/cm^2.
Z/A = 0.5399

Barkas and Berger Value: I = 65.6 eV

TABLE 2

DETERMINATION OF MEAN IONIZATION POTENTIAL, I, OF NYLON

Absorber Thickness $\rho\Delta x$ ±.001 (g/cm^2)	Measured ΔE (MeV)	Monte Carlo Calculated I = 57.0 eV ΔE (MeV)	The Change In ΔE Produced By A Change In: $\rho\Delta x$ of .001 $\Delta(\Delta E)$ (MeV)	I of 1 eV $\Delta(\Delta E)$ (MeV)	E_o of .1 MeV $\Delta(\Delta E)$ (MeV)	Most Probable Value of I (eV)
			E_o = 185.6 MeV			
1.449	7.06 ±.08	7.078	.005	.011	.002	58.66
2.895	14.34 ±.10	14.337	.005	.031	.003	57.10
			E_o = 159.75 MeV			
1.449	7.82 ±.04	7.838	.006	.012	.002	58.66
2.174	11.87 ±.03	11.866	.006	.025	.003	56.84
2.895	15.99 ±.03	15.953	.006	.033	.003	55.88
			E_o = 99.9 MeV			
0.727	5.51 ±.03	5.537	.009	.013	.006	59.08
1.449	11.28 ±.03	11.283	.009	.019	.009	57.16
2.174	17.37 ±.04	17.357	.009	.041	.010	56.68
2.895	23.73 ±.03	23.762	.010	.054	.010	57.59
					Average Value =	57.55

Nylon: $(C_{12} H_{22} O_2 N_2)$.
ρ = 1.1399 g/cm^2.
Z/A = 0.5486

If NAS-NRC Publication 1133 I-values are used, I is calculated to equal 63.35 eV.

TABLE 3

DETERMINATION OF MEAN IONIZATION POTENTIAL, I, OF POLYETHYLENE

Absorber Thickness $\rho\Delta x$ $\pm.001$ (g/cm^2)	Measured ΔE (MeV)	Monte Carlo Calculated I = 47.3 eV ΔE (MeV)	The Change In ΔE Produced By A Change In: $\rho\Delta x$ of .001 $\Delta(\Delta E)$ (MeV)	I of 1 eV $\Delta(\Delta E)$ (MeV)	E_o of .1 MeV $\Delta(\Delta E)$ (MeV)	Most Probable Value of I (eV)
			E_o = 185.6 MeV			
1.200	6.24 ±.05	6.230	.005	.014	.002	46.64
			E_o = 159.75 MeV			
1.200	6.93 ±.04	6.898	.006	.016	.002	45.35
1.802	10.44 ±.03	10.438	.006	.024	.003	46.93
2.402	14.00 ±.04	14.031	.006	.032	.003	48.32
			E_o = 99.9 MeV			
0.600	4.87 ±.10	4.853	.009	.012	.005	45.93
1.200	9.93 ±.04	9.908	.009	.025	.006	46.47
1.802	15.23 ±.03	15.198	.009	.039	.006	46.53
2.402	20.79 ±.05	20.744	.010	.054	.006	46.50
					Average Value =	46.58

Polyethylene: $(C\ H_2)^n$. Barkas and Berger Value: I = 54.6 eV

ρ = 0.9458 g/cm^2.
Z/A = 0.57137

TABLE 4

DETERMINATION OF MEAN IONIZATION POTENTIAL, I, OF A PLASTIC ($C_{27}\ H_{21}\ O\ N$)

Absorber Thickness $\rho\Delta x$ $\pm.001$ (g/cm^2)	Measured ΔE (MeV)	Monte Carlo Calculated I = 61.5 eV ΔE (MeV)	The Change In ΔE Produced By A Change In: $\rho\Delta x$ of .001 $\Delta(\Delta E)$ (MeV)	I of 1 eV $\Delta(\Delta E)$ (MeV)	E_o of .1 MeV $\Delta(\Delta E)$ (MeV)	Most Probable Value of I (eV)
			E_o = 185.6 MeV			
2.098	9.96 ±.05	9.969	.005	.018	.002	62.02
2.794	13.36 ±.05	13.363	.005	.025	.003	61.65
			E_o = 159.75 MeV			
1.398	7.29 ±.06	7.309	.006	.014	.003	62.88
2.098	11.10 ±.05	11.059	.006	.021	.003	59.57
2.794	14.85 ±.05	14.857	.006	.028	.003	61.77
			E_o = 99.9 MeV			
0.698	5.18 ±.04	5.135	.009	.010	.004	57.02
1.271	10.44 ±.04	10.496	.009	.021	.005	64.18
2.098	16.07 ±.05	16.112	.009	.032	.006	62.82
2.794	22.00 ±.05	22.003	.010	.047	.006	61.58
					Average Value =	61.50

ρ = 1.100 g/cm^2
Z/A = 0.52776

TABLE 5

STOPPING POWER VALUES AND RANGES IN LUCITE

I = 62.9eV Z/A = 0.5399 ρ = 1.1892 g/cm^2 Lucite ($C_5 H_8 O_2$)

ENERGY	STOPPING POWER	RANGE	SHIELDING RANGE DELTA RANGE	RANGE	ENERGY LOST
MEV	MEV*CM2/GM	G/CM2	G/CM2	CM	PER CM
2.0	160.03665	.0200	.0000	.0168	
4.0	94.84854	.0368	.0169	.0310	4.000
6.0	68.83682	.0620	.0252	.0522	6.000
8.0	54.76396	.0948	.0328	.0798	8.000
10.0	45.77099	.1349	.0401	.1135	10.000
14.0	34.84438	.2362	.1012	.1986	14.000
18.0	28.39169	.3641	.1279	.3062	18.000
22.0	24.10331	.5176	.1535	.4353	22.000
26.0	21.03379	.6957	.1781	.5851	26.000
30.0	18.72150	.8977	.2020	.7549	30.000
34.0	16.91327	1.1228	.2251	.9442	34.000
38.0	15.45823	1.3705	.2477	1.1525	38.000
42.0	14.26068	1.6402	.2697	1.3792	42.000
46.0	13.25689	1.9313	.2912	1.6241	46.000
50.0	12.40269	2.2435	.3122	1.8866	50.000
60.0	10.73442	3.1129	.8695	2.6177	52.069
70.0	9.51471	4.1047	.9918	3.4517	36.639
80.0	8.58247	5.2132	1.1085	4.3838	30.619
90.0	7.84591	6.4334	1.2202	5.4099	26.833
100.0	7.24876	7.7608	1.3274	6.5261	24.131
120.0	6.33871	10.7205	2.9597	9.0149	20.434
140.0	5.67723	14.0618	3.3413	11.8246	17.972
160.0	5.17444	17.7578	3.6960	14.9326	16.195
180.0	4.77930	21.7845	4.0267	18.3186	14.844
200.0	4.46063	26.1203	4.3358	21.9647	13.780
250.0	3.88175	38.1872	12.0669	32.1117	11.893
300.0	3.49300	51.8027	13.6155	43.5610	10.654
350.0	3.21500	66.7508	14.9481	56.1309	9.780
400.0	3.00721	82.8526	16.1018	69.6709	9.132
450.0	2.84674	99.9584	17.1058	84.0552	8.634
500.0	2.71967	117.9416	17.9832	99.1773	8.241
550.0	2.61701	136.6945	18.7529	114.9466	7.924
600.0	2.53275	156.1247	19.4302	131.2855	7.665
650.0	2.46268	176.1526	20.0279	148.1270	7.451
700.0	2.40377	196.7094	20.5569	165.4133	7.271
750.0	2.35378	217.7353	21.0259	183.0940	7.117
800.0	2.31104	239.1780	21.4427	201.1252	6.987
850.0	2.27425	260.9917	21.8136	219.4683	6.875
900.0	2.24241	283.1360	22.1443	238.0895	6.777
950.0	2.21472	305.5755	22.4395	256.9589	6.693
1000.0	2.19053	328.2787	22.7032	276.0500	6.620
1200.0	2.11986	421.2145	92.9358	354.1999	6.406
1400.0	2.07690	516.6087	95.3942	434.4171	6.276
1600.0	2.05062	613.5717	96.9629	515.9533	6.193
1800.0	2.03497	711.5112	97.9395	598.3108	6.146
2000.0	2.02638	810.0240	98.5128	681.1504	6.120

TABLE 6

STOPPING POWER VALUES AND RANGES IN NYLON

I = 57.6 eV Z/A = 0.5486 ρ = 1.1399g/cm^2 Nylon (C_{12} H_{22} O_2 N_2)

ENERGY	STOPPING POWER	SHIELDING RANGE	DELTA RANGE	RANGE	ENERGY LOST
MEV	MEV*CM2/GM	G/CM2	G/CM2	CM	PER CM
2.0	166.09961	.0200	.0000	.0175	
4.0	98.12151	.0362	.0163	.0318	4.000
6.0	71.11168	.0606	.0243	.0532	6.000
8.0	56.52280	.0924	.0318	.0811	8.000
10.0	47.21148	.1313	.0389	.1152	10.000
14.0	35.91072	.2294	.0982	.2013	14.000
18.0	29.24410	.3536	.1242	.3103	18.000
22.0	24.81669	.5027	.1491	.4410	22.000
26.0	21.64931	.6757	.1730	.5928	26.000
30.0	19.26429	.8720	.1963	.7650	19.381
34.0	17.39981	1.0908	.2188	.9569	15.712
38.0	15.89992	1.3315	.2408	1.1682	13.586
42.0	14.66576	1.5937	.2622	1.3982	12.106
46.0	13.63149	1.8769	.2831	1.6466	10.988
50.0	12.75152	2.1805	.3036	1.9129	10.104
60.0	11.03336	3.0263	.8458	2.6549	8.507
70.0	9.77757	3.9913	.9650	3.5014	7.421
80.0	8.81800	5.0701	1.0788	4.4478	6.626
90.0	8.06000	6.2578	1.1877	5.4898	6.015
100.0	7.44558	7.5500	1.2922	6.6234	5.530
120.0	6.50940	10.4318	2.8818	9.1515	4.805
140.0	5.82909	13.6858	3.2539	12.0061	4.286
160.0	5.31207	17.2857	3.6000	15.1643	3.896
180.0	4.90581	21.2084	3.9227	18.6055	3.592
200.0	4.57821	25.4326	4.2243	22.3113	3.348
250.0	3.98319	37.1910	11.7584	32.6266	2.908
300.0	3.58366	50.4610	13.2699	44.2679	2.613
350.0	3.29797	65.0320	14.5710	57.0506	2.404
400.0	3.08444	80.7297	15.6977	70.8218	2.247
450.0	2.91954	97.4081	16.6784	85.4533	2.126
500.0	2.78895	114.9438	17.5357	100.8368	2.031
550.0	2.68345	133.2316	18.2878	116.8802	1.953
600.0	2.59684	152.1816	18.9499	133.5043	1.891
650.0	2.52481	171.7159	19.5344	150.6413	1.837
700.0	2.46424	191.7676	20.0517	168.2320	1.793
750.0	2.41285	212.2782	20.5105	186.2253	1.757
800.0	2.36889	233.1966	20.9184	204.5764	1.724
850.0	2.33105	254.4781	21.2815	223.2460	1.697
900.0	2.29829	276.0834	21.6053	242.1997	1.672
950.0	2.26979	297.9779	21.8945	261.4071	1.651
1000.0	2.24490	320.1307	22.1529	280.8411	1.634
1200.0	2.17209	410.8242	90.6934	360.4037	1.583
1400.0	2.12775	503.9318	93.1076	442.0842	1.552
1600.0	2.10055	598.5838	94.6520	525.1196	1.531
1800.0	2.08428	694.2010	95.6172	609.0017	1.521
2000.0	2.07526	790.3886	96.1876	693.3842	1.510

TABLE 7

STOPPING POWER VALUES AND RANGES IN POLYETHYLENE

I = 46.6 eV Z/A = 0.57137 ρ = 0.9458 g/cm^2 Polyethelene (C H_2)

ENERGY MEV	STOPPING POWER MEV*CM2/GM	SHIELDING RANGE G/CM2	DELTA RANGE G/CM2	RANGE CM	ENERGY LOST PER CM
2.0	181.11624	0.0200	0.0	0.0211	
4.0	106.27518	0.0350	0.0150	0.0370	4.000
6.0	76.79439	0.0575	0.0225	0.0608	6.000
8.0	60.92497	0.0869	0.0295	0.0920	8.000
10.0	50.82202	0.1230	0.0361	0.1301	10.000
14.0	38.58868	0.2143	0.0913	0.2267	14.000
18.0	31.38773	0.3300	0.1156	0.3489	18.000
22.0	26.61258	0.4689	0.1389	0.4958	22.000
26.0	23.20013	0.6303	0.1614	0.6665	26.000
30.0	20.63283	0.8135	0.1832	0.8602	30.000
34.0	18.62723	1.0179	0.2043	1.0762	34.000
38.0	17.01479	1.2428	0.2250	1.3140	33.250
42.0	15.68866	1.4879	0.2451	1.5731	25.372
46.0	14.57782	1.7526	0.2647	1.8530	21.864
50.0	13.63306	2.0365	0.2839	2.1532	19.533
60.0	11.78938	2.8278	0.7913	2.9899	15.852
70.0	10.44278	3.7312	0.9033	3.9450	13.586
80.0	9.41435	4.7415	1.0103	5.0131	12.007
90.0	8.60234	5.8541	1.1127	6.1895	10.828
100.0	7.94435	7.0651	1.2109	7.4698	9.908
120.0	6.94225	9.7666	2.7015	10.3261	8.557
140.0	6.21438	12.8182	3.0517	13.5526	7.607
160.0	5.66143	16.1956	3.3773	17.1233	6.898
180.0	5.22706	19.8766	3.6811	21.0153	6.349
200.0	4.87689	23.8417	3.9651	25.2075	5.911
250.0	4.24105	34.8828	11.0410	36.8810	5.122
300.0	3.81424	47.3483	12.4655	50.0606	4.599
350.0	3.50910	61.0406	13.6923	64.5373	4.225
400.0	3.28104	75.7959	14.7553	80.1378	3.948
450.0	3.10492	91.4767	15.6809	96.7169	3.734
500.0	2.96543	107.9672	16.4904	114.1520	3.565
550.0	2.85273	125.1682	17.2011	132.3384	3.428
600.0	2.76019	142.9952	17.8270	151.1865	3.316
650.0	2.68321	161.3750	18.3798	170.6192	3.224
700.0	2.61847	180.2443	18.8693	190.5694	3.146
750.0	2.56350	199.5481	19.3038	210.9790	3.080
800.0	2.51648	219.2384	19.6903	231.7973	3.022
850.0	2.47598	239.2730	20.0346	252.9795	2.974
900.0	2.44090	259.6147	20.3418	274.4863	2.931
950.0	2.41037	280.2309	20.6163	296.2834	2.895
1000.0	2.38369	301.0927	20.8619	318.3403	2.862
1200.0	2.30552	386.5217	85.4291	408.6631	2.771
1400.0	2.25773	474.2551	87.7336	501.4221	2.714
1600.0	2.22824	563.4707	89.2158	595.7483	2.677
1800.0	2.21042	653.6201	90.1496	691.0618	2.656
2000.0	2.20035	744.3291	90.7090	786.9668	2.646

TABLE 8

STOPPING POWER VALUES AND RANGES IN TISSUE EQUIVALENT PLASTIC

I = 61.5 eV Z/A = 0.52776 ρ = 1.100 g/cm^2 Plastic (C_{27} H_{21} ON)

ENERGY MEV	STOPPING POWER MEV*CM2/GM	SHIELDING RANGE G/CM2	DELTA RANGE G/CM2	RANGE CM	ENERGY LOST PER CM
2.0	159.57516	.0200	.0000	.0182	
4.0	94.49740	.0369	.0169	.0336	4.000
6.0	68.55762	.0621	.0253	.0565	5.000
8.0	54.52949	.0951	.0330	.0865	8.000
10.0	45.56787	.1354	.0403	.1231	10.000
14.0	34.68241	.2371	.1017	.2156	14.000
18.0	28.25573	.3656	.1285	.3324	18.000
22.0	23.98539	.5199	.1542	.4727	22.000
26.0	20.92919	.6989	.1790	.6354	26.000
30.0	18.62717	.9019	.2030	.8199	30.000
34.0	16.82713	1.1281	.2263	1.0256	34.000
38.0	15.37877	1.3771	.2490	1.2519	38.000
42.0	14.18680	1.6482	.2711	1.4984	42.000
46.0	13.18773	1.9408	.2927	1.7644	46.000
50.0	12.33759	2.2546	.3138	2.0497	39.055
60.0	10.67736	3.1287	.8741	2.8443	27.668
70.0	9.46362	4.1258	.9971	3.7508	22.861
80.0	8.53601	5.2403	1.1145	4.7640	19.852
90.0	7.80313	6.4672	1.2269	5.8793	17.722
100.0	7.20901	7.8019	1.3347	7.0927	16.112
120.0	6.30360	10.7780	2.9761	9.7982	13.810
140.0	5.64554	14.1379	3.3599	12.8527	12.224
160.0	5.14536	17.8548	3.7168	16.2316	11.059
180.0	4.75230	21.9043	4.0496	19.9131	10.162
200.0	4.43531	26.2648	4.3605	23.8772	9.450
250.0	3.85950	38.4010	12.1362	34.9100	8.177
300.0	3.47283	52.0953	13.6943	47.3594	7.336
350.0	3.19632	67.1304	15.0352	61.0277	6.740
400.0	2.98965	83.3266	16.1962	75.7515	6.296
450.0	2.83004	100.5332	17.2066	91.3938	5.954
500.0	2.70364	118.6228	18.0896	107.8389	5.686
550.0	2.60154	137.4869	18.8642	124.9882	5.469
600.0	2.51773	157.0329	19.5459	142.7572	5.290
650.0	2.44803	177.1805	20.1476	161.0732	5.143
700.0	2.38942	197.8606	20.6801	179.8733	5.018
750.0	2.33970	219.0129	21.1523	199.1027	4.913
800.0	2.29718	240.5848	21.5719	218.7135	4.823
850.0	2.26058	262.5302	21.9454	238.6639	4.746
900.0	2.22890	284.8087	22.2784	258.9170	4.680
950.0	2.20134	307.3843	22.5757	279.4403	4.621
1000.0	2.17728	330.2255	22.8412	300.2051	4.570
1200.0	2.10695	423.7292	93.5036	385.2084	4.422
1400.0	2.06416	519.7101	95.9810	472.4638	4.333
1600.0	2.03798	617.2729	97.5627	561.1572	4.276
1800.0	2.02237	715.8213	98.5484	650.7467	4.245
2000.0	2.01378	814.9493	99.1280	740.8630	4.229

CHAPTER 8

TABLES OF STOPPING POWERS FOR ELEMENTS, MIXTURES, AND COMPOUNDS

by George W. Crawford

Proton Stopping Power Values for Elements Z=1.5
(MeV cm^2/g)

Energy (MeV)	H I=13.53	He I=37.99	Li I=43.35	Be I=52.63	B I=60.89
2.0	401.88989	167.69778	140.68589	137.30641	138.72147
4.0	229.54524	97.49554	82.20788	81.04784	81.71642
6.0	163.86041	70.27145	59.38127	58.77296	59.47741
8.0	128.68013	55.53735	46.99099	46.61385	47.26903
10.0	106.58253	46.21529	39.13808	38.88251	39.48205
14.0	80.15462	34.98526	29.66303	29.52757	30.03457
18.0	64.77953	28.40390	24.10185	24.02266	24.46204
22.0	54.66457	24.05148	20.42041	20.37228	20.76121
26.0	47.47867	20.94701	17.79263	17.76347	18.11348
30.0	42.09741	18.61470	15.81729	15.80053	16.11962
34.0	37.90936	16.79472	14.27515	14.26690	14.56080
38.0	34.55287	15.33282	13.03594	13.03375	13.30672
42.0	31.79982	14.13140	12.01721	12.01945	12.27475
46.0	29.49911	13.12566	11.16414	11.16971	11.40986
50.0	27.54640	12.27075	10.43884	10.44694	10.67395
60.0	23.74702	10.60373	9.02403	9.03626	9.23695
70.0	20.98195	9.38725	7.99115	8.00568	8.18652
80.0	18.87633	8.45888	7.20262	7.21847	7.38379
90.0	17.21774	7.72630	6.58018	6.59679	6.74962
100.0	15.87643	7.13295	6.07596	6.09300	6.23554
120.0	13.83854	6.22980	5.30823	5.32557	5.45216
140.0	12.36221	5.57421	4.75076	4.76805	4.88283
160.0	11.24299	5.07641	4.32736	4.34444	4.45011
180.0	10.36520	4.68550	3.99482	4.01164	4.11007
200.0	9.65849	4.37046	3.72677	3.74332	3.83585
250.0	8.37734	3.79861	3.24013	3.25604	3.33775
300.0	7.51879	3.41491	2.91353	2.92890	3.00327
350.0	6.90553	3.14064	2.68006	2.69501	2.76409
400.0	6.44736	2.93567	2.50558	2.52020	2.58532
450.0	6.09350	2.77739	2.37083	2.38520	2.44726
500.0	5.81312	2.65201	2.26410	2.27828	2.33793
550.0	5.58643	2.55070	2.17787	2.19191	2.24961
600.0	5.40012	2.46750	2.10706	2.12100	2.17712
650.0	5.24494	2.39827	2.04815	2.06201	2.11682
700 0	5.11421	2.34003	1.99860	2.01241	2.06613
750.0	5.00305	2.29057	1.95653	1.97031	2.02312
800.0	4.90776	2.24824	1.92052	1.93430	1.98633
850.0	4.82550	2.21176	1.88951	1.90329	1.95467
900.0	4.75408	2.18015	1.86265	1.87644	1.92727
950.0	4.69174	2.15263	1.83926	1.85308	1.90343
1000.0	4.63709	2.12856	1.81882	1.83267	1.88261
1200.0	4.47556	2.05791	1.75888	1.77292	1.82176
1400.0	4.37481	2.01454	1.72216	1.73646	1.78473
1600.0	4.31076	1.98761	1.69946	1.71404	1.76202
1800.0	4.27019	1.97117	1.68568	1.70056	1.74885
2000.0	4.24527	1.96171	1.67783	1.69302	1.74109

Proton Stopping Power Values for Elements Z=6-10.
(MeV cm^2/g)

Energy (MeV)	C I=72.11	N I=86.59	O I=100.10	F I=117.48	Ne I=138.95
2.0	143.14277	136.27698	130.93244	118.58397	116.32197
4.0	85.28596	81.79220	79.00391	71.97639	72.16500
6.0	62.03787	59.68443	58.05151	53.06494	53.39846
8.0	49.42652	47.68836	46.29055	42.53592	42.90816
10.0	41.35149	39.97231	38.86715	35.65546	36.12159
14.0	31.52241	30.54413	29.76352	27.37160	27.71988
18.0	25.70802	24.94813	24.34326	22.42149	22.74579
22.0	21.83944	21.21690	20.72215	19.10701	19.40677
26.0	19.06805	18.53986	18.12056	16.72196	16.99979
30.0	16.97897	16.51957	16.15519	14.91803	15.17687
34.0	15.34442	14.93740	14.61478	13.50283	13.74526
38.0	14.02855	13.66273	13.37293	12.36106	12.58928
42.0	12.94512	12.61258	12.34925	11.41927	11.63508
46.0	12.03669	11.73156	11.49003	10.62836	10.83327
50.0	11.26341	10.98127	10.75801	9.95422	10.14948
60.0	9.75256	9.51435	9.32598	8.63453	8.80992
70.0	8.64738	8.44045	8.27690	7.66699	7.82695
80.0	7.80233	7.61881	7.47381	6.92586	7.07348
90.0	7.13444	6.96908	6.83847	6.33925	6.47676
100.0	6.59282	6.44197	6.32284	5.86296	5.99206
120.0	5.76710	5.63796	5.53602	5.13582	5.25165
140.0	5.16671	5.05303	4.96333	4.60628	4.71213
160.0	4.71022	4.60811	4.52756	4.20318	4.30125
180.0	4.35138	4.25825	4.18480	3.88602	3.97785
200.0	4.06194	3.97598	3.90819	3.63000	3.71672
250.0	3.53604	3.46292	3.40529	3.16438	3.24164
300.0	3.18279	3.11819	3.06727	2.85132	2.92211
350.0	2.93014	2.87159	2.82545	2.62731	2.69343
400.0	2.74130	2.68724	2.64466	2.45983	2.52244
450.0	2.59546	2.54488	2.50505	2.33049	2.39039
500.0	2.47997	2.43216	2.39451	2.22810	2.28585
550.0	2.38669	2.34112	2.30524	2.14542	2.20146
600.0	2.31014	2.26643	2.23201	2.07760	2.13225
650.0	2.24648	2.20433	2.17115	2.02125	2.07476
700.0	2.19297	2.15215	2.12001	1.97392	2.02649
750.0	2.14759	2.10790	2.07666	1.93381	1.98559
800.0	2.10879	2.07009	2.03963	1.89956	1.95068
850.0	2.07540	2.03757	2.00779	1.87013	1.92070
900.0	2.04652	2.00945	1.98027	1.84470	1.89481
950.0	2.02141	1.98501	1.95638	1.82263	1.87235
1000.0	1.99949	1.96370	1.93554	1.80339	1.85279
1200.0	1.93552	1.90160	1.87492	1.74753	1.79609
1400.0	1.89674	1.86411	1.83845	1.71407	1.76228
1600.0	1.87313	1.84144	1.81652	1.69407	1.74223
1800.0	1.85918	1.82819	1.80383	1.68264	1.73092
2000.0	1.85164	1.82120	1.79727	1.67687	1.72538

Proton Stopping Power Values for Elements Z=11-15.
(MeV cm^2/g)

Energy (MeV)	Na I=149.40	Mg I=157.00	Al I=163.00	Si I=171.10	P I=182.00
2.0	110.68256	113.23468	109.95879	112.32408	107.22694
4.0	68.36726	68.80263	66.73718	68.39978	65.58739
6.0	50.66441	51.61926	49.91098	50.58032	48.51909
8.0	40.75000	41.54680	40.19077	41.09494	39.04034
10.0	34.33482	35.02242	33.89142	34.67409	33.21574
14.0	26.42519	26.98015	26.12502	26.74831	25.64864
18.0	21.66034	22.12216	21.46535	21.99124	21.10175
22.0	18.49284	18.89708	18.31030	18.79124	18.04167
26.0	16.20706	16.56770	16.05855	16.46245	15.82957
30.0	14.47463	14.80108	14.34982	14.71544	14.13708
34.0	13.11327	13.41219	13.00588	13.34063	12.82027
38.0	12.01349	12.28974	11.91939	12.22871	11.75473
42.0	11.10533	11.36257	11.02167	11.30968	10.87365
46.0	10.34196	10.58302	10.26670	10.53656	10.13221
50.0	9.69077	9.91787	9.62242	9.87663	9.49913
60.0	8.41457	8.61392	8.35904	8.58213	8.25681
70.0	7.47767	7.65631	7.43094	7.63080	7.34339
80.0	6.75926	6.92181	6.71892	6.90075	6.64219
90.0	6.19016	6.33986	6.15466	6.32208	6.08622
100.0	5.72775	5.86692	5.69604	5.85165	5.63415
120.0	5.02125	5.14417	4.99506	5.13246	4.94284
140.0	4.50628	4.61724	4.48391	4.60791	4.43848
160.0	4.11401	4.21580	4.09443	4.20816	4.05403
180.0	3.80520	3.89973	3.78775	3.89334	3.75121
200.0	3.55582	3.64446	3.54004	3.63904	3.50657
250.0	3.10204	3.17989	3.08919	3.17612	3.06117
300.0	2.79678	2.86735	2.78584	2.86461	2.76139
350.0	2.57829	2.64362	2.56868	2.64159	2.54675
400.0	2.41491	2.47632	2.40629	2.47482	2.38624
450.0	2.28874	2.34713	2.28089	2.34602	2.26228
500.0	2.18886	2.24486	2.18162	2.24407	2.16416
550.0	2.10824	2.16230	2.10149	2.16178	2.08496
600.0	2.04212	2.09461	2.03579	2.09431	2.02004
650.0	1.98721	2.03838	1.98122	2.03828	1.96612
700.0	1.94110	1.99119	1.93542	1.99126	1.92088
750.0	1.90205	1.95121	1.89663	1.95144	1.88257
800.0	1.86872	1.91711	1.86353	1.91746	1.84990
850.0	1.84010	1.88782	1.83512	1.88830	1.82186
900.0	1.81539	1.86254	1.81060	1.86314	1.79766
950.0	1.79396	1.84062	1.78934	1.84132	1.77670
1000.0	1.77531	1.82154	1.77084	1.82235	1.75846
1200.0	1.72128	1.76632	1.71731	1.76747	1.70577
1400.0	1.68913	1.73350	1.68554	1.73495	1.67461
1600.0	1.67013	1.71415	1.66683	1.71585	1.65637
1800.0	1.65947	1.70335	1.65643	1.70528	1.64633
2000.0	1.65434	1.69820	1.65151	1.70033	1.64170

Proton Stopping Power Values for Elements Z=16-20.
(MeV cm^2/g)

Energy (MeV)	S I=192.30	Cl I=205.30	Ar I=221.00	K I=242.70	Ca I=248.80
2.0	108.73717	102.42215	94.01163	98.25334	100.15466
4.0	66.80159	63.25131	58.40646	61.43927	62.72057
6.0	49.43501	46.84268	43.30304	45.69020	46.71417
8.0	39.78445	37.71573	34.88956	36.85165	37.67654
10.0	33.56076	31.82466	29.45322	31.13353	31.82980
14.0	26.11647	24.74464	22.76169	24.08487	24.62187
18.0	21.50003	20.38585	18.86841	19.95744	20.29630
22.0	18.39127	17.44786	16.15894	17.10521	17.47037
26.0	16.14291	15.32192	14.19712	15.03801	15.36209
30.0	14.43528	13.70638	12.70551	13.46483	13.75755
34.0	13.07976	12.43392	11.53009	12.22433	12.49206
38.0	11.99555	11.39475	10.57813	11.21932	11.46640
42.0	11.09868	10.54532	9.78286	10.38713	10.61730
46.0	10.34371	9.83000	9.12137	9.67883	9.90172
50.0	9.69888	9.21884	8.55600	9.08122	9.28332
60.0	8.43302	8.01854	7.44506	7.90617	8.08377
70.0	7.50189	7.13515	6.62695	7.04022	7.19946
80.0	6.78683	6.45651	5.99817	6.37428	6.51925
90.0	6.21974	5.91811	5.49915	5.84555	5.97906
100.0	5.75851	5.48011	5.09307	5.41512	5.53926
120.0	5.05302	4.80996	4.47155	4.75606	4.86570
140.0	4.53819	4.32075	4.01768	4.27456	4.37353
160.0	4.14567	3.94769	3.67147	3.90714	3.99792
180.0	3.83645	3.65374	3.39862	3.61750	3.70179
200.0	3.58660	3.41619	3.17809	3.38335	3.46238
250.0	3.13165	2.98357	2.77636	2.95671	3.02609
300.0	2.82541	2.69229	2.50584	2.66933	2.73219
350.0	2.60612	2.48370	2.31209	2.46347	2.52165
400.0	2.44212	2.32770	2.16717	2.30949	2.36416
450.0	2.31546	2.20722	2.05525	2.19058	2.24254
500.0	2.21521	2.11185	1.96667	2.09646	2.14627
550.0	2.13430	2.03489	1.89519	2.02052	2.06860
600.0	2.06797	1.97181	1.83660	1.95828	2.00495
650.0	2.01290	1.91944	1.78797	1.90662	1.95212
700.0	1.96669	1.87549	1.74717	1.86330	1.90782
750.0	1.92757	1.83830	1.71264	1.82665	1.87034
800.0	1.89421	1.80659	1.68321	1.79541	1.83840
850.0	1.86558	1.77938	1.65796	1.76863	1.81101
900.0	1.84088	1.75592	1.63620	1.74554	1.78741
950.0	1.81949	1.73560	1.61735	1.72556	1.76699
1000.0	1.80088	1.71793	1.60098	1.70821	1.74925
1200.0	1.74717	1.66697	1.55378	1.65826	1.69822
1400.0	1.71545	1.63694	1.52604	1.62900	1.66835
1600.0	1.69694	1.61948	1.50998	1.61215	1.65117
1800.0	1.68681	1.60999	1.50132	1.60316	1.64205
2000.0	1.68221	1.60576	1.49754	1.59936	1.63822

Proton Stopping Power Values for Elements Z=21-25.
(MeV cm^2/g)

Energy (MeV)	Sc I=255.50	Ti I=262.30	V I=269.00	Cr I=275.70	Mn I=283.10
2.0	92.98543	90.66705	88.40622	89.65421	87.60356
4.0	58.32698	56.96815	55.63907	56.51720	55.32564
6.0	43.51199	42.56862	41.61523	42.30086	41.44038
8.0	35.09627	34.33821	33.59468	34.18405	33.52505
10.0	29.65010	29.01065	28.38451	28.88512	28.33217
14.0	22.93652	22.44279	21.95972	22.34871	21.92403
18.0	18.90776	18.50150	18.10397	18.42560	18.07701
22.0	16.26108	15.84909	15.50957	15.78574	15.48806
26.0	14.30147	13.98511	13.63300	13.87674	13.61617
30.0	12.80989	12.52851	12.25298	12.46385	12.19366
34.0	11.63335	11.37943	11.13063	11.32354	11.10540
38.0	10.67969	10.44780	10.22066	10.39908	10.19979
42.0	9.88979	9.67625	9.46674	9.63309	9.44952
46.0	9.22428	9.02584	8.83137	8.98724	8.81692
50.0	8.65522	8.46985	8.28790	8.43497	8.27573
60.0	7.53221	7.37169	7.21925	7.34855	7.21105
70.0	6.70928	6.56734	6.42796	6.54356	6.42582
80.0	6.07613	5.94831	5.82278	5.92823	5.81857
90.0	5.57322	5.45652	5.34190	5.43918	5.33913
100.0	5.16369	5.05599	4.95019	5.04075	4.94847
120.0	4.53641	4.44239	4.34999	4.43015	4.34965
140.0	4.07796	3.99384	3.91117	3.98364	3.91167
160.0	3.72804	3.65144	3.57615	3.64270	3.57719
180.0	3.45213	3.38143	3.31193	3.37378	3.31335
200.0	3.22905	3.16310	3.09826	3.15630	3.09994
250.0	2.82249	2.76516	2.70877	2.75982	2.71086
300.0	2.54858	2.49703	2.44631	2.49262	2.44862
350.0	2.35235	2.30492	2.25826	2.30116	2.26070
400.0	2.20556	2.16122	2.11759	2.15793	2.12012
450.0	2.09220	2.05024	2.00894	2.04731	2.01154
500.0	2.00248	1.96240	1.92295	1.95976	1.92561
550.0	1.93008	1.89153	1.85357	1.88913	1.85628
600.0	1.87076	1.83345	1.79673	1.83125	1.79947
650.0	1.82153	1.78526	1.74955	1.78322	1.75233
700.0	1.78024	1.74484	1.70999	1.74296	1.71281
750.0	1.74531	1.71066	1.67654	1.70890	1.67939
800.0	1.71555	1.68153	1.64803	1.67988	1.65092
850.0	1.69004	1.65656	1.62360	1.65502	1.62653
900.0	1.66805	1.63505	1.60255	1.63359	1.60551
950.0	1.64903	1.61644	1.58434	1.61506	1.58733
1000.0	1.63251	1.60028	1.56853	1.59898	1.57156
1200.0	1.58500	1.55382	1.52310	1.55278	1.52626
1400.0	1.55721	1.52668	1.49658	1.52583	1.49987
1600.0	1.54127	1.51112	1.48141	1.51044	1.48482
1800.0	1.53282	1.50291	1.47343	1.50237	1.47696
2000.0	1.52931	1.49953	1.47018	1.49911	1.47383

Proton Stopping Power Values for Elements Z=26-30.
(MeV cm^2/g)

Energy (MeV)	Fe I=290.90	Co I=298.70	Ni I=306.30	Cu I=314.00	Zn I=323.40
2.0	88.74861	86.57579	89.32921	84.73145	84.28085
4.0	56.15700	54.88736	56.73808	53.91866	53.75574
6.0	42.09662	41.17737	42.59830	40.51256	40.42816
8.0	34.08856	33.35962	34.52618	32.85040	32.80000
10.0	28.81735	28.22362	29.23384	27.83412	27.80177
14.0	22.30383	21.84900	22.63583	21.55917	21.55139
18.0	18.39191	18.01904	18.67000	17.78416	17.78151
22.0	15.75940	15.44075	16.00005	15.24217	15.24185
26.0	13.85558	13.57657	14.06916	13.40363	13.40473
30.0	12.40911	12.16016	12.60203	12.00664	12.00870
34.0	11.26962	11.04420	11.44621	10.90611	10.90877
38.0	10.37535	10.14050	10.51017	10.01480	10.01798
42.0	9.61312	9.41692	9.75557	9.27706	9.28057
46.0	8.97039	8.78816	9.10493	8.67239	8.65939
50.0	8.42061	8.25020	8.54833	8.14272	8.14312
60.0	7.33859	7.19139	7.45252	7.10022	7.10184
70.0	6.54037	6.41000	6.64367	6.33044	6.33288
80.0	5.92269	5.80849	6.02085	5.73754	5.74050
90.0	5.43527	5.32787	5.52576	5.26628	5.26950
100.0	5.03802	4.93892	5.12021	4.87997	4.88560
120.0	4.42901	4.34250	4.50253	4.29186	4.29541
140.0	3.98348	3.90610	4.05047	3.86133	3.86504
160.0	3.64318	3.57273	3.70509	3.53242	3.53612
180.0	3.37471	3.30969	3.43255	3.27281	3.27651
200.0	3.15755	3.09691	3.21206	3.06276	3.06643
250.0	2.76158	2.70886	2.80991	2.67962	2.68319
300.0	2.49466	2.44726	2.53878	2.42127	2.42475
350.0	2.30338	2.25978	2.34445	2.23609	2.23949
400.0	2.16027	2.11951	2.19905	2.09753	2.10086
450.0	2.04974	2.01117	2.08675	1.99052	1.99379
500.0	1.96227	1.92543	1.99787	1.90582	1.90906
550.0	1.89170	1.85626	1.92617	1.83750	1.84070
600.0	1.83387	1.79958	1.86743	1.78152	1.78470
650.0	1.78590	1.75256	1.81870	1.73509	1.73825
700.0	1.74568	1.71315	1.77784	1.69616	1.69931
750.0	1.71167	1.67982	1.74330	1.66325	1.66639
800.0	1.68269	1.65143	1.71389	1.63523	1.63837
850.0	1.65787	1.62710	1.68868	1.61122	1.61436
900.0	1.63649	1.60616	1.66698	1.59055	1.59369
950.0	1.61800	1.58805	1.64822	1.57268	1.57583
1000.0	1.60195	1.57233	1.63194	1.55718	1.56033
1200.0	1.55590	1.52724	1.58526	1.51275	1.51594
1400.0	1.52910	1.50103	1.55815	1.48696	1.49021
1600.0	1.51384	1.48614	1.54277	1.47237	1.47568
1800.0	1.50599	1.47842	1.53483	1.46485	1.46823
2000.0	1.50277	1.47541	1.53177	1.46200	1.46544

Proton Stopping Power Values for Elements Z=31-35.
(MeV cm^2/g)

Energy (MeV)	Ga I=329.40	Ge I=337.50	As I=348.00	Se I=357.70	Br I=369.54
2.0	81.11993	79.70239	78.71092	76.13977	76.46245
4.0	51.81271	51.00655	50.49991	48.96350	49.31049
6.0	38.98930	38.41302	38.07057	36.94684	37.25108
8.0	31.64322	31.18991	30.93033	30.03363	30.30096
10.0	26.82738	26.45131	26.24181	25.49040	25.72879
14.0	20.80899	20.53217	20.38699	19.81964	20.01672
18.0	17.17046	16.94521	16.82948	16.36426	16.53709
22.0	14.71885	14.52718	14.43051	14.03385	14.18509
26.0	12.94509	12.77764	12.69409	12.34651	12.48146
30.0	11.59738	11.44796	11.37424	11.06377	11.18598
34.0	10.53542	10.40037	10.33428	10.05286	10.16492
38.0	9.67541	9.55179	9.49182	9.23406	9.33774
42.0	8.96347	8.84945	8.79449	8.55607	8.65280
46.0	8.36370	8.25768	8.20692	7.98487	8.07573
50.0	7.85105	7.75181	7.70459	7.49650	7.58231
60.0	6.85765	6.76927	6.71689	6.53619	6.61187
70.0	6.11579	6.03776	6.00063	5.83803	5.90463
80.0	5.54416	5.47399	5.44103	5.29423	5.35531
90.0	5.08954	5.02559	4.99585	4.86152	4.91819
100.0	4.71907	4.66006	4.63284	4.50868	4.56166
120.0	4.14929	4.09780	4.07609	3.96734	4.01455
140.0	3.73388	3.68793	3.66728	3.56973	3.61257
160.0	3.41635	3.37459	3.35604	3.26708	3.30665
180.0	3.16571	3.12723	3.11030	3.02808	3.06524
200.0	2.96287	2.92703	2.91139	2.83462	2.86943
250.0	2.59282	2.56174	2.54842	2.48154	2.51240
300.0	2.34323	2.31535	2.30356	2.24333	2.27148
350.0	2.16432	2.13871	2.12800	2.07252	2.09873
400.0	2.03044	2.00653	1.99662	1.94470	1.96944
450.0	1.92703	1.90444	1.89515	1.84597	1.86957
500.0	1.84520	1.82364	1.81484	1.76783	1.79054
550.0	1.77918	1.75846	1.75006	1.70480	1.72679
600.0	1.72510	1.70507	1.69700	1.65318	1.67458
650.0	1.68023	1.66078	1.65298	1.61036	1.63128
700.0	1.64264	1.62366	1.61610	1.57448	1.59499
750.0	1.61085	1.59229	1.58493	1.54415	1.56433
800.0	1.58379	1.56558	1.55839	1.51834	1.53823
850.0	1.56061	1.54279	1.53566	1.49624	1.51589
900.0	1.54065	1.52301	1.51610	1.47722	1.49667
950.0	1.52341	1.50599	1.49920	1.46079	1.48006
1000.0	1.50845	1.49124	1.48455	1.44655	1.46567
1200.0	1.46562	1.44899	1.44263	1.40581	1.42454
1400.0	1.44081	1.42455	1.41840	1.38230	1.40083
1600.0	1.42681	1.41079	1.40479	1.36912	1.38757
1800.0	1.41966	1.40378	1.39790	1.36247	1.38092
2000.0	1.41700	1.40121	1.39541	1.36011	1.37861

Proton Stopping Power Values for Elements Z=36-40.
(MeV cm^2/g)

Energy (MeV)	Kr I=383.	Rb I=388.	Sr I=393.	Y I=400.	Zr I=407.
2.0	73.89377	74.03804	73.75754	74.12289	73.66246
4.0	47.81181	47.96689	47.84595	48.15378	47.98175
6.0	36.16681	36.30280	36.22961	36.48407	36.39198
8.0	29.44154	29.56100	29.51006	29.72736	29.67029
10.0	25.01199	25.11852	25.08018	25.27060	25.23241
14.0	19.47227	19.56035	19.53554	19.68973	19.67046
18.0	16.09814	16.17760	16.16411	16.29695	16.28664
22.0	13.81212	13.88115	13.87003	13.98684	13.99138
26.0	12.15559	12.21692	12.20782	12.31139	12.32321
30.0	10.89552	10.95076	10.94304	11.03639	11.05141
34.0	9.90213	9.95267	9.94578	10.03095	10.04707
38.0	9.09726	9.14385	9.13768	9.21626	9.23226
42.0	8.43085	8.47412	8.46858	8.54157	8.55693
46.0	7.86915	7.90973	7.90473	7.97297	7.98742
50.0	7.38890	7.42710	7.42249	7.48685	7.50020
60.0	6.44425	6.47786	6.47412	6.53052	6.54133
70.0	5.74752	5.77770	5.77455	5.82513	5.83376
80.0	5.21952	5.24576	5.23601	5.28206	5.28893
90.0	4.79410	4.81850	4.81509	4.85652	4.85585
100.0	4.44703	4.46992	4.46698	4.50568	4.50293
120.0	3.91432	3.93480	3.93254	3.96696	3.96183
140.0	3.52418	3.54281	3.54097	3.57219	3.56590
160.0	3.22486	3.24201	3.24154	3.27032	3.26341
180.0	2.98953	3.00558	3.00427	3.03103	3.02470
200.0	2.79899	2.81413	2.81302	2.83821	2.83157
250.0	2.45113	2.46460	2.46383	2.48611	2.47931
300.0	2.21638	2.22869	2.22812	2.24842	2.24179
350.0	2.04803	2.05950	2.05907	2.07794	2.07156
400.0	1.92203	1.93287	1.93254	1.95034	1.94422
450.0	1.82470	1.83506	1.83481	1.85177	1.84590
500.0	1.74768	1.75765	1.75746	1.77376	1.76812
550.0	1.68556	1.69522	1.69508	1.71085	1.70541
600.0	1.63468	1.64408	1.64398	1.65932	1.65407
650.0	1.59248	1.60168	1.60162	1.61660	1.61152
700.0	1.55713	1.56616	1.56612	1.58080	1.57588
750.0	1.52726	1.53614	1.53613	1.55056	1.54577
800.0	1.50184	1.51060	1.51062	1.52483	1.52017
850.0	1.48008	1.48873	1.48877	1.50281	1.49826
900.0	1.46137	1.46993	1.46999	1.48388	1.47943
950.0	1.44520	1.45369	1.45377	1.46752	1.46317
1000.0	1.43119	1.43962	1.43972	1.45336	1.44910
1200.0	1.39118	1.39943	1.39959	1.41292	1.40897
1400.0	1.36815	1.37632	1.37653	1.38970	1.38599
1600.0	1.35531	1.36345	1.36370	1.37680	1.37329
1800.0	1.34891	1.35705	1.35734	1.37043	1.36709
2000.0	1.34674	1.35490	1.35523	1.36833	1.36514

Proton Stopping Power Values for Elements Z=41-45.
(MeV cm^2/g)

Energy (MeV)	Nb I=415.	Mo I=422.	Tc I=430.	Ru I=438.	Rh I=445.
2.0	73.53273	72.42401	72.39059	70.94986	70.74481
4.0	47.92371	47.27919	47.34377	46.47893	46.42497
6.0	36.35593	35.89043	35.96532	35.33147	35.31445
8.0	29.64461	29.27605	29.34927	28.84288	28.84023
10.0	25.21269	24.90553	24.97478	24.55006	24.55423
14.0	19.65727	19.42418	19.48528	19.16023	19.17001
18.0	16.27687	16.08731	16.14169	15.87581	15.88743
22.0	13.97911	13.82134	13.87205	13.64563	13.65778
26.0	12.30639	12.16825	12.21494	12.01883	12.03295
30.0	11.03327	10.91012	10.95277	10.77764	10.79098
34.0	10.02905	9.91760	9.95695	9.79833	9.81103
38.0	9.21511	9.11305	9.14971	9.00430	9.01637
42.0	8.54105	8.44673	8.48102	8.34650	8.35808
46.0	7.97291	7.88511	7.91741	7.79207	7.80310
50.0	7.48708	7.40486	7.43536	7.31788	7.32845
60.0	6.53151	6.46008	6.48719	6.38502	6.39456
70.0	5.82658	5.76317	5.78764	5.69676	5.70559
80.0	5.28381	5.22656	5.24899	5.16681	5.17505
90.0	4.85239	4.79998	4.82079	4.74547	4.75324
100.0	4.50601	4.45230	4.47179	4.40206	4.40942
120.0	3.96801	3.92487	3.94165	3.87979	3.88585
140.0	3.57367	3.53508	3.55048	3.49502	3.50075
160.0	3.27203	3.23687	3.25119	3.20060	3.20604
180.0	3.03380	3.00136	3.01479	2.96800	2.97319
200.0	2.84015	2.80986	2.82334	2.77966	2.78464
250.0	2.48827	2.46197	2.47330	2.43522	2.43977
300.0	2.25069	2.22706	2.23748	2.20318	2.20746
350.0	2.08027	2.05854	2.06830	2.03670	2.04078
400.0	1.95270	1.93239	1.94165	1.91208	1.91599
450.0	1.85415	1.83494	1.84381	1.81580	1.81959
500.0	1.77617	1.75782	1.76639	1.73961	1.74330
550.0	1.71327	1.69563	1.70394	1.67816	1.68177
600.0	1.66176	1.64469	1.65281	1.62785	1.63139
650.0	1.61905	1.60246	1.61041	1.58613	1.58963
700.0	1.58327	1.56709	1.57490	1.55119	1.55465
750.0	1.55305	1.53721	1.54491	1.52168	1.52510
800.0	1.52734	1.51179	1.51939	1.49658	1.49997
850.0	1.50534	1.49004	1.49756	1.47510	1.47847
900.0	1.48642	1.47133	1.47879	1.45664	1.46000
950.0	1.47008	1.45519	1.46259	1.44070	1.44405
1000.0	1.45594	1.44121	1.44857	1.42691	1.43024
1200.0	1.41559	1.40134	1.40858	1.38759	1.39091
1400.0	1.39245	1.37850	1.38569	1.36511	1.36844
1600.0	1.37963	1.36587	1.37305	1.35271	1.35607
1800.0	1.37334	1.35969	1.36689	1.34668	1.35007
2000.0	1.37132	1.35773	1.36497	1.34484	1.34827

Proton Stopping Power Values for Elements Z=46-50.
(MeV cm^2/g)

Energy (MeV)	Pd I=454.	Ag I=461.	Cd I=470.	In I=476.	Sn I=483.
2.0	69.39070	69.43909	67.48833	67.08928	65.78435
4.0	45.62152	45.73032	44.53510	44.32764	43.53577
6.0	34.72867	34.83441	33.95055	33.80896	33.22580
8.0	28.37372	28.47081	27.76082	27.65279	27.18553
10.0	24.16385	24.25266	23.65495	23.56731	23.17462
14.0	18.87215	18.94772	18.48798	18.42397	18.12262
18.0	15.64425	15.71023	15.33289	15.28221	15.03527
22.0	13.45101	13.50980	13.18769	13.14558	12.93502
26.0	11.85446	11.90823	11.62591	11.58978	11.40540
30.0	10.63153	10.68163	10.43098	10.40081	10.23738
34.0	9.66664	9.71273	9.48546	9.45828	9.31035
38.0	8.88418	8.92699	8.71861	8.69387	8.55827
42.0	8.23588	8.27586	8.08309	8.06038	7.93500
46.0	7.68926	7.72690	7.54723	7.52618	7.40933
50.0	7.22179	7.25730	7.08879	7.06918	6.95963
60.0	6.30196	6.33329	6.18671	6.16981	6.07452
70.0	5.62326	5.65151	5.52102	5.50606	5.42128
80.0	5.10062	5.12642	5.00834	4.99490	4.91818
90.0	4.68506	4.70896	4.60068	4.58845	4.51809
100.0	4.34632	4.36863	4.26837	4.25711	4.19196
120.0	3.82677	3.84663	3.75859	3.74881	3.69163
140.0	3.45061	3.46821	3.38859	3.37663	3.32527
160.0	3.16032	3.17663	3.10391	3.09566	3.04833
180.0	2.93096	2.94622	2.87893	2.87138	2.82762
200.0	2.74520	2.75959	2.69669	2.68971	2.64882
250.0	2.40541	2.41820	2.36384	2.35788	2.32220
300.0	2.17653	2.18825	2.13871	2.13340	2.10123
350.0	2.01230	2.02325	1.97757	1.97274	1.94309
400.0	1.88935	1.89971	1.85692	1.85245	1.82469
450.0	1.79436	1.80428	1.76371	1.75952	1.73321
500.0	1.71920	1.72875	1.68994	1.68597	1.66082
550.0	1.65857	1.66784	1.63046	1.62666	1.60243
600.0	1.60894	1.61797	1.58175	1.57810	1.55464
650.0	1.56778	1.57662	1.54138	1.53785	1.51501
700.0	1.53332	1.54200	1.50756	1.50414	1.48184
750.0	1.50422	1.51276	1.47901	1.47568	1.45382
800.0	1.47946	1.48790	1.45473	1.45147	1.43001
850.0	1.45829	1.46663	1.43397	1.43077	1.40964
900.0	1.44009	1.44835	1.41612	1.41298	1.39213
950.0	1.42438	1.43257	1.40073	1.39764	1.37703
1000.0	1.41079	1.41892	1.38741	1.38436	1.36397
1200.0	1.37208	1.38006	1.34949	1.34658	1.32681
1400.0	1.34997	1.35789	1.32788	1.32506	1.30567
1600.0	1.33782	1.34572	1.31604	1.31329	1.29411
1800.0	1.33196	1.33987	1.31037	1.30766	1.28861
2000.0	1.33022	1.33816	1.30874	1.30607	1.28708

Proton Stopping Power Values for Elements Z=51-55.
(MeV cm^2/g)

Energy (MeV)	Sb I=492.	Te I=501.	I I=511.	Xe I=523.	Cs I=527.
2.0	64.90627	62.63232	63.57565	61.92856	62.10825
4.0	43.03595	41.61095	42.33749	41.35172	41.50543
6.0	32.86835	31.80444	32.38916	31.66763	31.79524
8.0	26.90427	26.04480	26.53729	25.96132	26.07053
10.0	22.94125	22.21487	22.64275	22.15994	22.25580
14.0	17.94661	17.38496	17.72774	17.35852	17.43625
18.0	14.89271	14.43016	14.71891	14.41704	14.48301
22.0	12.81452	12.41868	12.66978	12.41283	12.47050
26.0	11.30059	10.95298	11.17621	10.95148	11.00295
30.0	10.14434	9.83334	10.03501	9.83463	9.88128
34.0	9.22761	8.94663	9.13222	8.95092	8.99369
38.0	8.48268	8.22480	8.39592	8.23092	8.27141
42.0	7.86526	7.62652	7.78568	7.63321	7.67081
46.0	7.34453	7.12192	7.27095	7.12898	7.16416
50.0	6.89899	6.69011	6.83045	6.69746	6.73059
60.0	6.02202	5.84015	5.96320	5.84777	5.87680
70.0	5.37470	5.21269	5.32293	5.22032	5.24631
80.0	4.87614	4.72935	4.82967	4.73691	4.76051
90.0	4.47966	4.34502	4.43741	4.35244	4.37416
100.0	4.15645	4.03168	4.11757	4.03894	4.05915
120.0	3.66057	3.55092	3.62686	3.55792	3.57578
140.0	3.29748	3.19886	3.26748	3.20560	3.22173
160.0	3.02264	2.93204	2.99268	2.93620	2.95102
180.0	2.80393	2.72003	2.77838	2.72581	2.73933
200.0	2.62674	2.54826	2.60306	2.55396	2.56668
250.0	2.30304	2.23443	2.28271	2.23991	2.25116
300.0	2.08401	2.02205	2.06589	2.02776	2.03802
350.0	1.92728	1.87009	1.91077	1.87522	1.88474
400.0	1.80993	1.75631	1.79461	1.76134	1.77032
450.0	1.71926	1.66840	1.70487	1.67335	1.68191
500.0	1.64751	1.59883	1.63384	1.60371	1.61195
550.0	1.58965	1.54272	1.57657	1.54756	1.55554
600.0	1.54227	1.49679	1.52969	1.50159	1.50935
650.0	1.50301	1.45872	1.49082	1.46350	1.47108
700.0	1.47013	1.42685	1.45829	1.43160	1.43904
750.0	1.44237	1.39994	1.43082	1.40468	1.41199
800.0	1.41876	1.37706	1.40747	1.38179	1.38900
850.0	1.39858	1.35749	1.38751	1.36223	1.36934
900.0	1.38124	1.34069	1.37036	1.34543	1.35246
950.0	1.36628	1.32619	1.35557	1.33094	1.33791
1000.0	1.35334	1.31366	1.34278	1.31841	1.32532
1200.0	1.31655	1.27802	1.30644	1.28283	1.28959
1400.0	1.29563	1.25777	1.28582	1.26266	1.26934
1600.0	1.28421	1.24674	1.27461	1.25172	1.25837
1800.0	1.27880	1.24153	1.26934	1.24661	1.25325
2000.0	1.27732	1.24014	1.26797	1.24531	1.25196

Proton Stopping Power Values for Elements Z=56-60.
(MeV cm^2/g)

Energy (MeV)	Ba I=532.	La I=538.	Ce I=545.	Pr I=550.	Nd I=557.
2.0	60.92549	61.01828	61.20715	61.95500	62.31656
4.0	40.76033	40.87175	41.05614	41.61002	41.90985
6.0	31.23778	31.33754	31.49604	31.93596	32.18266
8.0	25.61960	25.70810	25.84599	26.21405	26.42427
10.0	21.87436	21.95374	22.07592	22.39435	22.57831
14.0	17.14098	17.20705	17.30740	17.56107	17.70976
18.0	14.23965	14.29659	14.38239	14.59535	14.72130
22.0	12.26213	12.31243	12.38781	12.57257	12.68252
26.0	10.81990	10.86513	10.93267	11.09662	11.19464
30.0	9.71745	9.75869	9.82006	9.96797	10.05673
34.0	8.84500	8.88300	8.93941	9.07453	9.15586
38.0	8.13593	8.17127	8.22358	8.34827	8.42350
42.0	7.54523	7.57899	7.62860	7.74532	7.81544
46.0	7.04705	7.07872	7.12520	7.23435	7.30074
50.0	6.62067	6.65054	6.69437	6.79708	6.85961
60.0	5.78103	5.80733	5.84592	5.93586	5.99075
70.0	5.16093	5.18457	5.21922	5.29969	5.34890
80.0	4.68315	4.70473	4.73629	4.80943	4.85422
90.0	4.30314	4.32304	4.35214	4.41945	4.46073
100.0	3.99330	4.01183	4.03893	4.10145	4.13984
120.0	3.51786	3.53429	3.55830	3.61351	3.64744
140.0	3.16963	3.18452	3.20626	3.25609	3.28677
160.0	2.90334	2.91705	2.93705	2.98275	3.01094
180.0	2.69306	2.70583	2.72445	2.76690	2.79310
200.0	2.52508	2.53687	2.55416	2.59214	2.61674
250.0	2.21480	2.22527	2.24058	2.27546	2.29701
300.0	2.00518	2.01474	2.02869	2.06037	2.07997
350.0	1.85442	1.86331	1.87664	1.90602	1.92422
400.0	1.74189	1.75030	1.76255	1.79018	1.80732
450.0	1.65495	1.66299	1.67467	1.70097	1.71731
500.0	1.58614	1.59389	1.60513	1.63037	1.64608
550.0	1.53066	1.53816	1.54905	1.57345	1.58864
600.0	1.48524	1.49255	1.50314	1.52685	1.54162
650.0	1.44760	1.45475	1.46510	1.48823	1.50266
700.0	1.41609	1.42310	1.43326	1.45591	1.47004
750.0	1.38949	1.39639	1.40638	1.42862	1.44252
800.0	1.36688	1.37369	1.38353	1.40544	1.41913
850.0	1.34756	1.35428	1.36401	1.38562	1.39913
900.0	1.33096	1.33762	1.34724	1.36860	1.33197
950.0	1.31665	1.32325	1.33279	1.35394	1.36717
1000.0	1.30428	1.31083	1.32030	1.34126	1.35439
1200.0	1.26915	1.27558	1.28484	1.30528	1.31811
1400.0	1.24926	1.25562	1.26478	1.28495	1.29762
1600.0	1.23849	1.24483	1.25395	1.27398	1.28658
1800.0	1.23348	1.23982	1.24893	1.26891	1.28149
2000.0	1.23224	1.23860	1.24773	1.26771	1.28031

Proton Stopping Power Values for Elements Z=77-81.
(MeV cm^2/g)

Energy (MeV)	Ir I=798.	Pt I=807.	Au I=816.	Hg I=827.	Tl I=833.
2.0	48.40581	47.99573	47.82642	47.20053	46.70691
4.0	34.30234	34.07639	34.02301	33.65271	33.34299
6.0	26.84924	26.69025	26.66684	26.39722	26.16595
8.0	22.28076	22.15694	22.14587	21.93132	21.74435
10.0	19.17187	19.06989	19.06508	18.88562	18.72758
14.0	15.17368	15.09756	15.09848	14.96166	14.83942
18.0	12.68550	12.62430	12.62757	12.51593	12.41524
22.0	10.97318	10.92172	10.92608	10.83119	10.74502
26.0	9.71583	9.67126	9.67615	9.59326	9.51757
30.0	8.74972	8.71030	8.71543	8.64159	8.57387
34.0	7.98205	7.94663	7.95185	7.88510	7.82365
38.0	7.35609	7.32385	7.32909	7.26804	7.21166
42.0	6.83507	6.80544	6.81065	6.75429	6.70211
46.0	6.39408	6.36664	6.37179	6.31936	6.27072
50.0	6.01562	5.99003	5.99509	5.94603	5.90040
60.0	5.26750	5.24548	5.25034	5.20783	5.16812
70.0	4.71250	4.69309	4.69772	4.66001	4.62466
80.0	4.28236	4.26511	4.26974	4.23590	4.20411
90.0	3.93950	3.92376	3.92816	3.89718	3.86800
100.0	3.65950	3.64499	3.64918	3.62052	3.59347
120.0	3.22911	3.21646	3.22030	3.19520	3.17141
140.0	2.91331	2.90199	2.90558	2.88305	2.86164
160.0	2.67152	2.66122	2.66458	2.64401	2.62444
180.0	2.48040	2.47090	2.47408	2.45505	2.43690
200.0	2.32554	2.31669	2.31972	2.30195	2.28496
250.0	2.04258	2.03490	2.03767	2.02216	2.00729
300.0	1.85145	1.84455	1.84713	1.83315	1.81971
350.0	1.71529	1.70888	1.71043	1.69756	1.68514
400.0	1.61293	1.60695	1.60923	1.59710	1.58538
450.0	1.53386	1.52822	1.53043	1.51894	1.50782
500.0	1.47131	1.46593	1.46809	1.45711	1.44648
550.0	1.42090	1.41574	1.41786	1.40730	1.39705
600.0	1.37951	1.37452	1.37660	1.36655	1.35662
650.0	1.34541	1.34058	1.34263	1.33268	1.32300
700.0	1.31690	1.31219	1.31423	1.30451	1.29506
750.0	1.29287	1.28827	1.29029	1.28078	1.27151
800.0	1.27243	1.26797	1.26998	1.26064	1.25153
850.0	1.25509	1.25066	1.25266	1.24346	1.23449
900.0	1.24018	1.23582	1.23781	1.22875	1.21989
950.0	1.22737	1.22307	1.22505	1.21610	1.20734
1000.0	1.21632	1.21207	1.21406	1.20520	1.19653
1200.0	1.18524	1.18115	1.18313	1.17456	1.16615
1400.0	1.16805	1.16406	1.16606	1.15766	1.14939
1600.0	1.15917	1.15525	1.15727	1.14897	1.14078
1800.0	1.15552	1.15164	1.15369	1.14545	1.13731
2000.0	1.15529	1.15144	1.15351	1.14530	1.13718

Proton Stopping Power Values for Elements Z=82-86
(MeV cm^2/g)

Energy (MeV)	Pb I=840.	Bi I=848.	Po I=856.	At I=865.	Rn. I=876.
2.0	46.39413	46.29276	46.32468	46.54370	44.20885
4.0	33.17189	33.15593	33.24281	33.47180	31.86600
6.0	26.04588	26.04881	26.13455	26.33415	25.09073
8.0	21.65114	21.66060	21.73981	21.91470	20.88896
10.0	18.65094	18.66302	18.73572	18.89143	18.01225
14.0	14.78236	14.79590	14.85800	14.98648	14.29412
18.0	12.36943	12.38284	12.43718	12.54735	11.97035
22.0	10.70655	10.71944	10.76791	10.86491	10.36692
26.0	9.48429	9.49656	9.54047	9.62749	9.18731
30.0	8.54446	8.55613	8.59637	8.67556	8.27968
34.0	7.79723	7.80833	7.84558	7.91842	7.55768
38.0	7.18764	7.19823	7.23297	7.30056	6.96843
42.0	6.68004	6.69017	6.72277	6.78596	6.47759
46.0	6.25029	6.25999	6.29075	6.35016	6.06189
50.0	5.88135	5.89067	5.91983	5.97598	5.70494
60.0	5.15175	5.16026	5.18619	5.23581	4.99878
70.0	4.61023	4.61809	4.64157	4.68628	4.47444
80.0	4.19136	4.19869	4.22024	4.26113	4.06873
90.0	3.85637	3.86340	3.88354	3.92150	3.74477
100.0	3.58275	3.58936	3.60818	3.64356	3.47948
120.0	3.16205	3.16802	3.18477	3.21617	3.07150
140.0	2.85328	2.85876	2.87398	2.90243	2.77200
160.0	2.61683	2.62191	2.63595	2.66214	2.54259
180.0	2.42989	2.43466	2.44775	2.47213	2.36120
200.0	2.27842	2.28293	2.29525	2.31817	2.21420
250.0	2.00162	2.00566	2.01658	2.03682	1.94557
300.0	1.81462	1.81834	1.82830	1.84673	1.76407
350.0	1.68046	1.68396	1.69324	1.71036	1.63386
400.0	1.58095	1.58421	1.59292	1.60830	1.53642
450.0	1.50365	1.50678	1.51511	1.53046	1.46204
500.0	1.44250	1.44554	1.45356	1.46833	1.40273
550.0	1.39323	1.39619	1.40397	1.41826	1.35494
600.0	1.35293	1.35584	1.36342	1.37733	1.31586
650.0	1.31943	1.32228	1.32969	1.34345	1.28352
700.0	1.29158	1.29438	1.30166	1.31499	1.25635
750.0	1.26811	1.27088	1.27805	1.29116	1.23360
800.0	1.24820	1.25095	1.25802	1.27094	1.21431
850.0	1.23122	1.23394	1.24094	1.25370	1.19786
900.0	1.21667	1.21938	1.22631	1.23894	1.18377
950.0	1.20417	1.20687	1.21374	1.22626	1.17167
1000.0	1.19340	1.19608	1.20291	1.21533	1.16124
1200.0	1.16313	1.16579	1.17249	1.18465	1.13198
1400.0	1.14645	1.14911	1.15575	1.16779	1.11591
1600.0	1.13790	1.14057	1.14719	1.15917	1.10772
1800.0	1.13446	1.13714	1.14378	1.15576	1.10448
2000.0	1.13435	1.13706	1.14372	1.15572	1.10448

Proton Stopping Power Values for Four Plastics
(MeV cm^2/g)

Energy (MeV)	Lucite I=62.9 eV	Nylon I=57.6 eV	Polyethelene I=46.6 eV	TE($C_{27}H_{21}ON$) I=61.5 eV
2.0	160.03665	166.09961	181.11624	159.57516
4.0	94.84854	98.12151	106.27518	94.49740
6.0	68.83682	71.11168	76.79439	68.55762
8.0	54.76396	56.52280	60.92497	54.52949
10.0	45.77099	47.21148	50.82202	45.56787
14.0	34.84438	35.91072	38.58868	34.68241
18.0	28.39169	29.24410	31.38773	28.25573
22.0	24.10331	24.81669	26.61258	23.98539
26.0	21.03379	21.64931	23.20013	20.92919
30.0	18.72150	19.26429	20.63283	18.62717
34.0	16.91327	17.39981	18.62723	16.82713
38.0	15.45823	15.89992	17.01479	15.37877
42.0	14.26068	14.66576	15.68866	14.18680
46.0	13.25689	13.63149	14.57782	13.18773
50.0	12.40269	12.75152	13.63306	12.33759
60.0	10.73442	11.03336	11.78938	10.67736
70.0	9.51471	9.77757	10.44278	9.46362
80.0	8.58247	8.81800	9.41435	8.53601
90.0	7.84591	8.06000	8.60234	7.80313
100.0	7.24876	7.44558	7.94435	7.20901
120.0	6.33871	6.50940	6.94225	6.30360
140.0	5.67723	5.82909	6.21438	5.64554
160.0	5.17444	5.31207	5.66143	5.14536
180.0	4.77930	4.90581	5.22706	4.75230
200.0	4.46063	4.57821	4.87689	4.43531
250.0	3.88175	3.98319	4.24105	3.85950
300.0	3.49300	3.58366	3.81424	3.47283
350.0	3.21500	3.29797	3.50910	3.19632
400.0	3.00721	3.08444	3.28104	2.98965
450.0	2.84674	2.91954	3.10492	2.83004
500.0	2.71967	2.78895	2.96543	2.70364
550.0	2.61701	2.68345	2.85273	2.60154
600.0	2.53275	2.59684	2.76019	2.51773
650.0	2.46268	2.52481	2.68321	2.44803
700.0	2.40377	2.46424	2.61847	2.38942
750.0	2.35378	2.41285	2.56350	2.33970
800.0	2.31104	2.36889	2.51648	2.29718
850.0	2.27425	2.33105	2.47598	2.26058
900.0	2.24241	2.29829	2.44090	2.22890
950.0	2.21472	2.26979	2.41037	2.20134
1000.0	2.19053	2.24490	2.38369	2.17728
1200.0	2.11986	2.17209	2.30552	2.10695
1400.0	2.07690	2.12775	2.25773	2.06416
1600.0	2.05062	2.10055	2.22824	2.03798
1800.0	2.03497	2.08428	2.21042	2.02237
2000.0	2.02638	2.07526	2.20035	2.01378